AGGREGATE RAYS IN THE XYLEM OF THE DICOTYLEDONS WITH EMPHASIS ON THE SPECIES OF *NOTHOFAGUS* INDIGENOUS TO NEW ZEALAND

A thesis
submitted in partial fulfilment
of the requirements for the Degree
of
Doctor of Philosophy in Botany
in the
University of Canterbury

by

Alan R. Dickson

University of Canterbury
1994

CONTENTS

LIST OF FIGURES

CHAPTER 4

CHAPTER 5

CHAPTER 6

APPENDIX 1

APPENDIX 3A

LIST OF TABLES

CHAPTER 5

CHAPTER 6

ABBREVIATIONS USED IN THE TEXT

ANOVA	Analysis of Variance
GA3	Gibberellic acid
IAA	Indole acetic acid
IBA	Indole butyric acid
PAS	Periodic Acid-Schiff
RLS	Radial Longitudinal Section
SAS	Statistical Analysis System (SAS Institute Inc.)
TLS	Transverse Longitudinal Section
TS	Transverse Section

ABSTRACT

This thesis investigates the aggregate rays present in the xylem of the New Zealand species of *Nothofagus*, and compares them with those present in other genera, particularly *Fagus* and *Dracophyllum*. The ontogeny of aggregate rays is investigated, and shown to be a feature largely of the 'leaf-gap' in *Fagus* and *Dracophyllum*. In *Nothofagus*, however, aggregate ray ontogeny relates more to the leaf-trace. Neither the 'synthetic' nor the 'dissection' theory is adequate for describing aggregate ray ontogeny.

The presence of aggregate rays in *Nothofagus* is correlated with an irregular (not circular) outline of the pith (TS) and may relate to light and hormonal factors and their effect on cell division and elongation within the elongating internode.

Certain regions within the growth increment are dominated by pseudo-transverse anticlinal divisions of cambial fusiform initials, other regions are dominated by fusiform initial elongation. An attempt was made to determine whether these regions could be distinguished based on deviations from the normal distribution recorded for axial element length data. The results are not conclusive, but may merit further investigation.

Certain features of the aggregate rays in *Nothofagus* such as: reduced element length; paucity of vessels; reduction of individual rays; and the formation of 'wound-like' areas, indicate that the fluting may actually be responsible for the presence of these aggregate rays.

CHAPTER 1

INTRODUCTION

The classical concept of the aggregate ray is defined by the prominent ray structures that give a striking figure to a number of woods, notably *Quercus* and other members of the Fagaceae. These rays are typically very high, wide and radially extensive, and occasionally incorporate fibres or other axial elements within their structure. The term 'aggregate ray' was first used by Bailey (1911), he believed that these large rays had arisen phylogenetically by the aggregation of smaller uniseriate rays. Bailey (1911) also traced aggregate rays back to the 'leaf-gap', suggesting they had evolved as a storage system. It was this association with the 'leaf-gap', that was responsible for an often heated debate from 1911 to 1922 on the origin of the herbaceous form in dicotyledons. It was in relation to this that the aggregate ray reached its peak as a topic of botanical discussion.

Eames (1911), Jeffrey (1917) and Jeffrey and Torrey (1921a, 1921b) in particular, placed much emphasis on the aggregate ray and its role in the evolution of the herbaceous form. Since Bailey (1911) had traced the origins of the aggregate ray to the leaf-trace and termed it the 'foliar ray', similar accumulations of parenchyma in relation to the leaf-trace were also termed 'foliar rays', and regarded as being synonymous with the aggregate ray. Jeffrey (1917) in particular, regarded the aggregate ray as importance saying:

> "The aggregate ray is evidently the result of the correlation of radial and longitudinal storage devices. Its appearance is a phenomenon of prime biological importance and is ultimately related to the origin of the herbaceous type in angiosperms on the one hand and the evolution of the highest vertebrates, the warm-blooded mammals on the other."

The theory involving aggregate rays in the origin of the herbaceous habit can be summed up in three stages. In the first stage rays begin to aggregate in the area directly below the leaf-trace, forming in effect, an aggregate ray (Figure 1.1a). In the second stage, the axial elements of the aggregate ray are gradually converted to parenchyma, resulting in a compound ray (Figure 1.1b). In the third stage, the vascular cylinder is reduced, leaving only the trace and individual bundles separated by the pith and the residual compound ray (Figure 1.1c).

Figure 1.1

The role of the aggregate ray in the evolution of the herbaceous habit in angiosperms (TS redrawn from Jeffrey [1917])

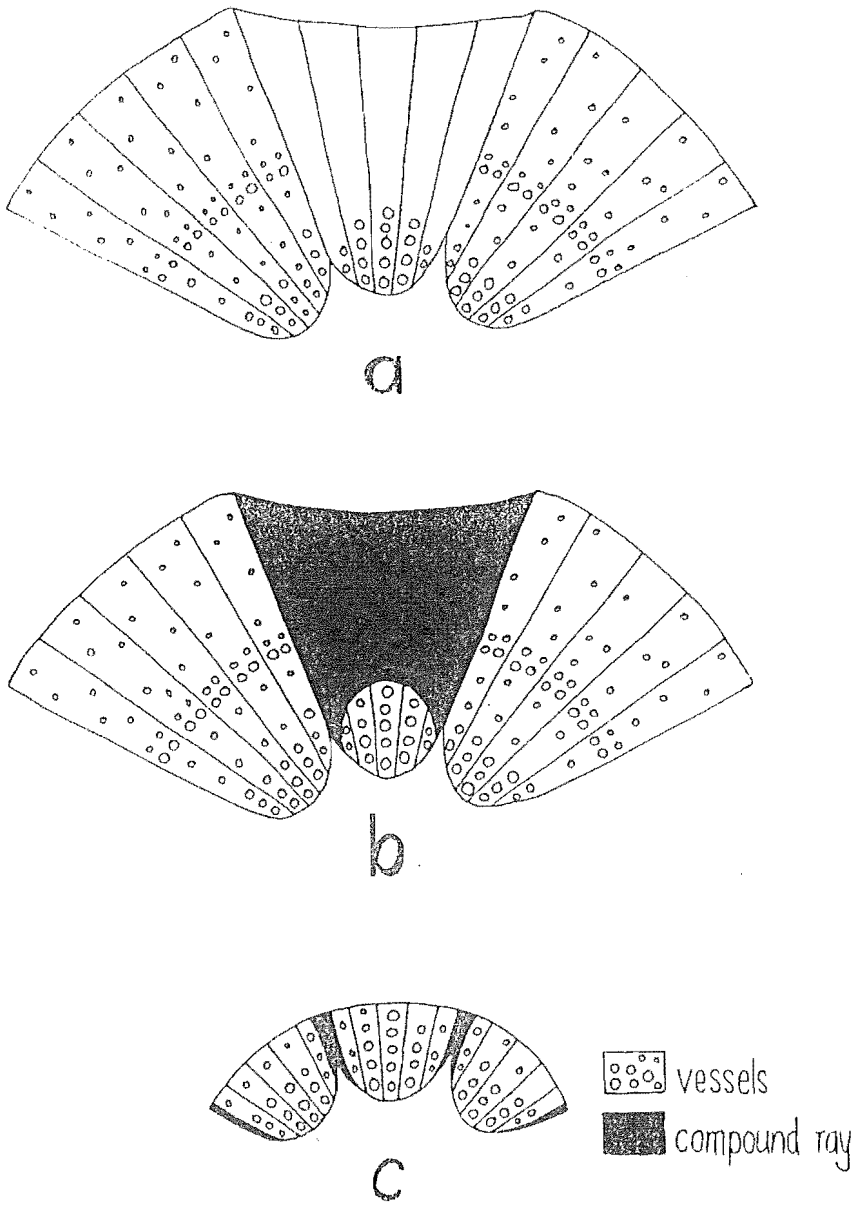

a. Three bundles in a woody stem. The middle bundle represents the area below the leaf trace just before its departure. This bundle has an indented outline and a paucity of vessels (i.e. an aggregate ray is present).

b. All the axial elements in the aggregate ray have been eliminated, resulting in a compound ray. The leaf trace bundle is now separated from the bundles on either side by pith and compound rays.

c. With the reduction of secondary growth, accompanied by the elaboration of the compound rays of surrounding bundles (also associated with leaf traces) an herbaceous stem is developed. Each of the bundles are separated from each other by pith and compound rays.

Sinnott and Bailey (1914, 1922) questioned the role of the foliar ray in the evolution of the herbaceous form. They pointed out that the herbaceous stem could be derived from the woody stem simply by a process of reduction, accompanied by the elaboration of multiseriate rays flanking the leaf-traces (where the herbaceous stem was in the form of discrete bundles). In this way, it was unnecessary to involve the foliar ray as an intermediary.

The broad definition of the foliar ray, used by Jeffrey and Torrey (1921a, 1921b), was also questioned by Sinnott and Bailey (1922), who suggested that it was not in all cases an obvious storage device, but was often just an area devoid of vessels.

The arguments of Eames (1911), Jeffrey (1917) and Jeffrey and Torrey (1921a, 1921b) relating to the evolution of the herbaceous habit depended almost entirely on their belief that the uniseriate ray was the primitive ray condition within the angiosperms. Kribs (1935), using statistical correlations of designated ray types with vessel element characteristics, showed that heterogeneous multiseriate rays in association with uniseriate rays were the primitive condition, and that woods with solely uniseriate rays represented a derived condition.

Parham (1930) recognised aggregate rays in *Nothofagus solandri* var. *cliffortioides* and *N. fusca*, relating them to the aggregate rays of *Quercus* described by Bailey (1911). However, he seemed uncertain about the nature of this relationship, seeing evidence for the formation of aggregate rays by a process of aggregation in mature wood, and evidence for dissection of aggregate rays in juvenile wood. As he seemed unable to reconcile these observations with the synthetic theory of aggregate ray ontogeny (Bailey 1911), his later papers on the wood anatomy of the New Zealand species of *Nothofagus* (Parham 1933a, 1933b) made no mention of aggregate rays, and referred instead, to the waviness of the growth rings. Parham (1930) also noted wavy growth rings in *N. truncata* and *N. solandri* var. *solandri*, but failed to correlate them with aggregate rays. His recognition of aggregate rays in *N. fusca* was not correlated with waviness or flutes in this taxon, though he did recognise that this was supposed to be a feature associated with aggregate rays. Subsequent studies on the wood of the New Zealand species of *Nothofagus* also refer to waviness or undulations of growth rings (Garrett 1924, Patel 1986), though Middleton (1987) does refer to aggregate rays.

The genus *Nothofagus* is traditionally regarded as a member of the Fagaceae (Allan 1961, Langdon 1947, Parham 1930), but there is now a school of thought suggesting the genus should be in its own family, Nothofagaceae Kuprianova (Cronquist 1988, Jones 1986, Nixon 1982), with Jones (1986) suggesting leaf data indicate that *Nothofagus* may be closer to the Betulaceae than the Fagaceae. Jenkins (1993), however, is not in favour of placing *Nothofagus* in its own family, preferring instead that it remain in the Fagaceae.

This thesis represents a study on the aggregate rays present in the New Zealand representatives of the genus *Nothofagus* Blume. The first section (Chapter 2) consists of an analysis of what constitutes an aggregate ray. This was seen as being necessary, as the aggregate rays described for *Nothofagus* (Middleton 1987) appeared to have a structure that was dissimilar to the classic aggregate ray structure, described for other taxa (Bailey 1910a, 1910b, 1911, 1912, Eames 1910, 1911, Carlquist 1988, Jeffrey 1917, Metcalfe and Chalk 1950, Metcalfe and Chalk 1983, Moseley 1948). The subsequent chapter deals with the ontogeny of the aggregate rays in *Nothofagus*, and compares it with the ontogeny of aggregate rays in other taxa. Chapter 4 attempts to relate the ontogeny of the aggregate rays in *Nothofagus* with features of the primary growth of the stem, and how these may be affected by environmental and/or physiological conditions. The final section of work (Chapter 6) deals with the woody tissue within the aggregate rays of *Nothofagus*, and how various features such as element dimensions and ray activity, reflect processes within the cambium. This is preceded by a study on how element length data may be used as an indicator of cambial activity (Chapter 5), and is the justification of a method used in the subsequent chapter.

CHAPTER 2

THE STRUCTURE OF AGGREGATE RAYS. WITH EMPHASIS ON THE NEW ZEALAND SPECIES OF *NOTHOFAGUS* BLUME

2.1. INTRODUCTION

The aggregate ray is defined by the IAWA Committee (1989) as:

> 'a number of individual rays so closely associated with one another that they appear macroscopically as a single large ray. The individual rays are separated by axial elements...'

Eames (1910) used the term 'false rays' to describe, collectively, closely associated small rays that appeared to make up one large ray assemblage. He also described the large rays typical of *Quercus* as being 'compounded' as he believed they had arisen by the fusion of the separate units that made-up the false rays. Bailey (1910a) appears to be the first to use the term 'compound ray' to describe the rays of *Quercus*. The term 'aggregate ray' appears to have been first used by Bailey (1911) in preference to false ray, to indicate that the compound ray had arisen by the 'aggregation' of uniseriate rays via this intermediate structure. Bailey (1911) also referred to both aggregate and compound rays as foliar rays, because of their relationship to the leaf-trace. Jeffrey (1917) used a further term, the 'diffuse ray', to describe ray assemblages with morphologies similar to the aggregate ray. Jeffrey's 'diffuse ray' terminology also had distinct phylogenetic and ontogenetic implications, with a diffuse ray being the product of the dissection of a compound ray. According to Metcalfe and Chalk (1983) the term 'compound ray' has fallen into disuse as "...there is no sharp distinction between fine (i.e. narrow), aggregate and compound rays even in the same genus."

Aggregate rays have been described in *Nothofagus* (Middleton 1987, Parham 1930), but other studies of this genus have used the terms 'undulations' or 'waviness' to describe these features of the wood (Garrett 1924, Parham 1933a 1933b, Patel 1986). In order to investigate these structures it was decided to compare the 'so called' aggregate rays of *Nothofagus* with those present in other woods, notably woods of the Betulaceae (Bailey 1910b 1911, Hoar 1916, IAWA committee 1989), Casuarinaceae (IAWA committee 1989, Jeffrey 1917, Moseley 1948), Epacridaceae

(Butterfield pers. comm.) and the Fagaceae (Bailey 1910, Eames 1910, IAWA committee 1989, Shimaji 1954a, 1954b). This study was not intended to provide a definitive description of the aggregate rays in the species examined, but was an investigation of the variability of the structures considered to be aggregate rays. A more detailed study, however, was also performed on species of *Nothofagus*, to ascertain the range of structures within these examples, that can be covered by the broad definition of the aggregate ray according to the IAWA Committee (1989).

2.2. MATERIAL

A number of specimens held in the wood collection of Dr. Brian Butterfield were examined. These are listed in Table 2.1. Most specimens had been fixed in FAA and stored in 70% alcohol, others were dry.

One mature stem specimen of each of *Quercus ilex* and *Casuarina* sp., were collected from the campus of the University of Canterbury. Samples of *Nothofagus fusca* were collected mainly from the Lewis Pass, and *N. solandri* var. *cliffortioides* from the Cass regions of the Southern Alps. Root material from two plants of *N. solandri* var. *cliffortioides* was also collected from the Castle Hill region of the Southern Alps Additional stem material was also available on the Campus of the University of Canterbury. Samples of *N. truncata* and *N. solandri* var. *solandri* were collected in Wellington by Dr. Brian Meylan. Stem specimens from mature trees were usually collected from breast height using a core borer, however, material from felled trees was also available for species of *Nothofagus*.

2.3. METHODS

2.3.1. Sliding microtomy

Dry samples were boiled in water until they were saturated. Samples were continuously washed in 50% ethanol in water as they were cut on a MSE sliding microtome. Sections were stained in a 1% safranin solution in 60% ethanol, for two minutes. This was followed by two quick washes in 100% ethanol and counterstaining in a 0.5% solution of fast green dissolved in equal parts of: ethanol; clove oil; and cellosolve, for 20 to 30 seconds. The sections were then transferred (briefly) to clove oil, followed by washes in three changes of xylene, with five minutes for each wash. Sections were mounted on glass slides using Depex[1] mountant.

---

1 BDH Limited Poole England.

Table 2.1

Specimens held in the wood collection of Dr. BG Butterfield and used in Chapter 2

specimen number	species	family
230	*Dracophyllum filifolium*	Epacridaceae
5	*Dracophyllum longifolium*	Epacridaceae
1016	*Dracophyllum longifolium*	Epacridaceae
229	*Dracophyllum pronum*	Epacridaceae
1056	*Dracophyllum subulatum*	Epacridaceae
323	*Dracophyllum traversii*	Epacridaceae
575	*Dracophyllum traversii*	Epacridaceae
840	*Dracophyllum uniflorum*	Epacridaceae
780	*Dracophyllum urvilleanum*	Epacridaceae
2058	*Carpinus betulus*	Betulaceae
2044	*Corylus avellana*	Betulaceae
2000	*Alnus glutinosa*	Betulaceae
2122	*Alnus glutinosa*	Betulaceae
2006	*Betula pendula*	Betulaceae
2130	*Betula pendula*	Betulaceae
2098	*Lithocarpus perclusa*	Fagaceae
2082	*Castanopsis accuminatissima*	Fagaceae
2008	*Quercus coccinia*	Fagaceae
2123	*Quercus palustris*	Fagaceae
2007	*Fagus sylvatica*	Fagaceae
2020	*Fagus sylvatica*	Fagaceae

2.3.2. SEM preparation

Samples were boiled in water for one hour and then trimmed with a razor blade. The samples were then dehydrated by sequential changes in solutions of 50%; 70%; 80%; 95%; and 100% ethanol, spending 24 hours in each solution. Samples were then transferred to 100% acetone for a further 24 hours, and then allowed to dry in a desiccator. The samples were gold palladium coated and examined under a Cambridge Stereoscan 250 Mark II.

2.3.3. Paraffin embedding

Samples of *N. solandri* var. *cliffortioides* were prepared and sectioned as in Appendix 1.

2.3.4. LR White[2] embedding

Samples that had been fixed in FAA, were cut into small sections of 1 mm or less in thickness. These samples were then dehydrated in an alcohol series of 20%; 40%; 60%; 80%; and three changes of 100% ethanol, spending 24 hours[3] in each. The samples were then transferred to 100% LR White, with three changes over three days. The resin was hardened with cold cure. Blocks were mounted on gelatin capsules that had been filled with araldite and cut at 5 µm on a Reichert-Jung Autocut rotary microtome. Sections were floated on 25% acetone, affixed to slides and placed in an oven overnight at 60° C.

Sections were stained with Periodic Acid-Schiff (PAS) and toluidine blue in a benzoate buffer at pH 4.4. Dimedone was used as the aldehyde block prior to the PAS staining (Feder and O'Brien 1968).

2.3.5. Staining for callose

Fresh sections of *N. fusca* and *N. solandri* var. *cliffortioides* were used. Sections were stained and mounted in 0.005% water-soluble aniline blue in a 0.15 Molar solution of K_2HPO_4 at pH 9.9 (Jensen 1962) and examined under fluorescent light on an Olympus BH2 microscope.

---

2 London Resin Company

3 Considerable difficulty was encountered in the cutting of woody samples in LR White, hence the extremely long dehydration and infiltration times. As the samples under investigation had been in FAA for some time it is likely a certain amount of the metabolites and secondary products in the cells had been leached out by ethanol, and this would have been exacerbated by the long dehydration times. This is, therefore, only good as a preliminary study to evaluate the possibility of general histochemical localisation in the aggregate rays of *Nothofagus*.

2.4. RESULTS

2.4.1. Field observations on *Nothofagus*

Observations were made on mainly *N. fusca* and *N. solandri* var. *cliffortioides* trees growing in the West Coast; Arthur's Pass; and Lewis Pass regions of the South Island, as well as trees growing in the grounds of the University of Canterbury.

Aggregate rays are visible on the outside of plants as longitudinal flutes in the bark (Figure 2.1). These flutes are most prominent on straight stemmed saplings with stem diameters of approximately 2-3 cm and greater, but are also frequently visible on large trees. In such cases the flutes are much broader and deeper, and accompanied by a group of aggregate rays. Figure 2.2 shows such a group associated with a large flute in a young tree of *N. solandri* var. *cliffortioides*. Aggregate rays, however, are not always associated with these flutes and also occur singly in other areas. Flutes are not usually visible on seedling material or on juvenile tissue from mature branches, though they are a feature of the mature tissue of mature branches. Some saplings and small branches of mature trees showed no signs of fluting but a simple section in the field, with a knife or razor blade, usually revealed the presence of aggregate rays. Occasionally it was possible to find a tree where most small branches (approximately 1 cm in diameter) appeared to have aggregate rays present, but some branches were almost totally devoid of aggregate rays toward their bases, with aggregate rays beginning to appear further up the branches. Such branches appear to have arisen on the main stem from previously suppressed lateral buds.

2.4.2. Aggregate ray morphology

The aggregate rays exhibited by samples of *Casuarina* sp., *Dracophyllum urvilleanum, Fagus sylvatica* and *Quercus coccinia* are high and broad multiseriate rays (Figure 2.3.a). These rays are occasionally dissected[4] by fibres. Samples of *Fagus sylvatica* also show further dissections of multiseriate rays into smaller units resulting in a continuum from dissected multiseriate rays to dissected biseriate rays and uniseriate rays (Figure 2.3.b). The definition of an aggregate ray (IAWA

4 Dissection and fusion cannot be confirmed without serial sectioning, therefore, the terms dissected and fused have been used here to convey the appearance of the rays. Often it will appear as though a ray has been split in two by an axial element and become dissected. At other times it may appear that 2 uniseriates have become fused by the loss of an intermediary axial element.

Figure 2.1

Mature trunk of *Nothofagus solandri* var. *cliffortioides*

Prominent longitudinal flutes (F) are a conspicuous external feature.

Figure 2.2

Stem of *Nothofagus solandri* var. *cliffortioides* (TS)

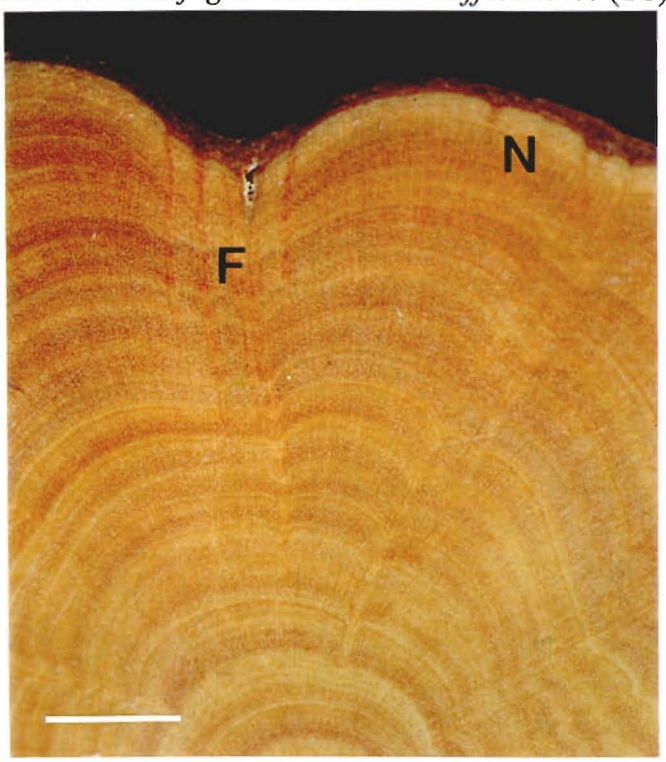

A group of aggregate rays associated with a flute (F), with other, usually single, aggregate rays in non-fluted regions (N) [scale bar = 5 mm]

Figure 2.3

High and wide, compound like, aggregate rays

a. Very high and wide multiseriate ray of *Quercus coccinia,* with very few dissections (TLS). [scale bar = 200 μm].
b. A collection of high and wide multiseriate rays of *Fagus sylvatica* where dissections have resulted in a number of rays of various sizes distributed throughout the tissue (TLS). [scale same as Figure 2.3.a].
c. A TS of *F. sylvatica* where the aggregate ray is represented by a very wide multiseriate ray. [scale bar = 100 μm].
d. High and wide multiseriate rays of *Q. ilex* where there are a number of axial elements included within the body of the ray (TLS). [scale same as Figure 2.3.a]
e. Multiseriate ray of *Q. palustris* showing dissections (D) at the tails, resulting in a close association of multiseriate, biseriate and uniseriate rays in this position (TLS). [scale same as Figure 2.3.a].
f. A TS of *Q. palustris* where the aggregate ray is represented by a broad multiseriate ray with closely associated uniseriate rays (U). [scale same as 2.3.c].

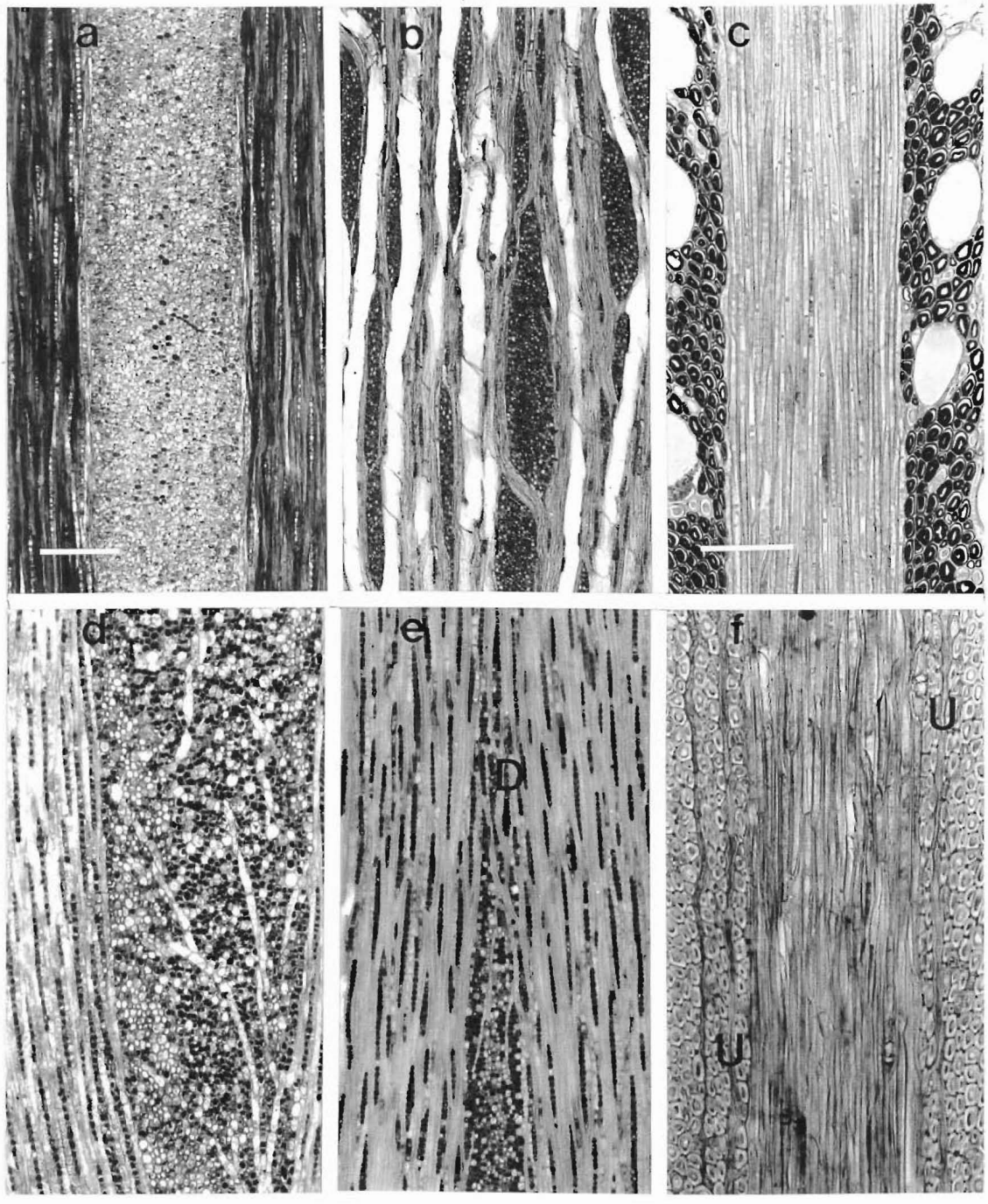
a
b
c
d
e
D
f
U
U

Committee 1989) is difficult in this situation, there being a gradation from large multiseriate rays to uniseriate rays. The rays of this type are best characterised in TS where the aggregate rays are defined by the broad multiseriate ray (Figure 2.3.c) and the dissections are not visible. In TLS (Figure 2.3.b) the situation is confused by these dissections and the compound nature is harder to define. Hence the sample of *F. sylvatica* is defined by the compound ray. The aggregate rays of samples of *Q. coccinia* and *D. urvilleanum* are also defined by the compound ray, but here the dissections by axial elements tend to be confined to the sides of the rays, so that in TS they appear as large multiseriate rays, often with associated uniseriate rays

The aggregate rays shown in the sample of *Q. ilex* are also defined in TS by what appears to be a compound ray. In TLS, however, it can be seen there are inclusions of what appear to be modified axial elements, within the broad multiseriate ray (Figure 2.3.d). Most of these modified axial elements are isolated from each other and therefore tend not to break up the multiseriate ray into smaller biseriate and uniseriate portions. The aggregate rays in samples of *D. traversii* and *Q. palustris* are similar to those in the *Casuarina* sp., *Dracophyllum urvilleanum, Fagus sylvatica* and *Quercus coccinia* samples in that there are areas of broad multiseriate rays, but other rays show a far greater degree of dissection, especially at the sides and tails (Figure 2.3.e). Unlike the dissections in the *F. sylvatica* sample, which seem to result in an even distribution of rays throughout the wood, the dissections shown by these samples result in multiseriate, biseriate and uniseriate rays in relatively close association. These examples are defined in TS (Figure 2.3.f) by the broad compound ray and a close association of uniseriate, biseriate and multiseriate rays (the aggregate ray according to the definition).

The samples of *D. filifolium, D. longifolium, D. pronum, D. subulatum* and *D. uniflorum* all have similar morphologies to the samples of *D. traversii* and *Q. palustris*, but there is a greater degree of dissection of the ray into smaller parts, although the overall structure is still reasonably well defined (Figure 2.4.a).

An even greater degree of dissection is shown in the samples of *Castanopsis accuminatissima* and *Lithocarpus perclusa*. The area of the aggregate ray is not well defined in TLS, and it is difficult to judge where one aggregate ray ends and another begins (Figure 2.4.b). As with the samples of *D. filifolium, D. longifolium, D. pronum, D. subulatum* and *D. uniflorum* above, these rays are represented in TS by multiseriate rays with associated uniseriate or biseriate rays (Figure 2.4.c).

Figure 2.4

Aggregate rays showing a high degree of 'dissections'

[scale bar = 100 μm]
a. A high aggregate ray of *Dracophyllum longifolium* dissected into a number of segments by axial elements (TLS).
b. Aggregate ray in *Castanopsis accuminatissima* represented by a collection of multiseriate, triseriate, biseriate and uniseriate rays, separated by axial (often deformed) elements. The boundaries of the rays are very difficult to determine (TLS).
c. A TS of *C. accuminatissima* with the aggregate ray represented by an association of multiseriate (M), triseriate (T) and uniseriate (U) rays.

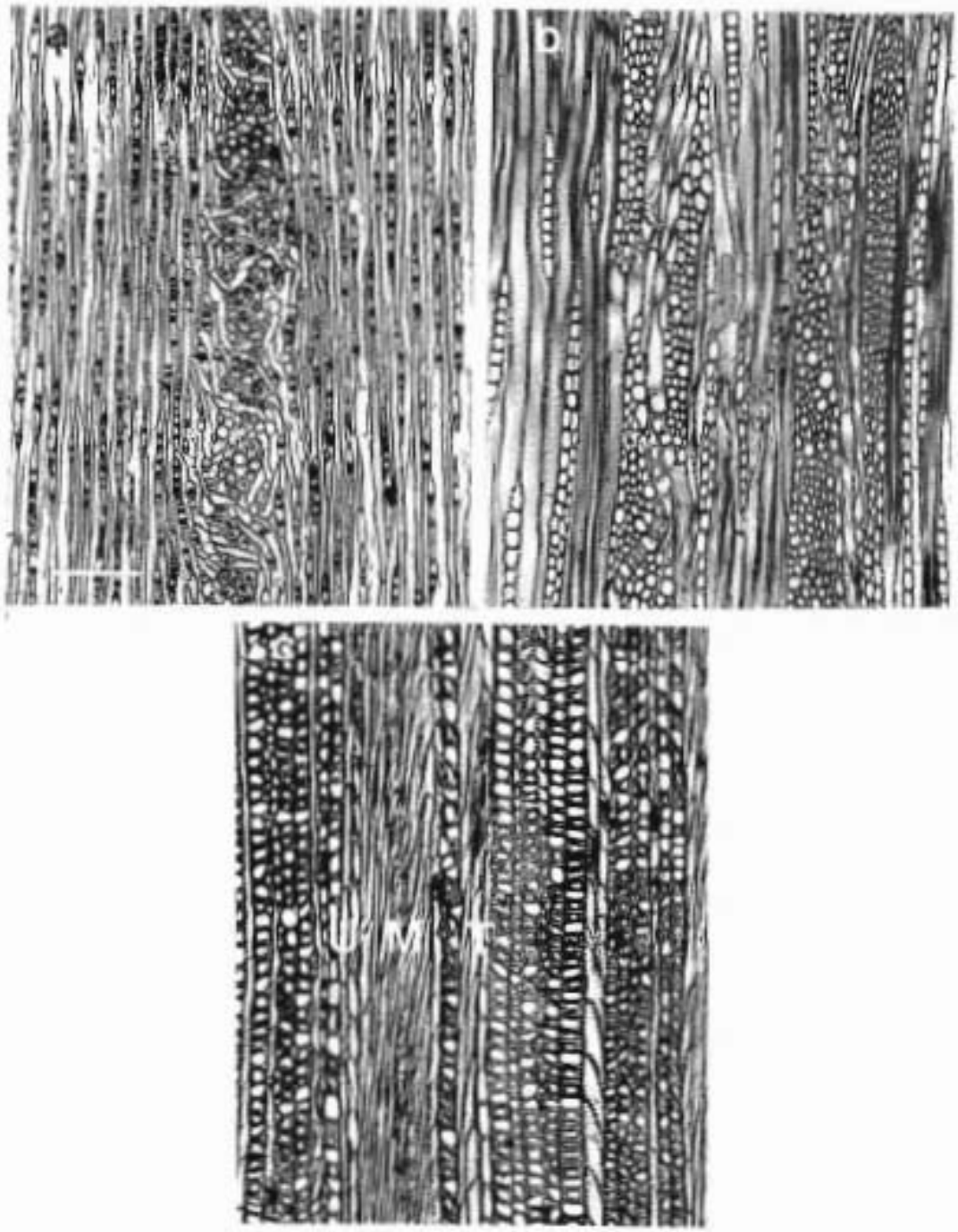
a
b
c

Figure 2.5

Highly 'dissected' aggregate rays

a. An aggregate ray in *Alnus glutinosa* flanked by vessels (V). Here the aggregate ray is represented by closely associated uniseriate, and occasionally biseriate, rays (TLS) [scale bar = 200 μm].
b. A TS of the aggregate ray of *A. glutinosa* with an associated indentation in the growth ring. [scale bar = 100 μm].

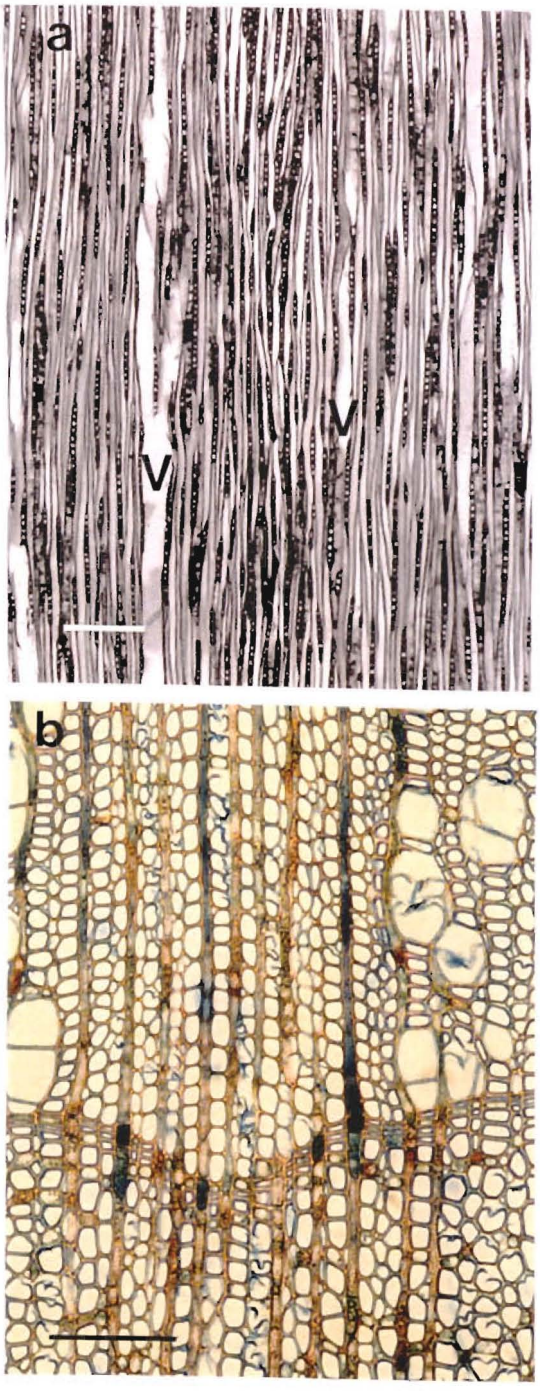
a
V
V
b

The greatest degree of dissection occurred in samples of *Alnus glutinosa, Carpinus* sp., *Corylus* sp., *Nothofagus fusca, N. solandri* var. *cliffortioides, N. solandri* var. *solandri* and *N. truncata*. No discrete aggregate ray structure was displayed in any of these samples. Instead aggregate rays consist of a reasonably ill-defined area of small rays, closely associated, devoid of vessels (Figure 2.5.a). Biseriate rays, or uniseriate rays with biseriate portions are occasionally present, with some showing signs of fusion. Aggregate rays were very difficult to distinguish in TLS for samples of *Carpinus* sp., and *Corylus* sp., In TS they tend to appear more as areas between aggregations of vessels than discrete ray structures. Aggregate rays of this type are defined in TS by groups of closely associated uniseriate rays usually devoid of vessels and usually, though not always, associated with indentations in the growth ring (Figure 2.5.b).

2.4.3. Aggregate rays of *Nothofagus*

The aggregate rays of *Nothofagus* are essentially vesselless zones extending radially and longitudinally in the wood. They are usually more readily discernible in TS than in longitudinal section, where owing to the presence of occasional vessels, they may be very difficult to see, unless one is already aware that an aggregate ray is, indeed, in section. Other sections may show greater degrees of 'aggregation' with uniseriate rays in association with septate fibres or axial parenchyma, or uniseriate rays in association with biseriate rays or having biseriate portions (Figure 2.6). Some individual rays may also be referred to as 'interconnected rays', a term coined by Carlquist (1988) to replace zusammengesetzt, a German term used to describe aggregate rays as a whole. Aggregate rays may rarely be almost compound in nature, consisting of a mass of parenchyma. Such areas are usually extensive longitudinally but of limited radial extent, and may have the appearance of small pith flecks (Figure 2.7.a). These features usually occur in the concave of the flutes (Figure 2.7.b), and not at the sides, and are within the body of the aggregate ray and not giving rise to it. They are almost certainly part of the aggregate ray structure of *Nothofagus* and not merely artefacts caused by insect injury or other wounding. They will henceforth be referred to as disruption zones.

Disruption zones arise rapidly, as evidenced in RLS, by the dissection of axial elements (Figure 2.7.c). The divisions giving rise to these dissections appear to be occurring in the cambial initial as they are able to be traced through the subsequent wood for some distance. Each dissection of the former axial element may then elongate independently and assume a deformed or irregular shape with some

Figure 2.6

Aggregate rays in *Nothofagus* showing varying signs of aggregation (TLS)

[scale bar = 200 μm]

a. Aggregate ray in *N. solandri* var. *cliffortioides* consisting entirely of uniseriate rays.

b. Aggregate ray in *N. solandri* var. *cliffortioides* with some uniseriate rays having biseriate portions (B).

c. Aggregate ray in *N. truncata* consisting mostly of uniseriate rays, but also septate fibres and some axial parenchyma (A).

d. Aggregate ray in *N. solandri* var. *cliffortioides* consisting almost solely of biseriate and triseriate rays, there is also some axial parenchyma. A vessel (V) is also incorporated into the aggregate ray structure.

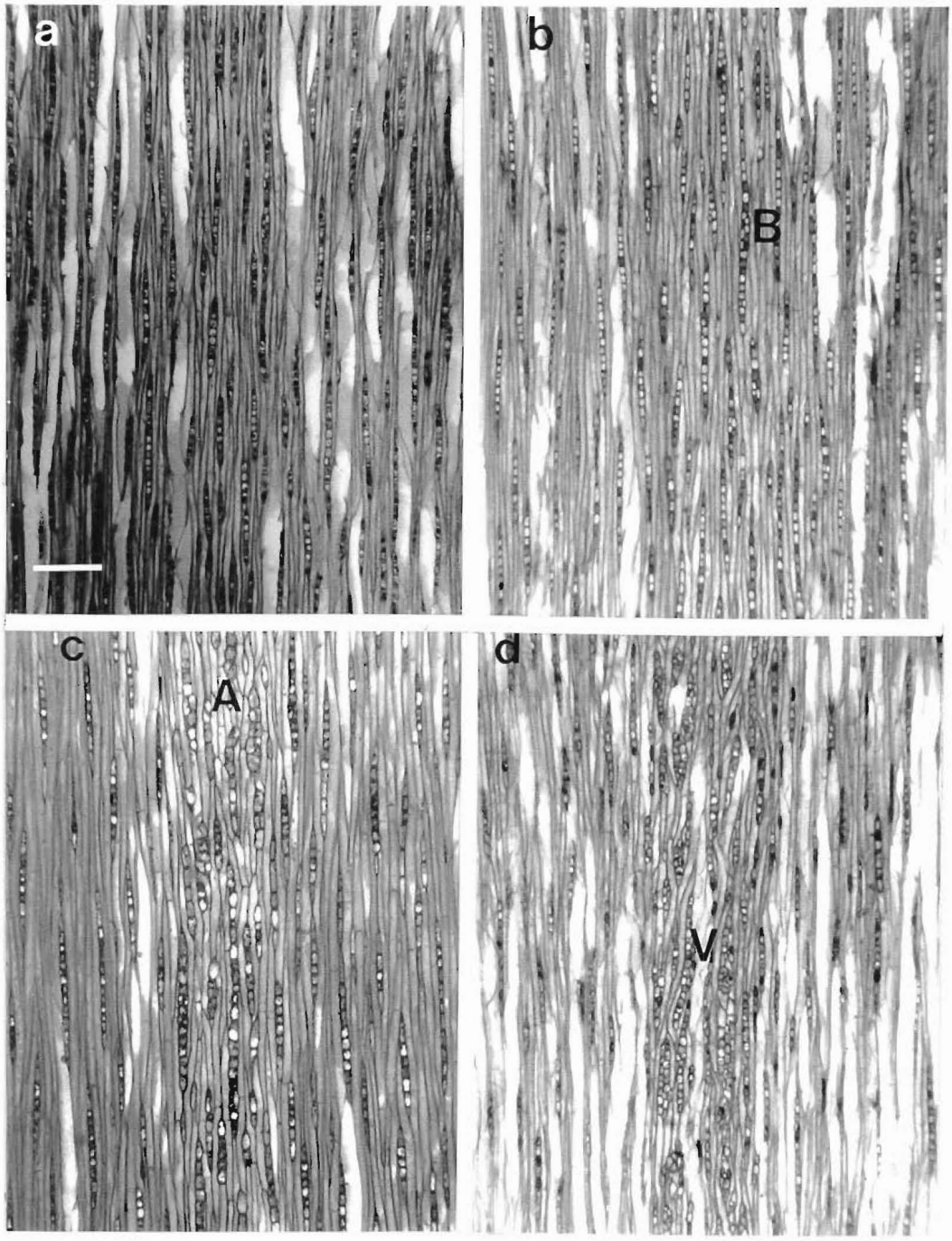
a
b
B
c
A
d
V

Figure 2.7

Disruption zones in the aggregate rays of *Nothofagus*

a. TLS of *N. solandri* var. *cliffortioides*. The disruption zone is nearly compound in nature, consisting mainly of parenchyma with some axial parenchyma. [scale bar = 200 μm].
b. TS of *N. truncata*. The disruption zone (D) is located in the centre of a flute. [scale bar = 50 μm].
c. RLS of *N. truncata* where 2 disruption zones are present. (P) indicates the direction towards the pith, and (C) indicates the direction to the cambium. The disruptions arise rapidly and dissipate more slowly with cambial development. [scale same as Figure 2.7.a].
d. TLS of *N. solandri* var. *cliffortioides*. (I) indicates an apparent invagination of cells. [scale bar = 20 μm].

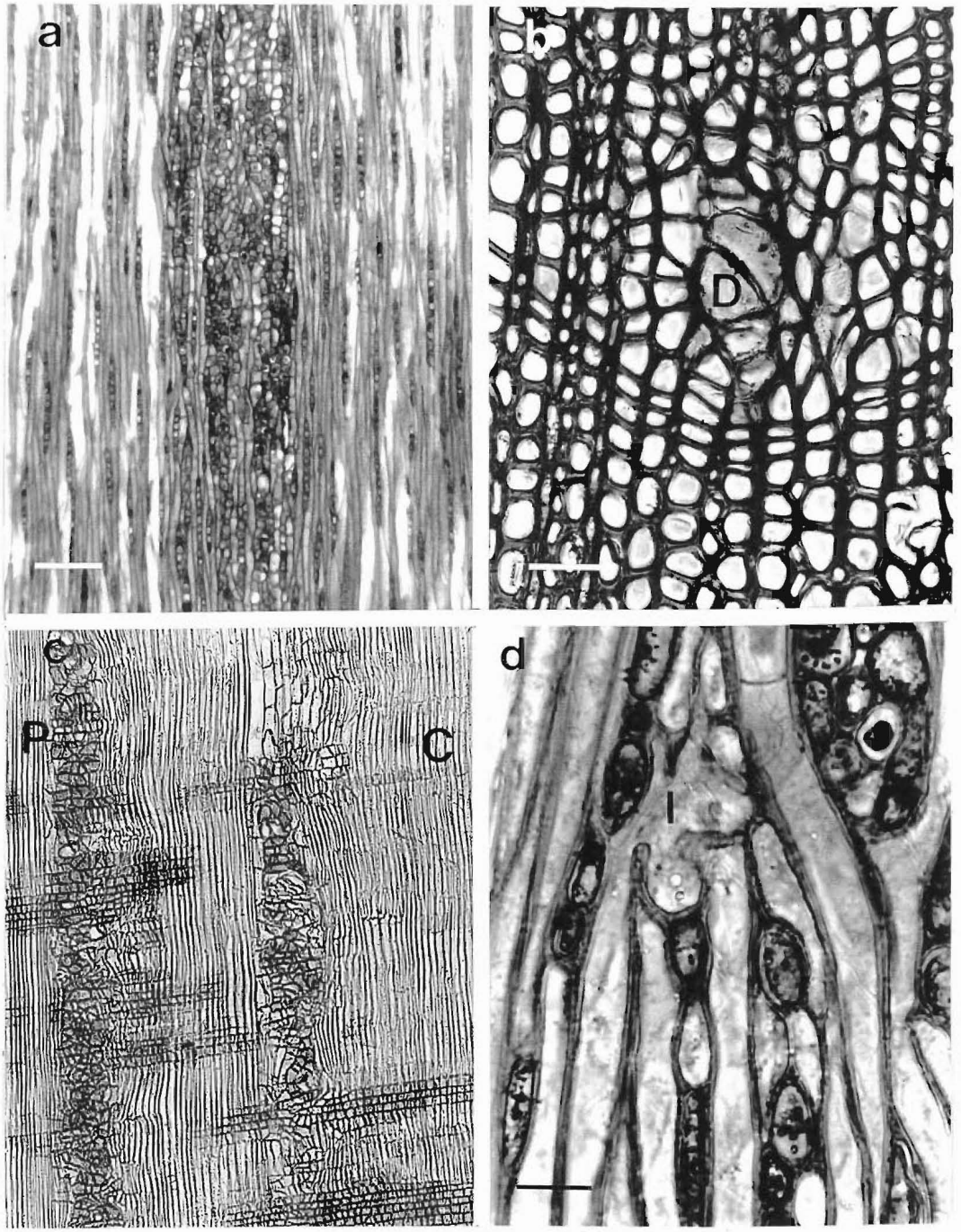
a
b
D
c
P
C
d
I

cells appearing to evaginate into others (Figure 2.7.d). These deformed axial elements may be heavily pitted with usually simple pits similar to those in normal ray cells (Figure 2.8). The walls of the axial elements may be variable, with some elements having secondary walls that appear to thicker than those in others. No attempt was made to measure the relative thickness of cell walls or their component layers.

Figures 2.9.a to 2.9.g depict serial tangential sections through a disruption zone. Figures 2.9.a displays the situation immediately prior to the disruption. There are five rays (numbered 1 to 5), and six axial elements of interest (A-F). Figure 2.9.b is 25 μ m further out, rays (2) and (3) have merged as have (4) and (5). As a result axial element (A) has been greatly reduced in length and has become segmented, probably by transverse divisions in the cambium prior to the xylem mother cell stage. The cell marked (Y) has arisen as a result of a transverse division of (D) at the xylem mother cell stage as it only persists for a few sections. The cell marked (X) has arisen by a transverse division of either (B) or (E) prior to the mother cell stage. Further sections show continued dissections of the remnants of fusiform (A) and the conversion of axial element tips to ray cells (element (E) Figure 2.9.c). Occasionally a ray cell will be lost and a neighbour will enlarge to replace it. In such a case it is difficult to establish which cell has survived. In Figure 2.9.d the hatched cell was either an enlarged cell of ray (5) or an enlarged segment of element (A), in Figure 2.9.e the same situation exists this time with ray (2). Figure 2.9.d shows a portion of element (C) (arrowed) that appears discontinuous with the remainder of the element. This, however, is probably due to the irregular shape of the element tip, with the remainder of the element being out of section. Most of the remnants of element (A) are lost between the surrounding elements (Figure 2.9.f), and finally replaced by element (C) (Figure 2.9.g). Ray (2) is only weakly represented and will eventually be lost by coalescing into ray (3) (Figure 2.9.g). Overall there was a reduction of fusiform cells by transverse division and the gradual loss of the initials from the cambium. There was also a reduction of the uniseriate rays by the merging of neighbouring rays to form biseriate rays. These tended to be reduced, however, by the loss of initials, back to the uniseriate condition.

The root material of *N. solandri* var. *cliffortioides* examined, has aggregate rays similar to those of the stem material (Figure 2.10), with aggregate rays radiating out from the centre of the root (Figure 2.10.a). No disruption zones are evident but the root samples are much younger than the stem sections. Large multiseriate rays are often associated with the aggregate rays in the roots (Figure 2.10.b),

Figure 2.8

Simple pitting in *Nothofagus truncata* (TS)

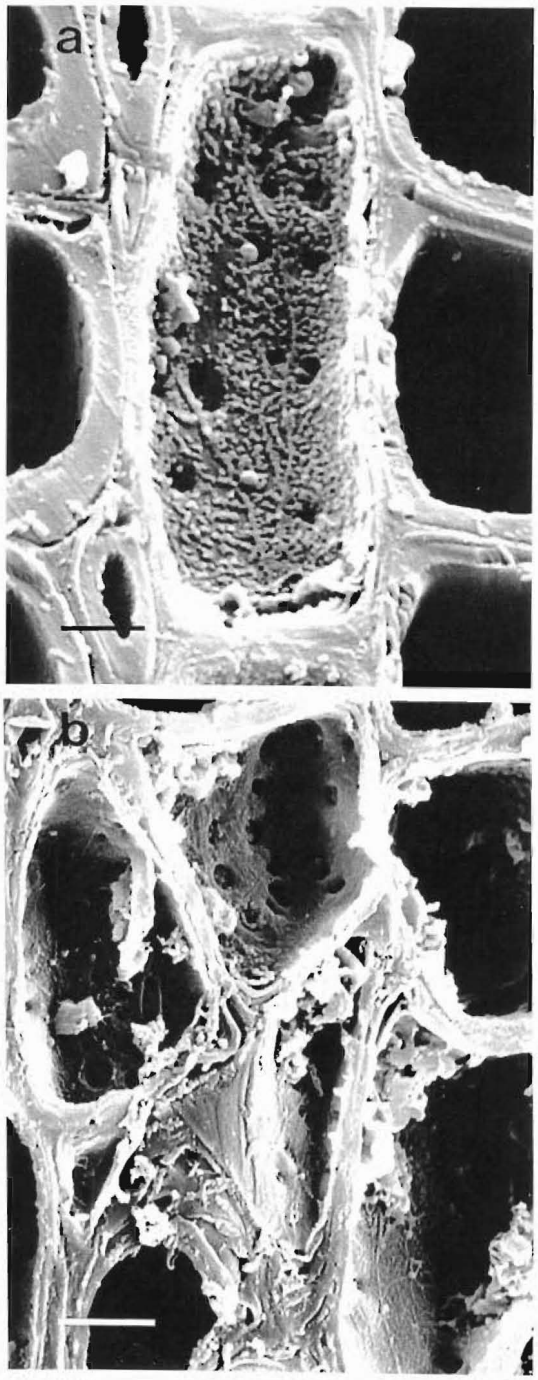

a. Ray cells of normal wood. [scale bar = 5 μm].
b. Deformed axials of a disruption zone. [scale bar = 10 μm].

Figure 2.9

Sequential sections through a disruption zone in *Nothofagus solandri* var. *cliffortioides* (TLS)

The derivatives of 6 fusiform initials (A to F) are labelled, as are 5 rays (1 to 5). See the text for details. [scale bar = 40 μm].

a. Immediately prior to the disruption zone.
b. Figure 2.9.a plus 25 μm.
c. Figure 2.9.a plus 50 μm.
d. Figure 2.9.a plus 75 μm.
e. Figure 2.9.a plus 100 μm.
f. Figure 2.9.a plus 250 μm.
g. Figure 2.9.a plus 350 μm.

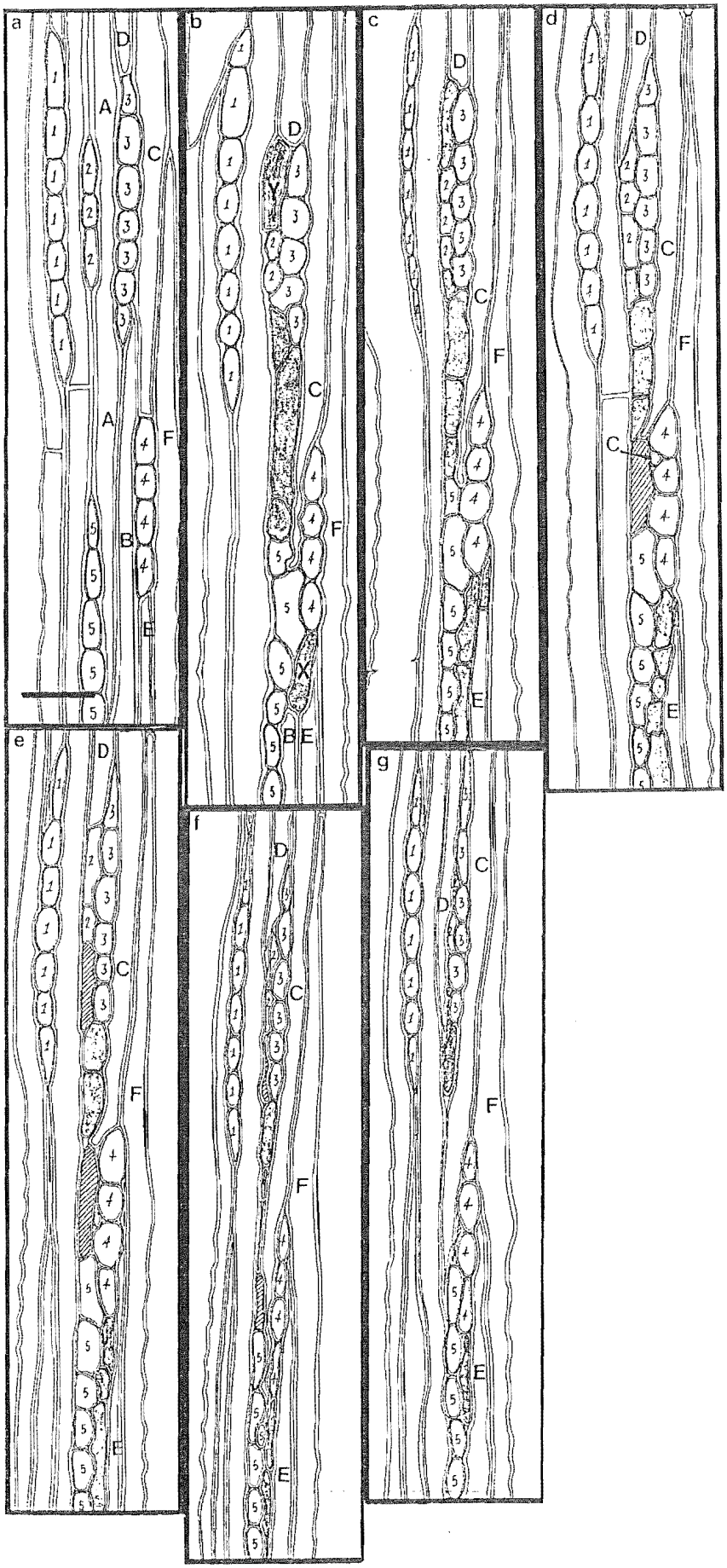
a
b
c
d
e
f
g
A
B
C
D
E
F
X
Y

Figure 2.10

Root material of *Nothofagus solandri* var. *cliffortioides*

a. TS showing a prominent aggregate ray (A) radiating out from the centre of the root. [scale bar = 400 μm].
b. TLS showing a large multiseriate ray (M) associated with an aggregate ray (A). [scale bar = 200 μm].
c. TLS showing a large multiseriate ray (M) with no associated aggregate ray. [scale bar = 200 μm].
d. RLS showing an aggregate ray (A) in association with a lateral root (L). [scale bar = 400 μm].

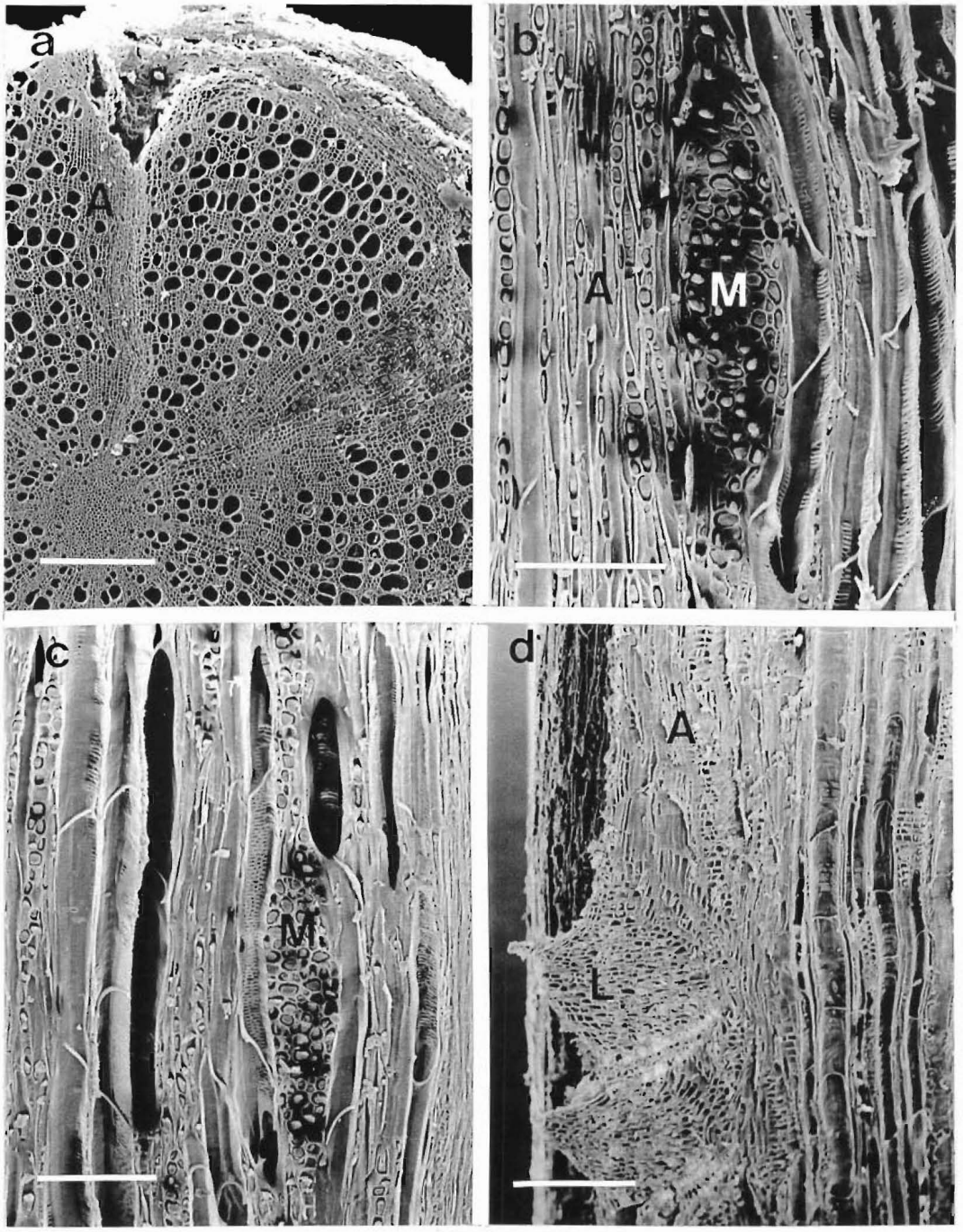
a
A
b
A
M
c
M
d
A
L

most aggregate rays contain multiseriate rays though not all of the multiseriate rays are associated with aggregate rays (Figure 2.10.c). These large multiseriate rays seem similar to the abnormal rays described by (Bhat 1980, 1983, Fink 1982 and Donaldson 1982) which have been attributed to adventitious root primordia. Some of the multiseriate rays and aggregate rays are also definitely related to lateral roots (Figure 2.10.d).

Staining for phenolics and polysaccharides showed no significant differences between the cells of the disruption zones, other ray cells within aggregate rays, or the ray cells in the remainder of the wood.

Stem flutes are usually accompanied by bundles of sclereids in the phloem. The degree to which sclereids are formed seems to depend on the magnitude of the flute, very shallow flutes may lack sclereids but they are usually prominent in deep flutes. Staining with aniline blue indicated that sieve tubes (as marked by the presence of callose) appear to be largely absent from the fluted zones, but are conspicuous in the non-fluted areas (Figure 2.11).

2.5. Discussion

It is clear that the range of structures considered to be aggregate rays is quite broad, ranging from large multiseriate rays, here represented by *Fagus*, to closely associated uniseriate rays of *Nothofagus*. It was with reference to the large rays of *Quercus* (compound rays) that the term aggregate ray was first used (Bailey 1911). It is ironic, therefore, that such compound rays are technically not covered by the current, accepted definition of the aggregate ray (IAWA 1989)[5], as they are definitely not 'a number of individual rays' but are, instead, essentially a single large mass of radial parenchyma. Such rays can only be included in this definition if it is accepted that they have arisen either phylogenetically or ontogenetically by the fusion of uniseriate rays, and thus represent *sensu lato* a group of narrow rays. Although this is currently the most accepted theory, evidence will be presented in Chapter 3 to show that this may be an over simplification of the situation.

---

5 'a number of individual rays so closely associated with one another that they appear macroscopically as a single large ray. The individual rays are separated by axial elements...'.

Figure 2.11

Stem of *Nothofagus solandri* var. *cliffortioides* stained for the presence of callose with aniline blue and examined under fluorescent light (TS)

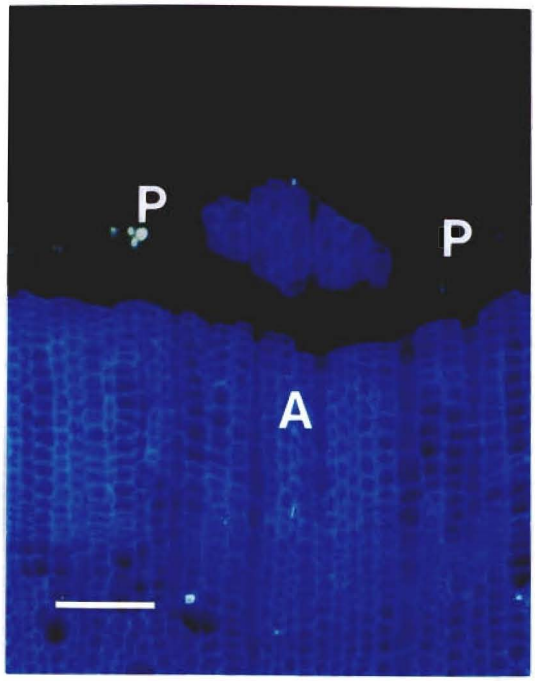

Sieve tubes marked by the presence of callose (P). Aggregate ray (A).

Three main types of aggregate ray may be defined on the basis of this study:

Type A. The broad and high rays commonly designated as compound, with only minimal signs of dissections or fusions. These are found in *Casuarina* sp, *Dracophyllum traversii, D. urvilleanum, Fagus sylvatica, Quercus coccinia, Q. ilex* and *Q. palustris* (Figure 2.3.a);

Type B. Closely associated uniseriate, biseriate and multiseriate rays. These are found in *Castanopsis accuminatissima, D. filifolium, D. pronum, D. subulatum, D. uniflorum* and *Lithocarpus perclusa* (Figure 2.4.a);

Type C. Morphologically indistinct zones consisting of closely associated uniseriate or biseriate rays, marked by the general absence of vessels. These are found in *Alnus glutinosa, Carpinus betulus*[6], *Corylus avellana, Nothofagus fusca, N. solandri* var. *cliffortioides, N. solandri* var. *solandri* and *N. truncata* (Figure 2.5.a).

It has been pointed out by Metcalfe and Chalk (1983), that attempting to designate discrete types within the continuum of aggregate ray structures is problematical, as a range of structures may be present in the one genus. This is reinforced by examples of *Dracophyllum* with rays of type A and B and more dramatically *Nothofagus*, where the disruption zones also present varied morphologies. This is really only a problem , however, in defining the aggregate rays in a designated genus, species or even individual sample. This study, however, is not a taxonomic one, and such considerations need not be of too much concern. Carlquist (1988) suggests that the individual ray components of an aggregate ray may be separated by libriform fibres, but where a vessel is incorporated within the confines of an aggregate ray then two aggregate rays would be present. This creates a problem with respect to the rays of type B, and in particular, type C. In these types of aggregate rays, vessels are often present sporadically throughout the structure. Therefore if Carlquist's reasoning is followed, one or a number, of aggregate rays may be present depending on the position of the section.

Since the term 'aggregate ray' has been in use for so long it would seem unwise to change it, even with its implied phylogeny and ontogeny. However, the existence of distinct, if broad ray types within the continuum of aggregate ray structure has been

---

6 Although the sample of *Carpinus betulus* examined showed no obvious aggregation of uniseriate rays into biseriates or higher levels, Carlquist (1988, figure 6.12.1, page 200) clearly shows this aggregation for *Carpinus caroliniana.*

recognised in this work. Those aggregate rays of type A could be referred to as '**entire aggregate rays**' as they appear to be largely undissected by axial elements. The aggregate rays of type B could be referred to as '**fasciculate aggregate rays**' as they appear as 'bundles' of closely associated rays. Finally the aggregate rays of type C could be referred to as '**diffuse aggregate rays**' as they are ill-defined zones often not recognised so much by the presence of rays as by the absence of vessels. Here the word 'diffuse' is used according to its dictionary meaning which is 'spread out, not concentrated, not concise' and should not be confused with the diffuse ray of Jeffrey (1917), which is an compound ray in the process of dissection. The intent here has been to remove phylogeny from the terminology and represent the different structures solely on their morphologies.

Another problem with the terminology is the use of the word 'ray' itself. According to the Committee on Nomenclature IAWA (1964) a ray is defined as:

> A ribbon-like aggregate of cells extending radially in the xylem and phloem.

There is generally little trouble in recognising the structures of type A within this definition as they can clearly be recognised as structures that fit the common concept of a well defined uniseriate, biseriate or multiseriate ray structure. The problem arises, however, with the 'rays' of type B and especially type C. Here the aggregate rays are not discrete structures but consist of a number of closely associated individual rays. It could, therefore, be argued that the use of the word 'ray' is misleading and the term 'aggregate ray' should be replaced with a descriptive term such as 'aggregation of rays' or 'vesselless zone'. In a number of circumstances such an approach is perfectly valid, and even necessary, as such terminology defines the morphology intrinsic to these structures. There is, however, nothing in the definition of the 'ray', as cited above, to preclude the inclusion of the aggregate ray within its boundaries. Even the requirement that a ray be represented in the phloem is met by aggregate rays of the type in *Nothofagus*. Even putting the semantics of the definition aside, aggregate rays must be regarded as rays as this term aids in the definition of their gross structure, When examined at low magnification[7] aggregate rays appear to radiate from the centre of the stem or at least have a radial orientation. Also any attempts to exclude types B and C from the definition of the ray would effectively isolate them from type A, therefore resulting in disunity within the continuum.

---

7 This is the situation from which the definition of the aggregate ray (IAWA Committee 1989) is to be applied.

The aggregate rays of *Nothofagus* present an interesting case, especially with reference to the disruption zones. The disruption zones have a relatively consistent ontogeny, arising from apparently spontaneous transverse divisions in the cambium. This is followed by disorganised elongation of the daughter initials. The gradual resumption of normal cambial behaviour leads to the reversion of multiseriate rays back to the uniseriate condition. Disruption zones always occur within the centre of the flutes, and can be readily discerned from wounds caused by external factors which tend not to be as limited in tangential extent. They are, however, generally similar to induced wounds (Kuroda and Shimaji 1985) which also had transverse divisions of fusiform initials and xylem mother cells followed by the resumption of normal activity. The indications are, that the disruption zones are indeed wounds, but only in the sense that they represent an abnormal development of the fusiform initials and derivatives induced within the aggregate ray by either the aggregate ray itself, or by the fluted nature of the growth ring associated with the aggregate ray.

The sclerotic bundles present in the bark of *Nothofagus* associated with the aggregate rays, have also been described for other plants with aggregate rays (Kucera, Bosshard and Katz 1980, Holdheide 1954). It has been suggested they have a structural significance by Kucera *et al* (1980) due to the presence of the aggregate rays on one hand, and the thinness of the bark on the other. The functional significance of these sclereids in *Nothofagus* was not investigated.

The aggregate rays in the root wood of *Nothofagus* are also of some interest. It is often the case that roots are neglected in the study of wood anatomy and this is also true for this study. The ontogeny of the aggregate rays in relation to the leaves will be investigated in a subsequent chapter. The ontogeny of aggregate rays in relation to lateral roots also merits investigation due to the different modes of origin of lateral roots and leaves.

CHAPTER 3

THE ONTOGENY AND 3-DIMENSIONAL ASSOCIATIONS OF AGGREGATE RAYS

3.1. INTRODUCTION

Structures that would later be referred to as aggregate rays (Bailey 1911) were first described by Eames (1910). He believed that the broad multiseriate rays characteristic of many species of *Quercus* had evolved by the fusion of numerous uniseriate rays. This view was subsequently supported by Bailey (1910a, 1910b, 1911, 1912). This conclusion was based on putative fossil oak wood with clusters of small rays representing the broad ray, characteristic of present day species. These clusters of smaller rays in the fossil material, and similar structures in living genera, were referred to as false rays, and the broad rays of *Quercus* as compound rays. Bailey (1911, 1912) and Eames (1911) traced aggregate rays back to the leaf-trace suggesting they had evolved as a large storage system, both above and below the leaf-trace, in a response to a cooling climate. Thompson (1911) believed that a return to warmer climates had resulted in the dissection of these aggregate rays and the formation of smaller multiseriate rays.

The early papers of both Bailey and Eames placed considerable phylogenetic significance on the presence of aggregate rays, believing the uniseriate ray to be the primitive ray condition in the dicotyledons, and multiseriate rays an advanced feature. Groom (1911), however, believed it was impossible to determine whether the broad ray of *Quercus* was primitive or advanced, there being evidence for both aggregation and dissection in the formation of aggregate rays. He suggested the presence of aggregate rays had a far greater significance physiologically than phylogenetically. Bailey (1912), although at first hostile to the suggestions of Groom (1911), changed his stance later on (Bailey and Sinnott 1914), where it was pointed out that:

> ....'multiseriate' rays are found in middle and upper cretaceous dicotyledons, although according to the 'aggregate' ray hypothesis they are the most recent development of the angiosperm ray. If 'aggregate' and 'compound' rays originated for purposes of storing the assimilates descending from the persistent leaves of mesozoic angiosperms, and were later replaced by 'multiseriate' rays as an adaptation to the advent of a severe winter season and the consequent acquirement of the

> deciduous habit by the leaves, we should hardly expect to find the 'multiseriate' ray well developed in cretaceous angiosperms or in families which have lived in moist, warm, tropical conditions since ancient times.

It was Kribs (1935), however, who showed that heterogeneous multiseriate rays together with uniseriate rays are the primitive ray condition in the angiosperms, and that the compound ray is 'merely an unusually wide multiseriate ray', and that the 'so-called aggregate ray is a specialisation which occurs sporadically'. Barghoorn (1940, 1941) carried this further, suggesting the aggregate ray was a large multiseriate ray in the process of dissection. Studies on the Betulaceae (Hoar 1916), *Casuarina* (Moseley 1948) and the Fagaceae (Shimaji 1954a, 1954b), however, support the opposite view, that aggregate rays are built-up of smaller rays. Moseley (1948) showed convincing figures (figures 12 and 27 of Moseley 1948) demonstrating the formation of aggregate rays at some distance from the pith, above the departure of the leaf-trace, apparently as the result of the fusion of uniseriate rays. According to Carlquist (1988) the latter 'synthetic' view has been widely accepted but with much reduced phylogenetic implications.

Aggregate rays occur in 4 of the 5 taxa of *Nothofagus* in New Zealand (Middleton 1987). In order to investigate the lack of aggregate rays in the fifth taxon (*N. menziesii)* it was decided to investigate the ontogeny of the aggregate rays in *Nothofagus* and how it compared with aggregate ray ontogeny in *Fagus sylvatica*, *Dracophyllum pronum* and *D. uniflorum.*

The aggregate rays of *Nothofagus* are usually associated with prominent fluting on the stem (Chapter 2). Newman (1956) noted an association of the fluting on stems with branch bases for *Pinus taeda.* He suggested the fluting had been caused by a suppression of lateral growth in the vicinity of the branch base, possibly due to an infection factor. Aggregate ray formation has also been attributed to disruptions in normal cambial development, there being some evidence that aggregate rays can arise from pith flecks (Bhat 1980, 1983, Noskowiak 1978) and adventitious root primordia (Donaldson 1982).

To study the possible relationship of the aggregate ray in *Nothofagus* with branching and/or wounding, it was also decided to investigate the 3-dimensional nature of the aggregate ray assemblage, and if the flutes on mature trees could be traced back to their supposed origin as aggregate rays at the leaf-trace. It was also decided to investigate the possible role of wounding in the formation of aggregate rays.

3.2. Materials and Methods

3.2.1. The aggregate ray assemblage of *N. solandri* var. *cliffortioides*

A single sample from a single specimen was examined for this section. The specimen was a mature straight stemmed tree of *Nothofagus solandri* var. *cliffortioides* collected from the Cass region of the Southern Alps. The sample was an approximately 400 mm long section of stem material, with three prominent branches and was approximately 35 mm in diameter.

3.2.1.1. Disking

A single longitudinal reference line was drawn extending the entire length of the sample. This line was as straight as possible, and in practice followed a flute. The sample was then cut into transverse disks 5 mm thick with a band-saw. Individual disks were then numbered and polished with an orbital sander. The resulting disks had a mean thickness of 4.7 mm. A light oil ('3 in 1') was then applied to the surface and allowed to soak into the wood.

3.2.1.2. Examination of the aggregate ray assemblage

Disks were photographed onto colour slides and images projected on to paper using a photographic enlarger. Three measurements were made for each aggregate ray on each disk (each disk was given its own identifier = Disk Number). The measurements were:

The radial extent of the aggregate ray as a percentage of the distance from the cambium to the pith (% Length);

The angle the aggregate ray, where it reached the cambium, formed with the reference line (Outside Angle);

The angle the inner extent of the aggregate ray formed with the reference line (Inside Angle).

Measurements were made as in Figure 3.1. If an aggregate ray was present in the wood but failed to extend all the way out to the cambium then no % Length or Outside Angle could be calculated for that ray and, therefore, no measurements were recorded. By plotting Disk Number against Outside Angle on a XY graph and carefully following individual aggregate rays from disk to disk (based not only on the position of the rays, but also on the size, shape and associations of rays when referring

Figure 3.1

Measurements made for the examination of the aggregate ray assemblage of *Nothofagus solandri* var. *cliffortioides* (TS)

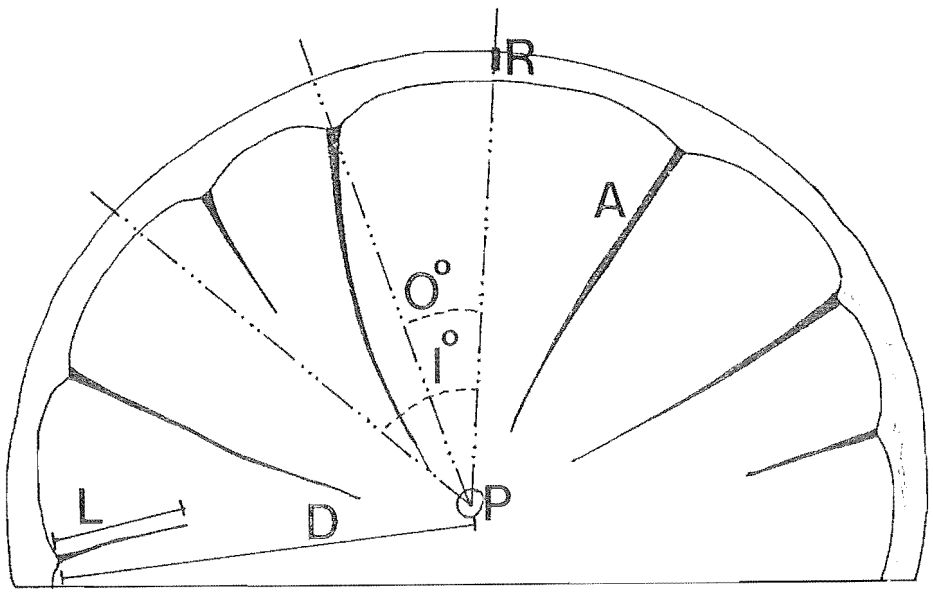

Reference line (R). Pith (P). Aggregate ray (A). Length of aggregate ray (L). Distance to pith (D). Outside angle (O^o). Inside angle (I^o). The percentage length of the aggregate ray is calculated as (L/D)*100 (to the nearest 10%)

back to the photographic slides) the longitudinal extent and connections between aggregate rays could be seen.

3.2.1.3. Three-Dimensional nature of the aggregate ray assemblage

The data from the above measurements were stored in two files. One file contained the variables Disk Number, % Length of aggregate ray, and Outside Angle The other file contained Disk Number, % Length of aggregate ray, and Inside Angle. Both files were treated in the following manner:

For each disk 90 sectors were created each comprising 4 degrees of circumference (Eg. 1-4°, 5-8°...357-360°). This was done solely for ease of data manipulation. Fifty disks had been cut, if each of these disks had 360 observations (the lack of an aggregate ray would have been an observation) then the total data set would have consisted of 18,000 observations, well beyond the capacity of a standard spreadsheet;

Individual rays were assigned to their appropriate sector for each disk;

The average % Length (to the nearest 10%) of aggregate ray was calculated for each sector;

The sectors were then divided into 3 groups depending on the average % Length of the aggregate rays.

> Group A = sectors where the average % Length of aggregate rays equals zero (those sectors with no rays present).
> Group B = sectors where the average % Length of aggregate rays is in the range of 10 - 80% (those sectors where rays are present but do not continue all the way to the pith).
> Group C = sectors where the average % Length of aggregate ray is 90% or greater (those sectors where the rays continue all the way to the pith. Ninety % was chosen as the arbitrary lower value for this group. Although at 90% the rays were not actually continuous with the pith was considered likely that they were connected with the pith somewhere within the 4.7 mm thickness of the disk);

Disk Number was plotted against angle on the circumference (for each sector) for each of the three groups

3.2.1.4. Classification of aggregate ray types

Individual aggregate rays were identified and numbered. It was often found that rays which appeared isolated on some disks were connected on other disks. All aggregate rays showing such connections were regarded as being part of the same ray and assigned the same number. Rays were then assigned to 2 groups:

group 1 = aggregate rays incomplete. Those rays which were not completely contained between disks 1 and 50.

type 1 = rays present on disk 1 which terminate on successive disks.
type 1.1 = rays present on disk 1 which continue to disk 50.

type 1.2 = rays present on disk 1 which terminate on abaxial side of branch.

type 4.1 = rays beginning on the adaxial side of a branch and present on disk 50.

type 5 = rays beginning after disk 1 but present on disk 50;

group 2 = aggregate rays complete. Those rays which are completely contained between disk 1 and disk 50.

type 0 = rays beginning after disk 1 which terminate before disk 50 and are not in association with any branch traces.

type 2 = rays beginning after disk 1 but terminate on abaxial side of branch.

type 3 = rays isolated (usually only on a single disk) and in association with a branch trace.

type 4 = rays that begin on the adaxial side of a branch and terminate before disk 50.

3.2.1.5. The skew of an aggregate ray

For each aggregate ray the maximum % distance to the pith was recorded for each disk. This was then converted to frequency data i.e. if the maximum % distance to the pith for disk 10 was 70 then disk 10 was recorded 70 times (in practice this was 7 as all % distance to the pith measurements were divided by 10 as % Length measurements were only made to the nearest 10%). The disks with the greatest maximum % distance to the pith have aggregate rays extending the greatest distance towards the pith and are, therefore, more likely to represent the inception of the aggregate ray at the leaf-trace. Disks above and below this point have progressively smaller values of maximum % distance to the pith recorded as the aggregate ray fans out (vertically) in the wood with consecutive growth rings. With the measurements recorded as frequency data the disks with the greatest maximum % distance to the pith are recorded more frequently than those with the smallest maximum % distance to the pith and, in terms of the standard frequency distribution, represent the 'mean' value (assuming a general similarity of mean with medium and mode). The disks with the smallest maximum % distance to the pith values, both above and below the inception of the aggregate ray, therefore, represent the 'tails' of the distribution. By calculating the skew of the distribution it is possible to determine if the tails extend further, from the mean, in any direction, i.e. do the aggregate rays extend further upwards or downwards from their inception? The skew for each aggregate ray was calculated using SAS and the sign of the skew recorded. A χ^2 test was then carried out for the type 0 aggregate ray (only '+' and '-' results were included, '0' and missing results were omitted).

3.2.1.6. Creation of an aggregate ray data file

A file was constructed that contained summary data for each aggregate ray. The variables were:

Ray Number - unique identifier for each aggregate ray;
Ray Extent - the number of disks on which the aggregate ray was present;
Maximum Length - the maximum % Distance to the Pith recorded for that aggregate ray;
Ray Type;
Skew.

3.2.1.7. Complete aggregate rays of limited radial extent

To investigate how aggregate rays of limited radial extent were related to branching and aggregate rays that could be traced to the pith, the data points for aggregate ray types 0, 2, 3, and 4 were superimposed over the 3-dimensional ray assemblage graphs. These data points were not converted to sectors, as with the 3-dimensional ray assemblage and, therefore, represent all points for these rays.

3.2.2. Aggregate rays arising in relation to the leaf-trace

One sample of each of *Nothofagus fusca, N. menziesii* and *Fagus sylvatica* were collected from the campus of the University of Canterbury. Samples of *Dracophyllum pronum* and *D. uniflorum* were collected from the Cass region of the Southern Alps.

Nodal samples from a range of juvenile and mature tissue were softened and sectioned in paraffin wax according to Appendix 1.

3.2.3. Aggregate rays arising in relation to pith flecks

Two specimens each of *Nothofagus fusca, N. menziesii* and *N. solandri* var. *cliffortioides* were used. Three mature internodes from each plant were wounded by the insertion of a needle through the bark into the woody tissue. The positions of the wounds were marked, above and below, by enamel paint. After a period of 35

months the internodes were collected, fixed in FAA, and softened and sectioned in paraffin wax according to Appendix 1.

3.3. RESULTS

3.3.1. The aggregate ray assemblage of *N. solandri* var. *cliffortioides*

3.3.1.1. Three-Dimensional nature of the aggregate ray assemblage

The most striking feature of the graphs illustrating the length of aggregate rays as percentage distance from the pith (Figures 3.2 and 3.3) is the alignment of the 90%+ points into 4, roughly defined, zones running lengthwise up the stem. These zones seem to correlate with where the leaf traces would have been in the juvenile tissue. To highlight this the four zones have been drawn on the graphs, each covering 90° of the circumference. These zones are based on a line connecting the centres of 2 branches (There are 3 branches represented on the graph labelled as X, Y, and Z - Figure 3.2) situated morphologically 1 above the other. (zone A). The number of 90%+ points completely occurring in each zone is recorded in the figure legends. Zones A and C represent the medial leaf-traces, and zones B and D represent the lateral traces. It can be seen that zones B and D have approximately twice as many pith connections as zones A and C.

When the graphs for the outside and inside angles are compared, it is noticeable that the 90%+ points are more tightly clustered into four zones on the outside than the inside. There are 2 major reasons for this. Firstly, angles very close to the pith were difficult to measure accurately. Secondly, there is a tendency for the rays to coalesce over a period of time.

3.3.1.2. Aggregate rays of limited radial extent

There seems to be a correlation between aggregate rays and leaf-traces. This impression is based solely on the arrangement of the aggregate ray assemblage, without taking into consideration the situation with individual aggregate rays. Table 3.1 shows the frequency of maximum length measurements for the 2 major aggregate ray groups. From this it can be seen that the complete aggregate rays are more limited in their radial extent than the incomplete aggregate rays, and that there are very few complete aggregate rays that have 90%+ points. This is contrary to what would be expected under the hypothesis that the presence of aggregate rays was

Figure 3.2

The aggregate ray assemblage of *Nothofagus solandri* var. *cliffortioides* (inside angles)

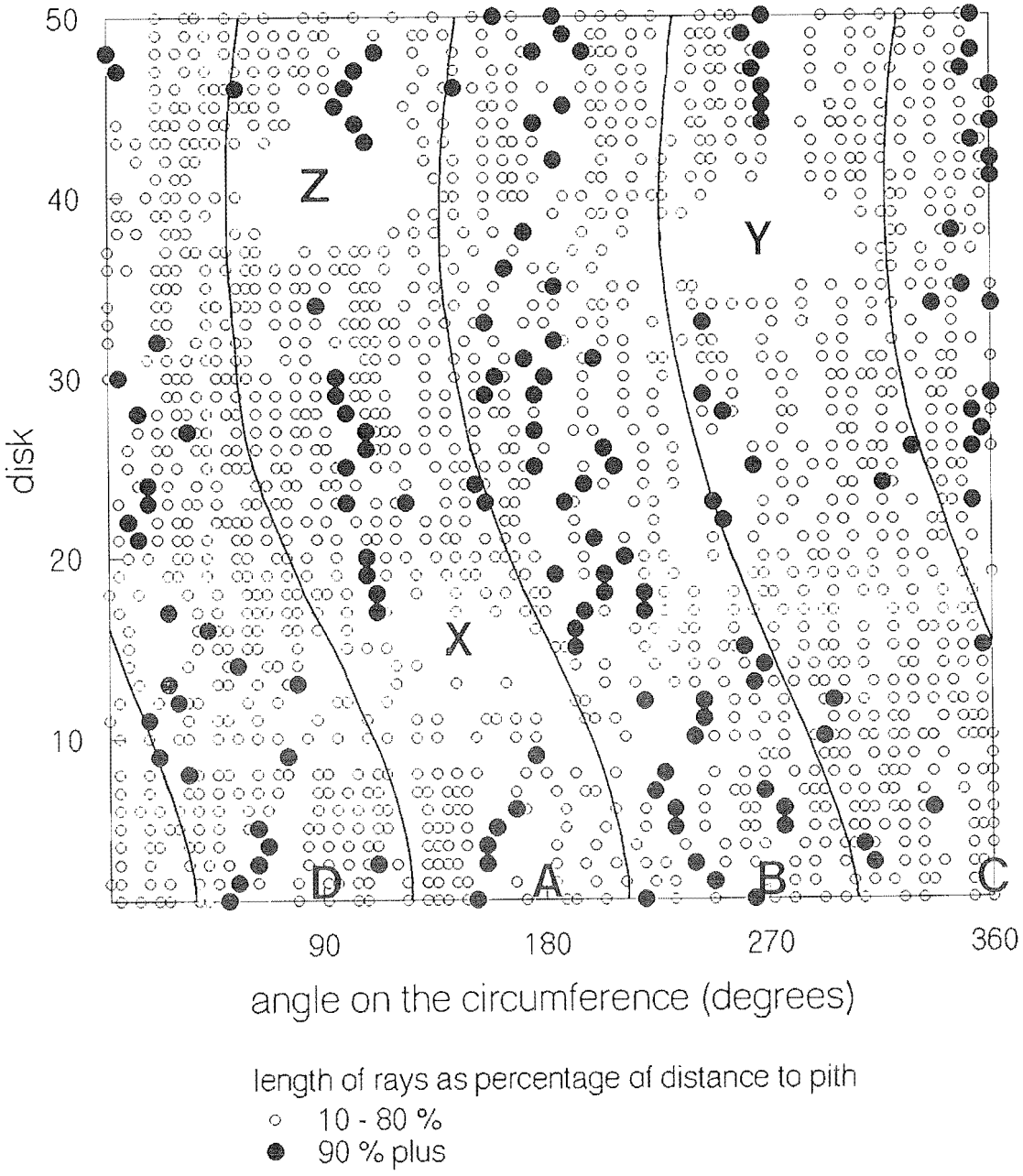

Branch traces are marked by X,Y and Z. Four zones have been marked off (A to D), these represent the alternate phyllotaxis of the primary stem (here based on the position of the branch traces). Zones A and C each represent 90° of circumference that would contain the medial leaf traces, and zones B and D each represent 90° of circumference that would contain the lateral leaf traces. Zone A contains 25 90% + points, zone B 53 90% + points, zone C 17 points and zone D 41 points.

Figure 3.3

The aggregate ray assemblage of *Nothofagus solandri* var. *cliffortioides* (outside angles)

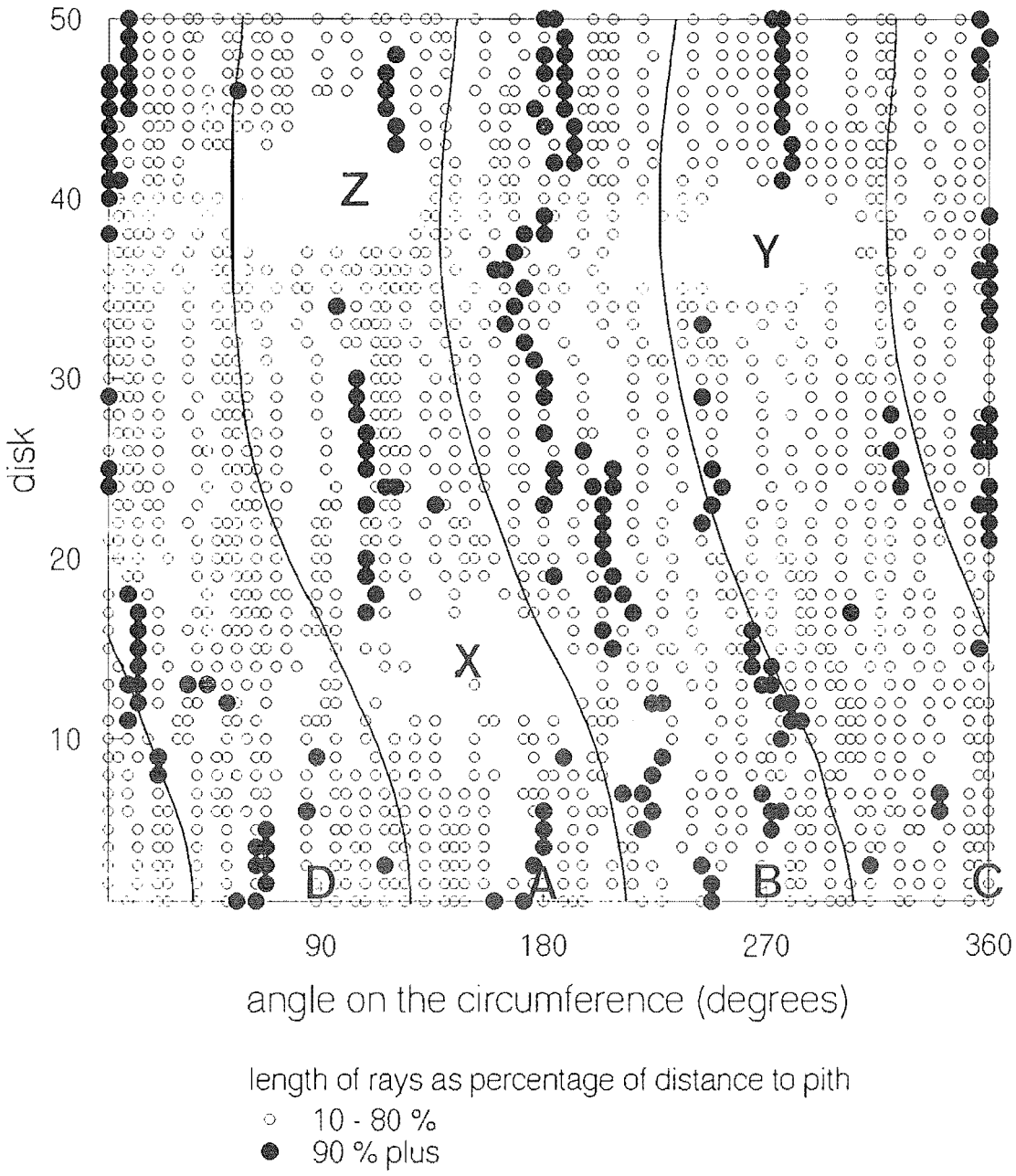

The labelling is the same as Figure 3.2. Zone A contains 28 90% + points, zone B 72 90% + points, zone C 25 points and zone D 60 points.

related to the leaf-traces. However, Table 3.1 also shows that the complete aggregate rays are, on average, far shorter than the incomplete ones, and suggests the complete aggregate rays are mostly recorded as such because their connections with other aggregate rays have been missed (i.e. occurring within the thickness of a disk). This is supported by Figures 3.4 and 3.5 where the complete aggregate rays have been plotted over the 3-dimensional aggregate ray assemblage. The complete aggregate rays are not randomly arranged around the stem but tend to fall into definite zones, either clustered around branch traces or in association with 90%+ points.

Table 3.1

The frequency of maximum length measurements and mean aggregate ray extent for complete and incomplete aggregate rays (types 1.1 and 3 excluded)

aggregate ray group	maximum length										mean aggregate ray extent*
	10	20	30	40	50	60	70	80	90	100	
complete	1	4	11	10	5	5	2	1	0	2	4
incomplete	0	1	1	2	8	7	10	6	13	3	19

* the average extent of aggregate rays in each group

3.3.1.3. The skew of aggregate rays

The χ^2test on the sign of the skew confirms there is a significant prevalence of negatively skewed complete aggregate rays to positively skewed aggregate rays (Table 3.2). This indicates that individual aggregate rays tend to be more developed below their disk containing their maximum length, than above it. In other words, if the maximum length can be regarded as the inception of an aggregate ray, then as the aggregate ray traverses out through the wood it tends to develop downwards more than upwards.

Table 3.2

χ^2 table for the sign of the skews for type 0 aggregate rays

(+) skew	(-) skew	χ^2
3	14	7.12**

^{ns} not significant, * P>0.05, ** P>0.01, *** P>0.0001

Figure 3.4

The aggregate ray assemblage of *Nothofagus solandri* var. *cliffortioides* with the addition of all complete rays not connected to the pith (inside angles)

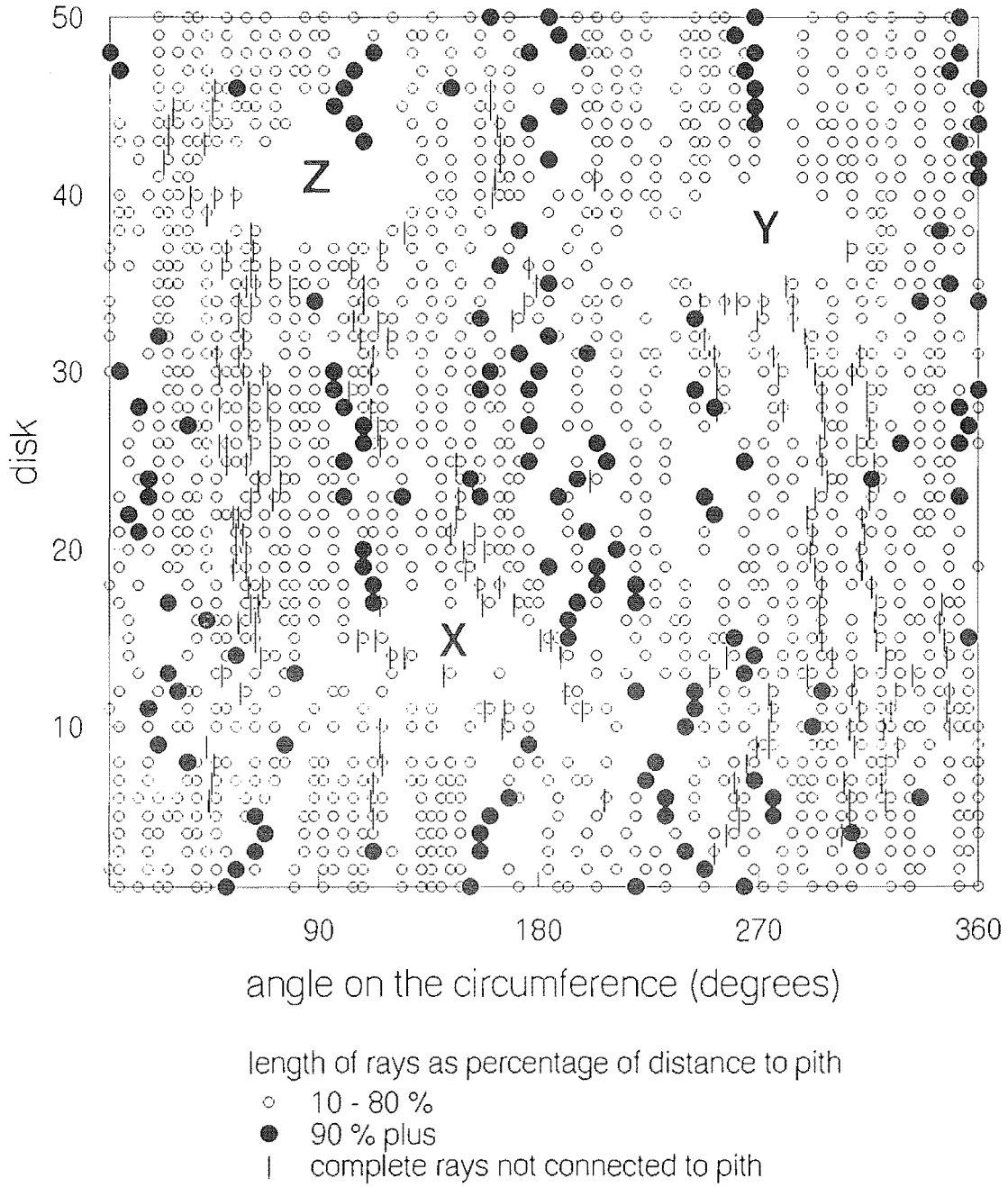

The same data as in Figure 3.2 with the addition of all complete rays (see text for details).

Figure 3.5

The aggregate ray assemblage of *Nothofagus solandri* var. *cliffortioides* with the addition of all complete rays not connected to the pith (outside angles)

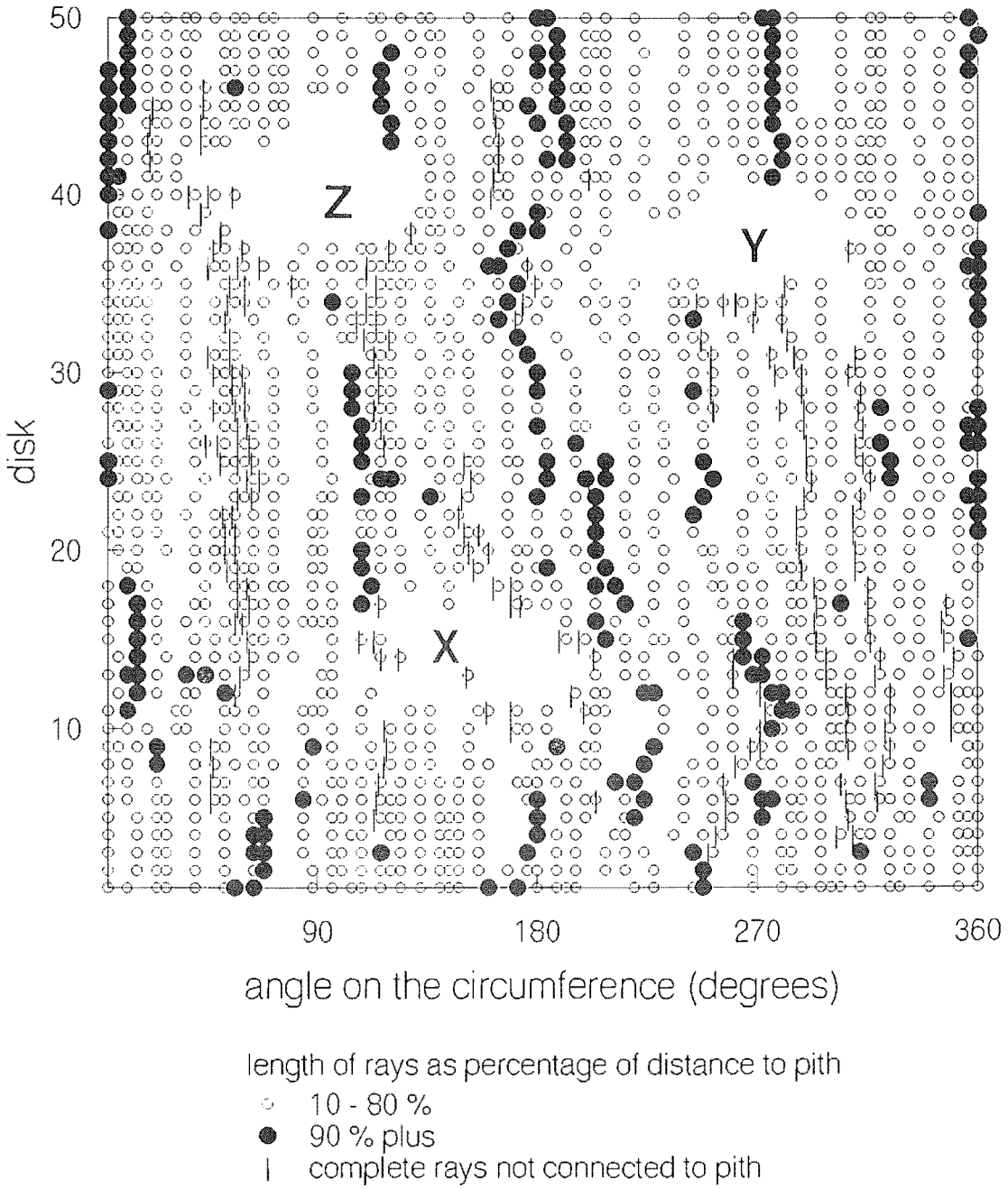

The same data as in Figure 3.3 with the addition of all complete rays (see text for details).

3.3.2. Aggregate rays arising in relation to the leaf-trace

3.3.2.1. *Nothofagus*

Below the node of *Nothofagus fusca*, before the leaf-trace has begun to depart, the leaf-trace bundle is more prominent than surrounding bundles[1]. The dominant feature of the bundle is the very wide vessels (along with a lack of fibres) in the metaxylem or very early secondary xylem. The secondary xylem immediately external to this area has smaller vessels, fibres and occasionally septate fibres or axial parenchyma (Figure 3.6.a). Other bundles at the same level tend to show the same pattern to a limited extent, or not at all (Figure 3.6.b). This seems to depend on how far away the bundle is from forming a leaf-trace, with bundles about to depart as leaf-traces having more prominent vessels than others.

Leaf-trace bundles of *N. menziesii* tend not to show the prominent wide vessels of the metaxylem, there being instead, a gradual increase in the width of vessels from the primary xylem into the secondary xylem (Figure 3.6.c). If wide vessels are prominent in the metaxylem, then all bundles at the same level tend to show the same pattern, to approximately the same extent (Figure 3.6.d).

Both species have leaf-trace bundles with associated indentations in the cambium that increase in magnitude further up the internode, as the departure of the leaf-trace bundle into the petiole becomes imminent. This indentation in *N. menziesii* tends not to extend as far down the internode, below the departure of the leaf-trace, as it does in *N. fusca.* With increasing secondary development both species display an aggregation of rays into radial files, associated with the indentation under the leaf-trace (Figure 3.6.a). These aggregations are equivalent to the foliar rays of Bailey (1911, 1912) and Eames (1911).

In both species indentations clearly associated with the leaf-traces are present in the growth rings. In *N. fusca* the indentations are prominent and accompanied by aggregate rays, whereas in *N. menziesii*, no aggregate rays are present and the indentations gradually decreased in size with continued secondary growth.

---

1 *Nothofagus* has a pseudosiphonostele (a review of stelar terminology is contained in Beck, Schmid and Rothwell 1982) with the separate bundles of the eustele having become confluent. It is, however, possible to distinguish the separate bundles to some degree even after secondary tissues have developed

Figure 3.6

Leaf-trace bundles of *Nothofagus fusca* and *N. menziesii* (TS)

a. *N. fusca.* Prominent vessels in the primary xylem and very early secondary xylem, with a general absence of vessels and an aggregation of ray tissue external to this. [scale bar = 200 μm].
b. *N. fusca.* Medial leaf-traces (M) and lateral leaf-traces (L) have prominent vessels in primary and early secondary xylem, whereas surrounding bundles do not. [scale same as Figure 3.6.a].
c. *N. menziesii.* No prominent vessels in the primary or very early secondary xylem. [scale bar = 100 μm].
d. *N. menziesii.* All bundles at the same level have a similar level of development. [scale bar = 100 μm].

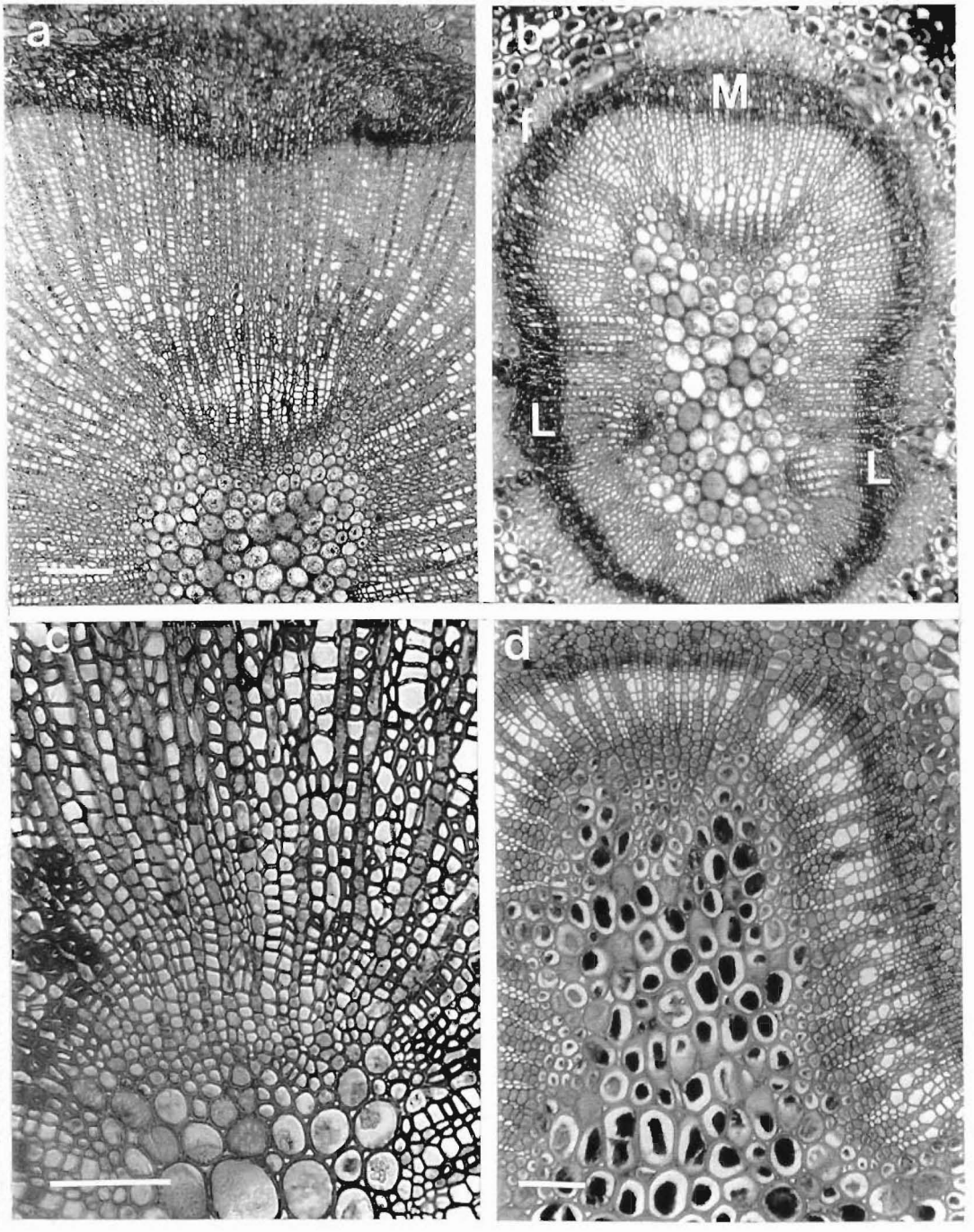
a
b
M
f
L
L
c
d

There is often an accumulation of axial parenchyma and/or septate fibres present under (or outside) the leaf-trace (or leaf-trace bundle) in *N. fusca*. This is a feature of the early secondary xylem and is first visible as a zone of septate fibres some distance below the departure point of the leaf-trace (Figure 3.7.a). Further up the internode axial parenchyma is also present (Figure 3.7.b). As the departing leaf-trace 'arches over' the axial parenchyma gives way to an accumulation of ray tissue (Figure 3.7.c).

This accumulation of ray parenchyma is also associated with the 'arching over' of the leaf trace in *N. menziesii*. However, there is no upward transition in the node from septate fibres. The relative positions of septate fibres, axial parenchyma and the accumulation of ray tissue under the leaf-trace in *N. fusca* and *N. menziesii* are shown in Figure 3.8.

The accumulation of ray material largely relates to the dissection of axial elements, into ray cells, via an axial parenchyma-like intermediary (Figure 3.9). Where the dissected axial element lies beside an existing high uniseriate ray, a biseriate ray is formed. A biseriate ray may also be formed by the fusion of 2 uniseriate rays, by the loss of an intermediary axial element. Greater degrees of dissections and fusions result in multiseriate rays. Due to the nature of its origin, the term accumulated parenchyma seems appropriate to describe tissue of this type, in this position.

With increasing secondary development individual ray cells are lost, and the biseriate rays are reduced to uniseriate rays. This is accompanied by the dissection, of these still very high rays, into shorter units by neighbouring axial elements. Multiseriate rays may also be dissected by the conversion of ray cells into axial elements.

Where the 'arching over' of the leaf-trace is at its maximum, the accumulation of parenchyma is at its greatest, with the leaf-trace completely surrounded by parenchyma, the accumulated parenchyma below, and the 'leaf-gap' above and to the sides (Figure 3.9).

The 'leaf-gap' of both species is not well developed with an interfascicular cambium[2] present just above leaf departure (Figure 3.10). The height of the 'leaf-gap', or

---

[2] leaf-gaps' in seed plants should be regarded as interfascicular regions (Beck, Schmid and Rothwell 1982)

Figure 3.7

Sequential sections through the departing leaf-trace of *Nothofagus fusca* (TLS)

[scale bar = 100 μm]
a. Zone of septate fibres (S) just below and outside the protoxylem (X).
b. Section further out with a zone of axial parenchyma (A) between the septate fibres (S) and the 'arching over' of the leaf-trace (X).
c. Section even further out where there is a zone where ray tissue (R) has accumulated under the leaf-trace.

Figure 3.8

The leaf-traces of *Nothofagus* (RLS)

a. *N. fusca.*
b. *N. menziesii.*

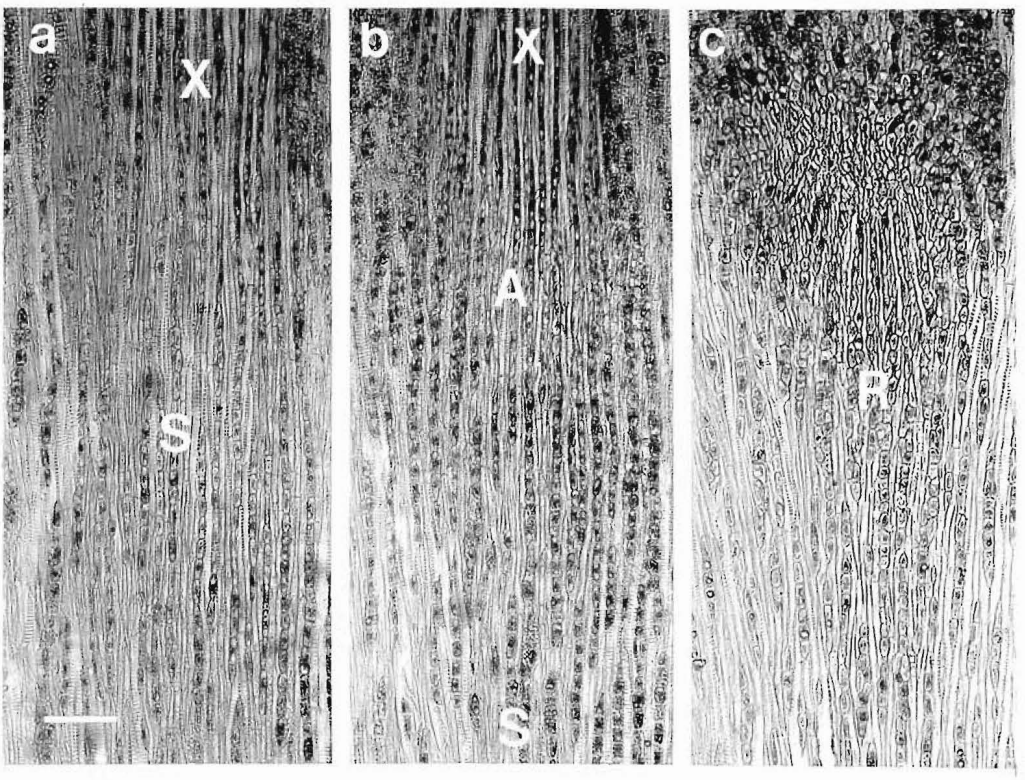
a
X
S
b
X
A
S
c
R

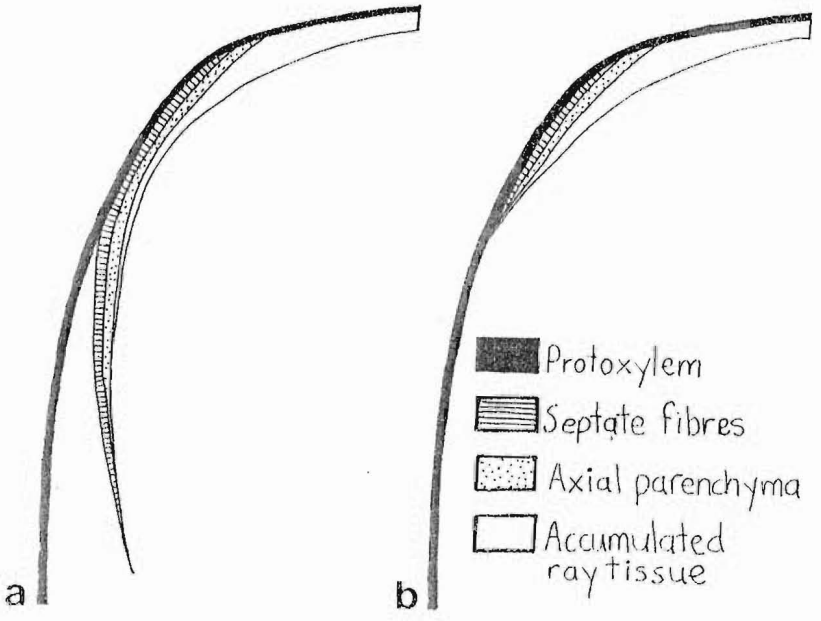
a
b
Protoxylem
Septate fibres
Axial parenchyma
Accumulated ray tissue

Figure 3.9

The sequence of aggregation, followed by dissection, of ray material under the leaf-trace in *Nothofagus menziesii* (TLS)

[scale bar = 100 μm]. 'Leaf gap' (G). Leaf-trace (T).

a. Mainly uniseriate rays under the leaf-trace.

b. Mainly uniseriate rays and axial parenchyma under the leaf-trace.

c. Mainly biseriate rays with some axial parenchyma under the leaf-trace.

d. Mainly biseriate and multiseriate rays under the leaf-trace.

e. Multiseriate rays are beginning to be dissected. (A) and (B) are just below such rays.

f. Multiseriates (A) and (B) are now mostly dissected into biseriate rays.

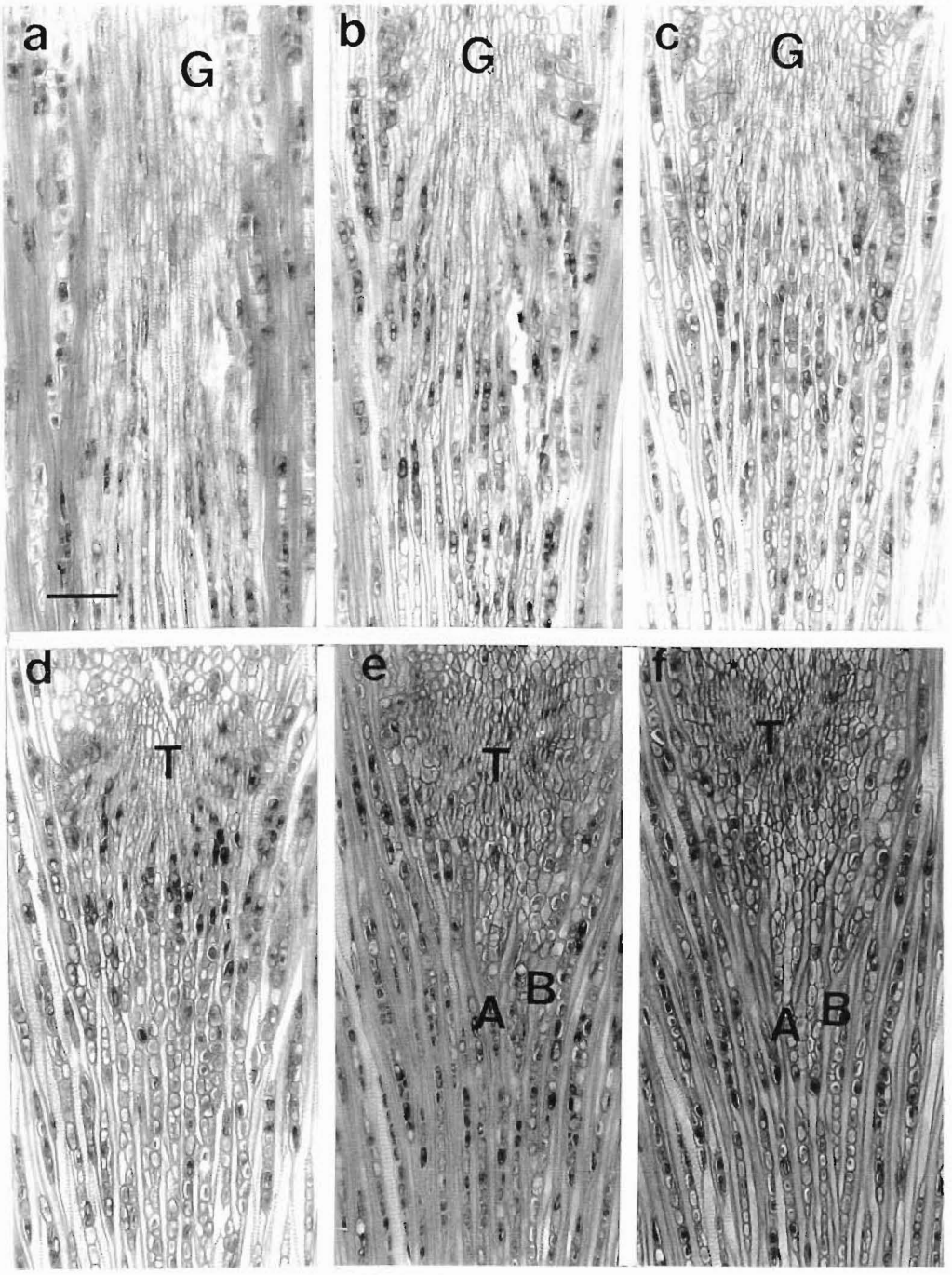
a
G
b
G
c
G
d
T
e
T
A
B
f
T
A
B

Figure 3.10

The interfascicular cambium in the 'leaf gap' of *Nothofagus menziesii* (TS)

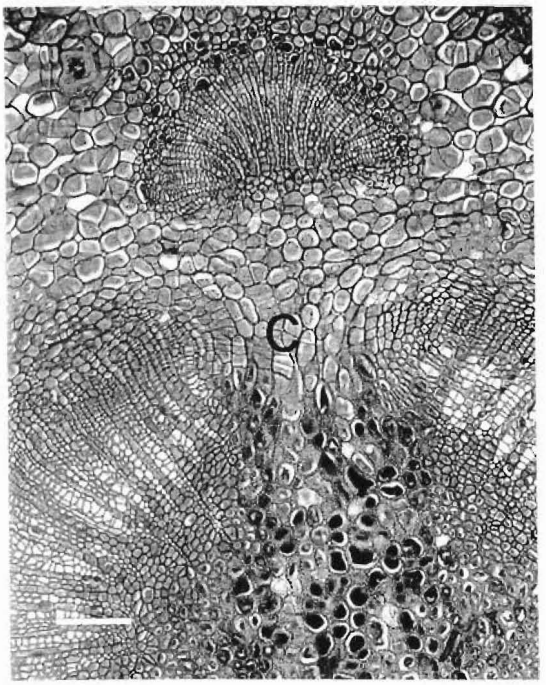

Interfascicular cambium (C). [scale bar = 100 μm].

interfascicular region, is controlled partially by the development of the bundles on either side as they expand tangentially and radially into it. With the formation of an interfascicular cambium the 'leaf-gap' is essentially a broad multiseriate ray, and will henceforth be termed a 'compound foliar' ray. With continuing secondary development this ray is reduced in width and height by the conversion of ray cells into axial cells at the margins (top and sides) of the ray, eventually resulting in uniseriate rays separated by fibres. This, essentially vesselless zone, can extend for some distance above the 'compound foliar' ray (Figure 3.11). There is generally no appreciable indentation in the cambium associated with the 'compound foliar' ray, and if there is, its influence is not lasting. Where the leaf-trace became ruptured the 'compound foliar' ray and the accumulated tissue became confluent and the process of dissection continued.

Occasionally the vesselless zone, formed by the dissection above the 'compound foliar' ray of a lateral leaf-trace, extends up the internode to such an extent it becomes confluent with the indentation below the lateral trace of the next leaf. A situation such as this occurs when the pith has a slightly crescent shaped outline, with successive lateral leaf-traces occurring within the indentation, and results in the confluence of two aggregate rays (Figure 3.12). In the limited specimens examined, the pith of the internodes of *N. fusca* tends to be more irregular in outline than those of *N. menziesii*, where they tend to be more circular in outline.

Biseriate rays and small multiseriate rays also form above and below branches, but these are also eventually reduced to uniseriates. Aggregate rays did not appear to develop above the branch, but there may be some limited development below. The formation of aggregate rays in relation to branches is complicated by the presence of a leaf-trace under the branch and leaf-traces produced by the branch itself, and was not extensively examined.

3.3.2.2. *Fagus sylvatica*

There is no obvious indentation, nor is there generally any appreciable aggregation of rays below the leaf-trace. Some accumulation tissue does form to a limited extent, and in the sections examined this is most common under the traces in the over wintering bud. Where accumulation tissue is present it tends to be vertically elongated, having the appearance of dissected axial elements (Figure 3.13). Normal vegetative leaves usually had a bipartite medial trace, consisting of 2 bundles (Figure 3.14). At a distance below the medial leaf-trace the leaf-trace consists of a single

Figure 3.11

Dissection of the 'compound foliar ray' above the leaf-trace in *Nothofagus menziesii* (TLS)

The sequence begins at the pith (Figure 3.11.a) and progresses outward through the secondary xylem. It is difficult to follow individual rays, though just to the left and below (R) there is a ray that can be followed through the sections.
[scale bar = 100 μm].

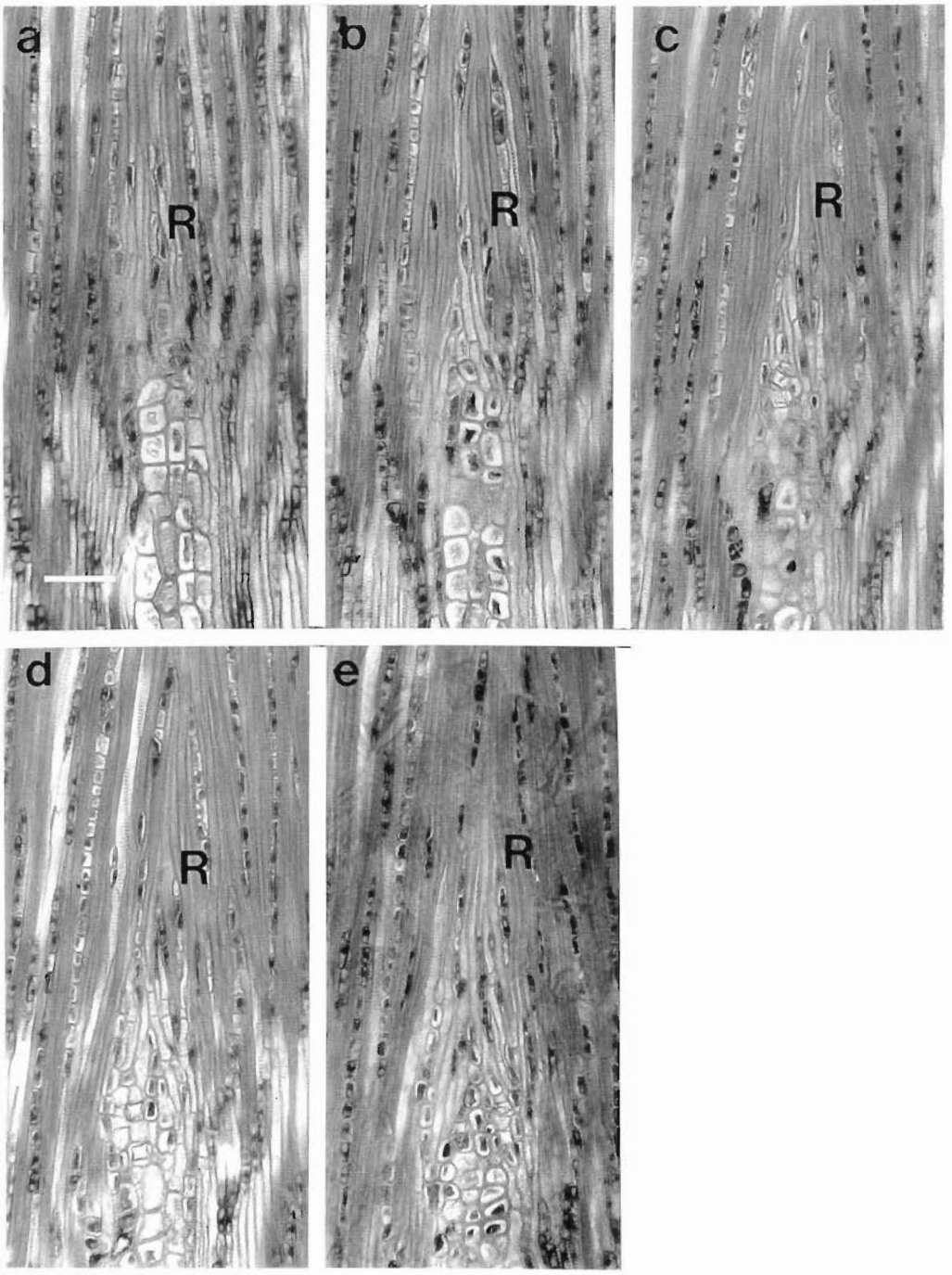
a
R
b
R
c
R
d
R
e
R

Figure 3.12

The vertical positioning of leaf-trace bundles in *Nothofagus* (TS)

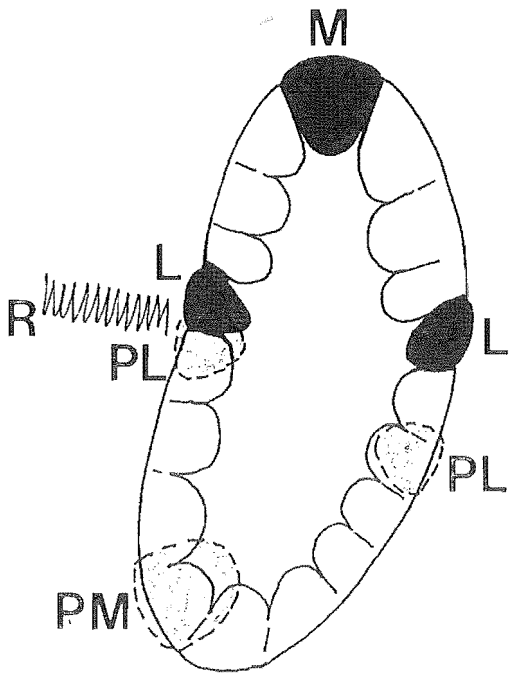

Medial leaf-trace bundle (M). Lateral leaf-trace bundle (L). Medial leaf-trace bundle for previous leaf (PM). Lateral leaf-trace bundle for previous leaf (PL). When the stem outline is vaguely crescent shaped, one of the lateral leaf-trace bundles may be positioned above one of the lateral leaf-trace bundles for the previous leaf. This allows for the dissections at the top of the 'compound foliar ray' to become continuous (R) with the indentation under the leaf-trace of the current leaf.

Figure 3.13

Leaf-trace of a bud scale of *Fagus sylvatica* (TLS)

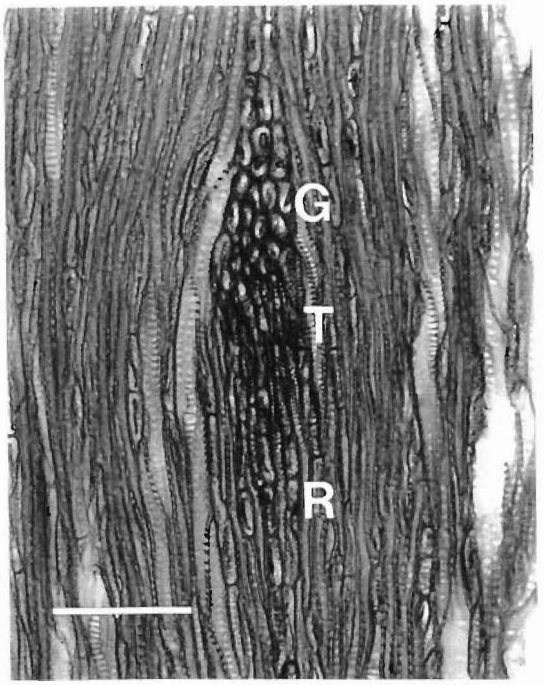

'Leaf gap'/'compound foliar ray' (G) with mainly procumbent cells. Leaf-trace (T). Accumulated ray tissue (R) with upright cells. [scale bar = 100 μm].

Figure 3.14

Sequential sections (TS) upward through the stem, node and petiole in *Fagus sylvatica*

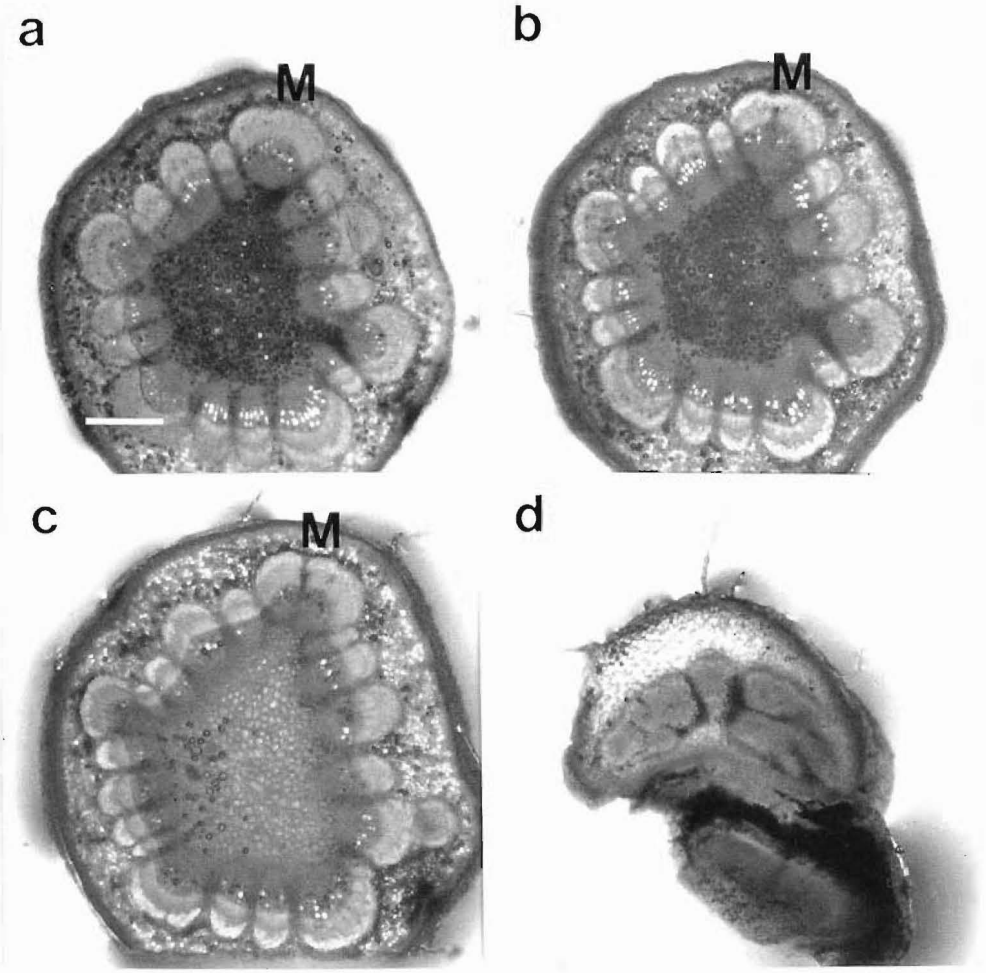

[scale bar = 200 μm].

a) to c) shows how the medial leaf-trace (M) becomes dissected into 2 discrete bundles separated by an interfascicular region.

d. The base of the petiole where the leaf-trace bundle has undergone further dissections.

bundle (Figure 3.14.a), further up the trace this bundle is split in two radially (Figure 3.14.b), and, as a result, a prominent interfascicular area is visible in the centre of the medial trace (Figure 3.14.c). Further dissections of the bundles occur in the petiole (Figure 3.14.d). This means there is an interfascicular region situated below the leaf-trace. With secondary development a multiseriate ray is formed. Further up the trace the multiseriate ray may be lost due to the fusion of the 2 bundles in the single trace.

There may be up to 4 interfascicular areas associated with each trace: The region reflecting the bipartite nature of the trace; the flanking regions on either side of the trace; and the 'leaf-gap'. These 4 regions are, of course, confluent at the pith, but with further secondary development separate broad multiseriate rays are formed. These multiseriate rays are synonymous with the 'compound foliar' rays of *Nothofagus* and also become slightly dissected at the edges by the conversion of ray cells into axial elements.

3.3.2.3. *Dracophyllum*

As with the species of *Nothofagus* above, there is a prominent indentation below the leaf-trace, and some accumulation tissue is present, similar in appearance to that described for *F. sylvatica.* The 'leaf-gap' can extend for an appreciable distance above the departure of the leaf-trace (but is not nearly as extensive as in *F. sylvatica*) and has an indentation associated with it. A 'compound foliar' ray is formed with the development of the interfascicular cambium and, as with *F. sylvatica,* a slight degree of dissection occurs at the margins.

The relationship of the aggregate ray with the leaf-trace is more striking in more mature stems, as represented in TS by Figure 3.15. Below the departure of the leaf-trace, the leaf-trace bundle is discernible, and the secondary xylem immediately outside it is not noticeably dissimilar to the surrounding woody tissue (Figure 3.15.a). Further up the leaf-trace an aggregate ray is present at the cambium, but it dissipates noticeably towards the trace (Figure 3.15.b). With the departure of the leaf-trace (Figure 3.15.c) an aggregate ray is present from the cambium to the leaf-trace. The cambium is now strongly indented in association with the aggregate ray. A 'compound foliar' ray is formed from the 'leaf-gap' (Figure 3.15.d) and this gradually dissipates with increasing height above the departure of the leaf-trace (Figure 3.15.e).

Figures 3.15.b and 3.15.e apparently show aggregate rays that have been formed by the fusion of uniseriate rays and thus support the 'synthetic' view on the origin of

Figure 3.15

Sequential sections (TS) through the stem of *Dracophyllum pronum* showing the relationship of the aggregate ray to the leaf-trace

[scale bar = 200 μm]. The figures are labelled with Figure 3.15.a at the base to show the relative positions of the sections.

a. Some distance below the departure of the leaf-trace. The approximate position of the leaf-trace bundle is marked by (T). The wood outside (T) shows no dissimilarity to the surrounding wood.

b. The wood just outside the leaf-trace bundle (T) appears to contain slightly more parenchyma tissue than the wood on either side (tangentially), further out toward the cambium there is a greater build-up of parenchyma until a prominent aggregate ray is formed. This figure apparently supports the 'synthetic' theory of aggregate ray formation.

c. The leaf-trace has reached its maximum radial extent (T) and ruptured. An aggregate ray now extends from the pith to the cambium with some signs of dissections (D) at the sides, these possible relate to the interfasiscular areas flanking the leaf-trace.

d. Just above the departure of the leaf-trace an aggregate ray extends from the pith to the cambium. There are no signs of dissections at the sides.

e. The aggregate ray is more prominent at the cambium than at the pith, again providing apparent support for the 'synthetic' theory on aggregate ray formation.

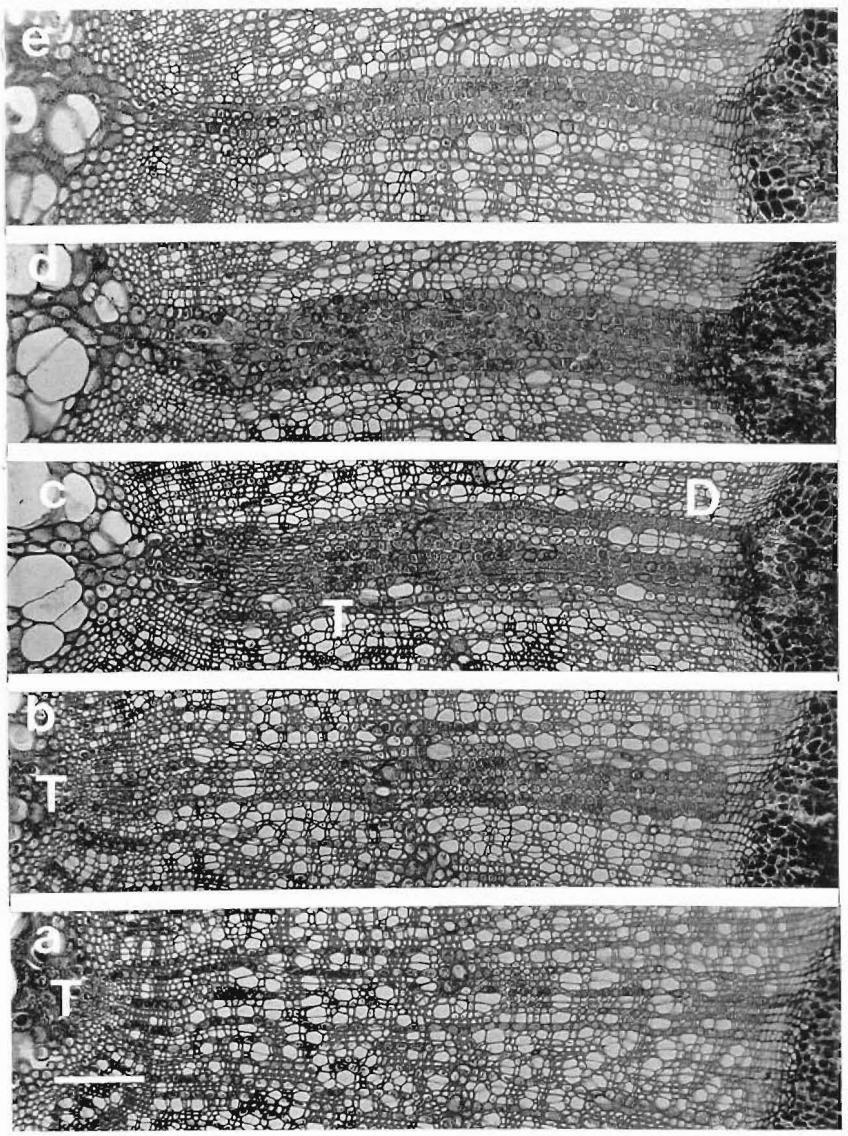
e
d
c
D
T
b
T
a
T

aggregate rays. This is, however, an over-simplification of the ontogeny of the aggregate ray. It is clear from serial tangential sections through the node of *Dracophyllum* (Figure 3.16), that the aggregate ray has its beginnings as a broad compound ray formed from the interfascicular region, above the departed leaf-trace. There is some accumulation of ray material under the leaf-trace, but this is in the form of a close association of uniseriate rays. In addition to the interfascicular region comprising the 'leaf-gap', there are also long, flanking, interfascicular regions on each side of the trace. With further cambial development the uniseriate rays under the leaf-trace begin to 'fuse' with the 'compound foliar' rays that comprise the flanking regions of the leaf-trace. Uniseriate rays that do not fuse with the flanking regions, tend to become more closely associated with each other, both in the region between the flanking regions, and at a distance below the trace. With the rupture of the leaf-trace further axial elements are converted to ray cells and the flanking regions become continuous with each other, forming 1 large compound ray. This compound ray extends downwards (and to a certain extent upwards) with further cambial activity as axial elements are lost between uniseriate rays below the compound ray.

The resulting structure can best be visualised in RLS (Figure 3.17) as a compound ray 'fanning out' from the 'leaf-gap'. Below and inside of this compound ray is an area where uniseriate rays are becoming closely associated. A TS below the departure of the leaf-trace will show the leaf-trace bundle with an area of closely associated uniseriate rays external to this, further out a compound ray is present.

3.3.3. Aggregate rays arising in relation to pith flecks

Initially only 2 internodes from 2 plants (1 of *N. fusca* and 1 of *N. menziesii*) were sampled. As none of these samples showed any development of aggregate rays in relation to the wounded tissue no further samples were collected. This is justified as other sections prepared for this chapter to investigate the relationship of the aggregate ray to the leaf-trace, and sections prepared for the previous chapter, often show natural wounds or pith flecks, none of which produced structures that could be considered aggregate rays. Wounding did result in a proliferation of parenchyma, but this was quickly dissected by axial elements during the subsequent secondary development leaving no lasting impression on the wood (Figure 3.18)

Figure 3.16

Sequential sections (slightly oblique TLS) through the stem of *Dracophyllum uniflorum* showing the relationship of the aggregate ray to the leaf-trace

[scale bar = 100 μm]

a. The protoxylem (P) of the leaf-trace is visible, with the 'leaf gap' (G) above, and a flanking interfascicular area (F) to the side.

b. Further out the leaf-trace has ruptured and is marked by the presence of deformed axial elements (T).

c. The leaf-trace has ruptured completely with a 'compound foliar ray' (G) above the position of the leaf-trace, and an accumulation of ray material (R) below.

d. The above and below regions of the trace have become confluent as the 'compound foliar ray' extends downwards.

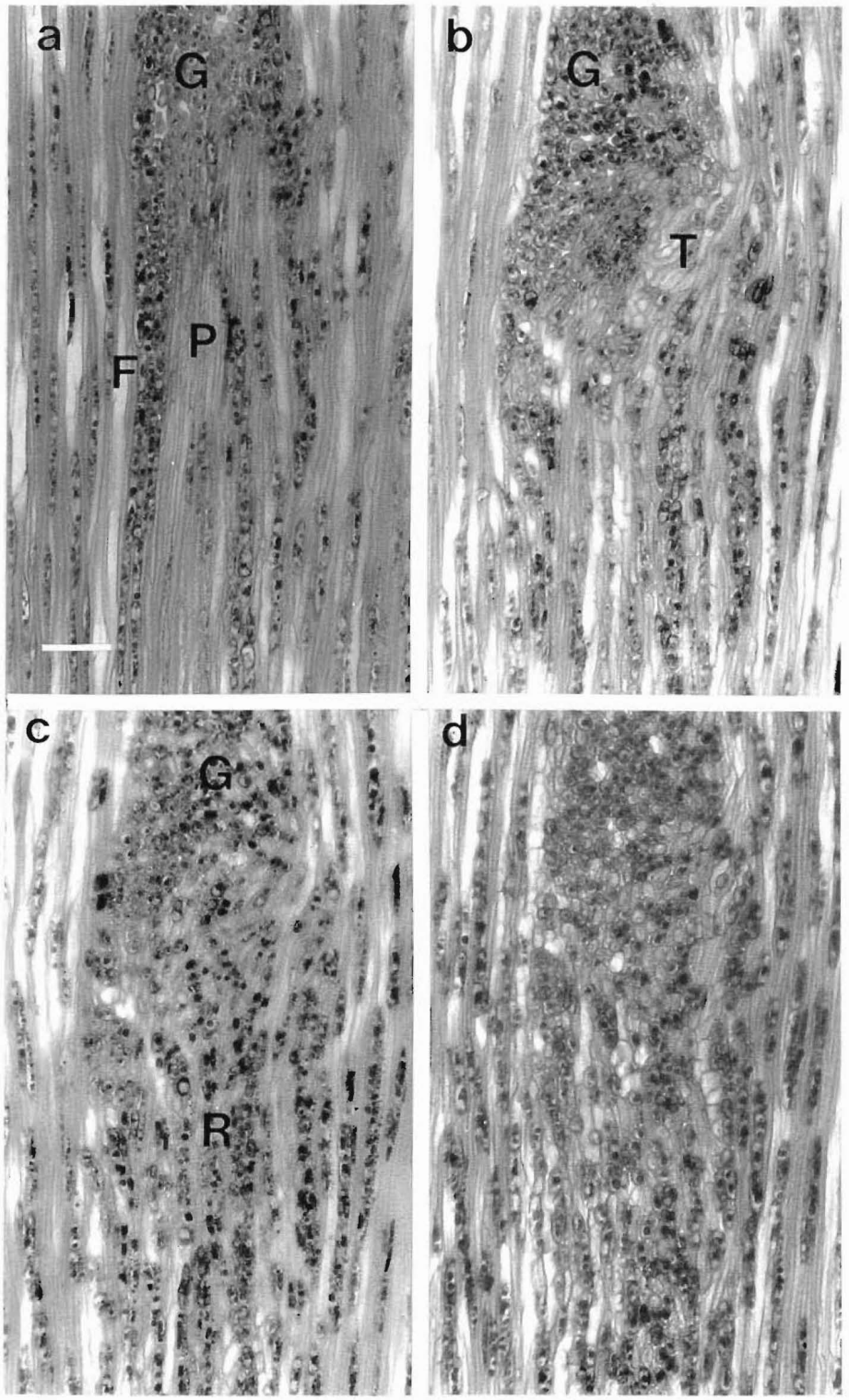
a
G
P
F
b
G
T
c
G
R
d

Figure 3.17

The leaf-trace of *Dracophyllum*

a. TS section from a'- a' apparently showing the formation of an aggregate ray by the enlargement of an existing ray.
b. TS section from b'- b' apparently showing the formation of an aggregate ray by the fusion of separate uniseriate rays.
c. TS section from c'- c' showing a leaf-trace with a small amount of accumulated ray tissue outside it.

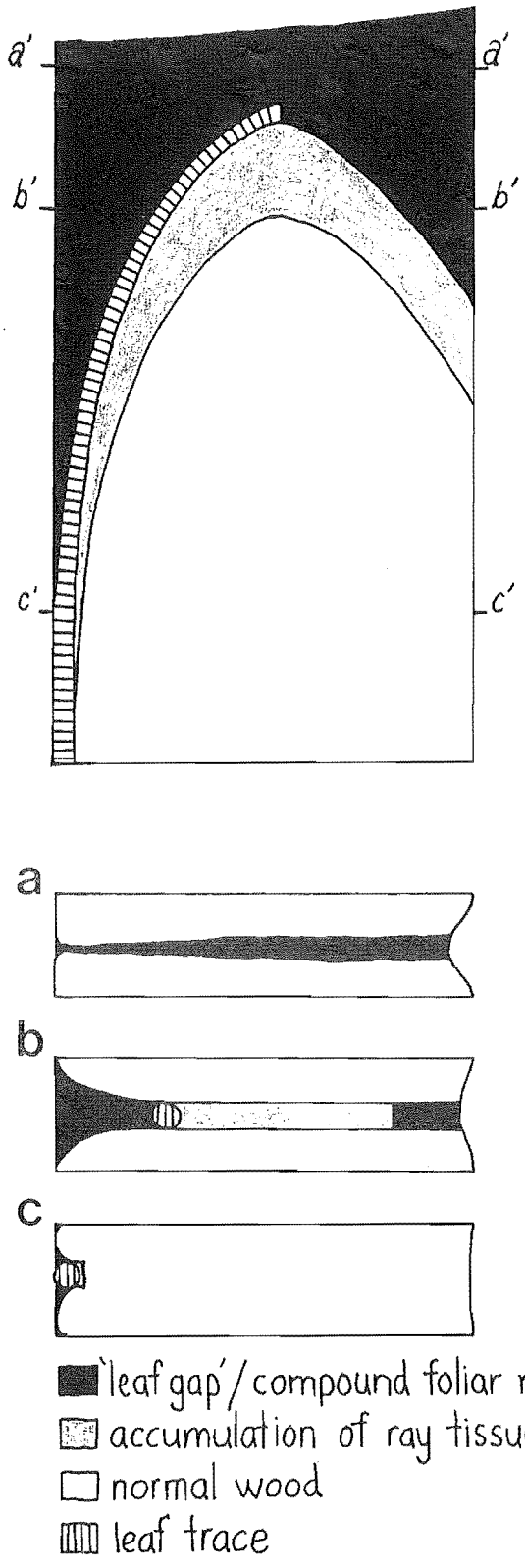
a'
a'
b'
b'
c'
c'
a
b
c
'leaf gap'/compound foliar ray
accumulation of ray tissue
normal wood
leaf trace

Figure 3.18

Aggregate rays in response to wounding in *Nothofagus fusca* (TLS)

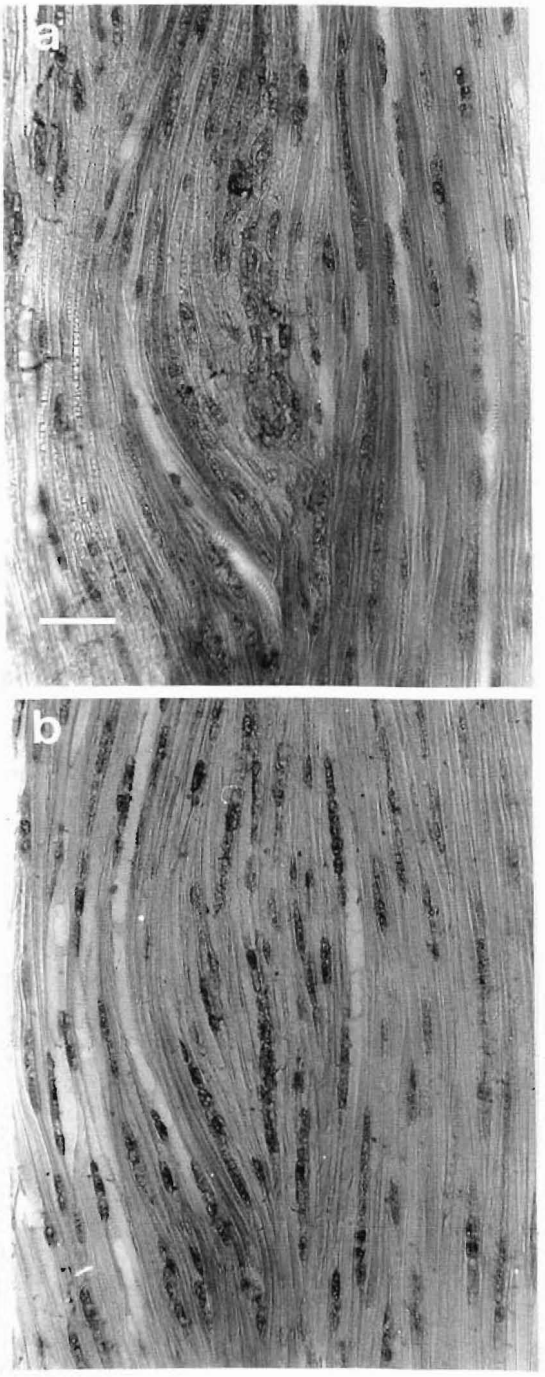

[scale bar = 100 μm].

a. Induced wound.

b. Resumption of normal growth with no signs of aggregate ray formation after a period of cambial activity.

3.4. Discussion

When the first papers relating to the 'synthetic' origin of aggregate rays (and aggregate rays themselves) were produced by Bailey (1910a, 1910b, 1911, 1912) and Eames (1910, 1911) it was widely believed that the uniseriate ray was the primitive ray structure, as it was the one that most commonly occurred in gymnosperms. Further more, 'leaf-gaps' were regarded as always being bridged by the widening of the secondary segments on either side (Jeffrey 1917). The assumption was that the 'leaf-gap' played no role in the formation of the compound ray, therefore, in order to obtain a compound ray that extended apparently all the way to the pith, it was necessary to have an intermediate form where the 'leaf-gap' had become bridged, but the uniseriate rays of the secondary xylem had begun to fuse with each other, eventually forming a compound ray. Further reduction would result in the loss of this intermediary and the apparent fusion of this compound ray with the pith. Bailey (1911 figure 23) illustrates this intermediate type above the leaf-trace in *Alnus japonica.* However, a feature similar to this can also exist in *Nothofagus* as a result of the dissection at the top of the compound foliar ray. A feature such as this, therefore, cannot be regarded as evidence for the formation of an aggregate ray by the fusion of uniseriate rays, especially where it occurs above the leaf-trace, but shows, instead, a compound ray in the process of dissection.

The interfascicular origin of the aggregate ray has been recognised by Philipson, Ward and Butterfield (1971) for *Fagus* and *Casuarina.* It has been with reference to *Casuarina*, however, that the most convincing arguments for the 'synthetic' origin of the aggregate ray are to be found (Jeffrey 1917, Moseley 1948). Both of these authors show figures depicting an apparently rapid widening of a multiseriate ray, originating from an interfascicular region, into a broad aggregate or compound ray.

A range of *Casuarina* species was not available for study, but a careful analysis of the figures of both Jeffrey (1917) and Moseley (1948) suggest comparisons may be made with *Dracophyllum.* It has been shown in examples of this genus that the apparent aggregation of uniseriate rays, to form an aggregate ray, under the leaf-trace is, in fact, the inclusion of these uniseriate rays into an existing compound ray developing downwards from the interfascicular region above the leaf-trace (the 'compound foliar' ray). Neither of the authors above made reference to using serial transverse or tangential longitudinal sections in their studies, apparently relying instead on isolated transverse and tangential sections from which to draw their conclusions. If the 'compound foliar' ray can develop downwards in *Dracophyllum*, it is not

inconceivable that it could develop upwards in *Casuarina*, thus giving the impression of the aggregation of uniseriate rays into aggregate rays above the leaf-trace.

A more likely explanation, however, can be found on a close examination of the figures of Jeffrey (1917 figures 66-67 pages 86-87). These figures are reproduced in Figure 3.19 and depict, moving outward from the pith, a 'compound foliar' ray which undergoes a rapid enlargement in width, with radially elongated cells. This is followed by an aggregate ray, which appears to be compounding further out towards the cambium. In this figure, the region of rapid ray enlargement looks suspiciously like a trace associated with the formation of a bud in the axil of the leaf. If this is the case, then the region of aggregation followed by the region of compounding, would be similar to the situation under the leaf-trace of *Dracophyllum*. Flores (1980) has shown that branch traces in *Casuarina* arise from the 2 stem bundles extending from either side of the leaf-trace of the subtending leaf. If the bud failed to develop then a similar situation would result with this trace, as with the ruptured leaf-trace of *Dracophyllum*.

The aggregate rays of *Dracophyllum* and *Fagus* have different, but related ontogenies. The aggregate ray of *Fagus* is essentially a radial and longitudinal continuation of the 'leaf-gap', and is clearly of the type designated 'compound' by early authors. This 'compound foliar' ray shows some signs of dissection at the top of the ray as ray cells are converted into axial elements. There may be some accumulation tissue under the trace, but this does not appear to play a significant role in the formation of the aggregate ray.

Dracophyllum also has a well developed 'compound foliar' ray which undergoes dissection at the top. However, the examples furnished by this genus also show a significant degree of accumulation tissue below the leaf-trace. The confluence of the above and below trace areas, associated with the rupture of the leaf-trace and the secondary development of the flanking regions, results in an aggregate ray with the 'compound' structure above and the 'aggregate' structure below. *Dracophyllum*, therefore, offers evidence for both the 'synthetic' hypothesis (Bailey 1910a, 1910b, 1911, 1912, Eames 1910, Jeffrey 1917, Moseley 1948, Shimaji 1954a 1954b) and the 'dissection' hypothesis (Bailey and Sinnott 1914, Barghoorn 1940, 1941, Kribs 1935) of aggregate ray formation, depending on the point of reference.

In *Nothofagus* the 'compound foliar' ray is only weakly developed and does not extend much beyond the rupture of the leaf-trace. Here the aggregate ray appears to be very

Figure 3.19

The formation of aggregate rays in *Casuarina fraseri* (TS) (a reproduction of Figures 66 and 67 from Jeffrey [1917])

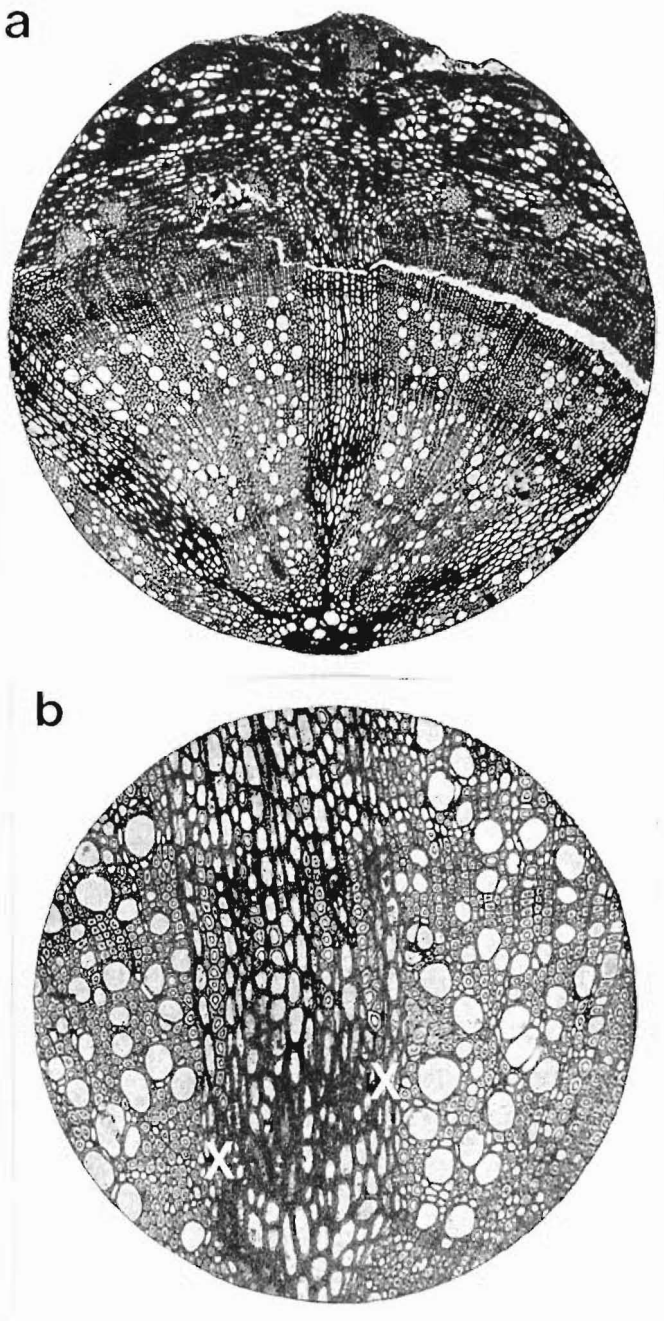

a. The apparent formation of an aggregate ray by the enlargement of an existing ray.
b. A more highly magnified region of above. (X) indicates possible lateral bud traces.
(see text for details).

much the product of the secondary xylem subtending the leaf-trace. There is, however, no evidence to suggest that the close association of uniseriate rays in this area will ultimately result in the formation of a compound ray. To the contrary, where there is fusion of neighbouring uniseriate rays to form biseriate rays, these are quickly reduced to uniseriate rays with subsequent cambial development.

No definitive differences could be found between *N. fusca* (with aggregate rays) and *N. menziesii* (without aggregate rays) that could lead to their extensive development in mature wood of the former species. There was some formation of axial parenchyma under the leaf-trace in *N. fusca*, however, this did not appear to extend for any great extent radially and its role in the formation of the aggregate rays in *Nothofagus* is unknown. No definitive explanation for the origin of the aggregate ray in *Nothofagus* was found in relation to the interfascicular regions or the leaf-traces. However, the indentation of the growth ring, which is a characteristic feature of the aggregate rays in this genus, could be traced back to the secondary xylem subtending the leaf-trace, and tended to be more conspicuous in *N. fusca* than *N. menziesii.*

Although there is some degree of commonality between the formation of the aggregate rays of *Dracophyllum* and *Fagus*, a similar relationship was not obvious in *Nothofagus*, except for an indentation under the leaf-trace.

Pith flecks, or wounds, did not appear to play any significant role in the formation of aggregate rays in *Nothofagus*. The fact that the resumption of normal cambial development after wounding is similar to that occurring after the rupture of a leaf-trace is further evidence that it is the indentation associated with the leaf-trace and not the rupture of the leaf-trace or the 'compound foliar' ray that is the major stimulus for the formation of aggregate rays in *Nothofagus.*

That wounding did not result in the formation of aggregate rays would seem contrary to the observations of Bhat (1980, 1983) and Noskowiak (1978) who showed aggregate rays formed in relation to pith flecks in the Betulaceae. There are, however, several points that may account for this discrepancy. As Bhat (1983) pointed out, aggregate rays occur only rarely in *Betula*, the genus studied. This makes it difficult to compare aggregate rays arising from pith flecks with those arising in association with the leaf-trace. The aggregate rays that arose from the pith flecks were essentially enlarged, abnormal rays and the extent of their radial development was not discussed. Noskowiak (1978) shows aggregate rays that trace their origins back to the pith, as well as those that relate to pith flecks. His study was, however,

conducted at a macroscopic level, and an anatomical comparison of these 2 types of aggregate ray was not attempted.

If the aggregate rays associated with pith flecks are comparable to those arising in association with the leaf-trace then there is a further factor that may account for the discrepancy. The studies of both Bhat and Noskowiak dealt with mature wood, whereas the material in this study was still relatively young and the formation of aggregate rays from pith flecks in mature wood of *Nothofagus* can not be ruled out.

Donaldson (1982) refers to aggregate rays occurring spasmodically in *Eucalyptus*, the formation of which he attributes to adventitious root primordia as suggested by Fink (1982). Fink, however, never refers to these rays as aggregate rays, preferring to call them abnormally broad xylem rays. Bannan (1950a) described similar structures in the gymnosperm *Chamaecyparis*, also referring to them as abnormal rays.

It would seem that these structures fit the general broad definition of an aggregate ray as suggested by the IAWA Committee (1989)[3], however, the term originally used by Bailey (1911), and by many authors subsequently, was used in reference to a structure associated with the leaf-trace. Aggregate rays of this sort tend to be major features of the woods in which they occur, whereas the structures associated with adventitious root primordia and pith flecks tend to be of erratic occurrence. It is therefore suggested the definition of an aggregate ray be narrowed to include only those structures tending to be persistent features of the wood, arising in relation to the leaf-trace.

3.5. Conclusions

No direct evidence could be found to support the theory that aggregate rays are formed by the aggregation of smaller uniseriate rays into a single large ray (the 'synthetic' theory). Where there seemed to be evidence to support this theory it was shown that uniseriate rays were actually being included into existing compound rays that were extending downwards from the region associated with the 'leaf-gap'.

The origin of the aggregate rays of *Nothofagus* does not appear to directly relate to the origins of those of *Fagus* and *Dracophyllum*. Although there is some relationship to the leaf-trace, there are no differences between *N. fusca* and *N. menziesii*

3 "a number of individual rays so closely associated with one another that they appear macroscopically as a single large ray. The individual rays are separated by axial elements...".

considered significant enough to account for the later development of aggregate rays in 1 and not the other.

Examples in the genus *Casuarina* which apparently support the 'synthetic' theory should be re-examined with special emphasis placed on weakly developed or latent branch traces.

CHAPTER 4

THE RELATIONSHIP OF PRIMARY GROWTH, AND THE APPLICATION OF GROWTH SUBSTANCES, TO THE PRESENCE OF AGGREGATE RAYS IN *NOTHOFAGUS*

4.1. INTRODUCTION

It was noted in Chapter 3 that internodes of *Nothofagus menziesii* tend to have more circular pith outlines in TS than internodes of *N. solandri var. cliffortioides* which tend to be more elongated. It was also noted that where the pith is depressed, there is a tendency for the secondary xylem, associated with that area of pith, to have an appearance similar to a diffuse aggregate ray. If the pith outline is irregular, then it is more likely to have depressed areas in it, than if it was circular in outline. Therefore, it is possible that an irregular pith outline may aid the longitudinal expansion of aggregate rays at their inception. To investigate this possibility pith and stem ratios from fluted and non-fluted species, and fluted and non-fluted areas of the same plant were compared.

The most pronounced affect of gibberellins on plants is cell elongation, though this may be accompanied by an increase in cell number (Métraux 1987). Auxins stimulate both cell enlargement and division (Davies 1987). It was noted in Chapter 3 that where the pith outline is elongated, this tends to correspond to the direction of the medial leaf-traces. Since the stem, node and leaf essentially form a continuum of structures (Howard 1974), it seems likely that this elongation of the pith, in the direction of the medial trace, is related to the formation of the leaves, especially with respect to cell elongation and division occurring in the procambium of the leaf-trace during internode elongation. It therefore seemed sensible to test the effects of factors that may change the ratio of cell elongation to cell division within the procambium, and how this affected pith outlines. It was therefore decided to investigate the affect of gibberellins and auxins on pith outlines.

In Chapter 2 it was shown that the phloem in the fluted region relating to the presence of aggregate rays, may have a deficit of sieve tubes in comparison to the non-fluted regions. Since sieve tube elements are a known pathway of non-polar auxin transportation, and auxin is an important factor in xylem differentiation (Roberts,

Gahan and Aloni 1988) it was decided to test the effects of applied auxin on the aggregate rays in mature wood.

4.2. MATERIAL

4.2.1. Three species comparison (stem ratios)

Material was selected from mature trees on the campus of the University of Canterbury. Ten trees each of *Nothofagus menziesii* and *N. solandri* were selected and 11 trees of *N. fusca*. From each tree two successive internodes (second and third from the apex) were selected from the current seasons growth.

4.2.2. Two species comparison (stem ratios)

Material was selected from mature trees on the campus of the University of Canterbury. Ten trees each of *N. menziesii* and *N. solandri* were selected, but only still expanding buds were chosen.

4.2.3. Two species comparison (pith ratios)

Material was selected from mature trees on the campus of the University of Canterbury. Seven trees each of *N. menziesii* and *N. solandri* were selected. Two fully expanded buds were selected from each tree. The middle three nodes were selected from each bud.

4.2.4. *Nothofagus solandri* var. *cliffortioides* comparison (pith ratios)

Material was collected from the Cass region in the Southern Alps of New Zealand. Individual trees were selected by line transect. In all, 39 plants were selected of varying ages. From each plant four internodes were selected.

4.2.5. *Nothofagus fusca* comparison

Material was selected from mature trees on the campus of the University of Canterbury. One obviously fluted branch and one not obviously fluted branch were selected from each of three trees.

4.3. METHODS

4.3.1. Stem ratios

Internodes were measured and then a TS cut from the middle. The long axis of the transverse outline of the stem (measured protophloem to protophloem, passing through the centre of the pith) and the axis perpendicular to the centre of the long axis (the short axis) were also measured. The stem ratio was calculated as short axis/long axis, this being the measurement of stem irregularity.

4.3.2. Pith ratios

These were calculated as per stem ratios except the long and short axes were measurements of the pith only (from protoxylem to protoxylem).

4.3.3. Two species comparison (stem ratios), marker for level of development

The sections were examined for the presence of phloem fibres (stained with aniline sulphate). Data were used for the first internode with phloem fibres (as measured from the apex) and the internode above it.

4.3.4. *Nothofagus solandri* var. *cliffortioides* comparison (pith ratios), variables collected

As well as the pith ratio, and the long and short axes lengths, classification variables were also collected for each tree. One classification variable was the relationship to the canopy, inside the canopy or outside the canopy. Large trees that were part of the canopy were regarded as being inside the canopy as this was where the internodes were sampled from. The other classification variable was whether the tree had any obvious fluting on the stem

4.3.5. *Nothofagus fusca* comparison (pith ratios - recent growth)

Internodes with two to three growth rings were selected. The branches from which they were selected all had ten or more growth rings.

4.3.6. *Nothofagus fusca* comparison (pith ratios - basal growth)

Three successive internodes were selected from the base of each branch.

4.3.7. The effect of applied GA3 and IAA

Seedling material of *N. fusca* and *N. menziesii* was used. Each species was subjected to three treatments (applied GA3, IAA, and shading) and a control. The GA3 and IAA treatments were applied at a concentration of 0.1%. The crystallised growth substances were firstly dissolved in 6 drops of ethanol and then made up to 5 ml with distilled water. The growth substances were applied as a spray from a small container. The container had a capacity that meant each plant received an average of 0.11 ml per application. Plants were sprayed every second day for 9 months. The control and the shade treatment were sprayed with distilled water. The shaded plants were placed under a canopy constructed of commercial shade cloth and received approximately 20% less light than other treatments.

4.3.8. Application of exogenous IBA

Six saplings of *N. solandri* var. *cliffortioides* all showing prominent fluting on their bark were selected. The stems were wounded as in Figure 4.1, and lanolin paste with 0.1% IBA was applied to the uppermost grooves of 3 plants. Three controls were also run, with the lanolin paste lacking IBA. The plants were left for 18 weeks, with the lanolin, and grooves, being refreshed every 2 weeks. After 18 weeks the stems were harvested and cut into 1 cm thick disks extending from 2 cm above the grooves, to 5 cm below. The surface of each disk was trimmed and examined with a dissecting microscope.

Figure 4.1

The position of the grooves cut in the stem of *Nothofagus solandri* var. *cliffortioides* for the application of IBA

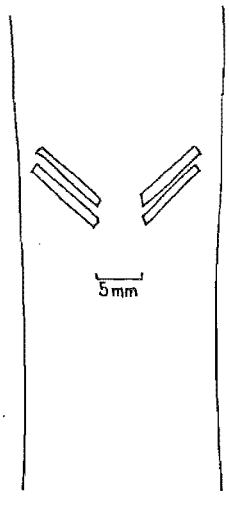

4.3.9. Statistical analysis

Where possible untransformed data or the best transformation available was used. A one-way ANOVA was calculated and significant means were examined by Gabriel's comparison of means for unplanned comparisons (95% confidence intervals). Correlation analysis was performed using Pearson's correlation coefficient. Where no acceptable transformation was available, non-parametric analysis was required. The Kruskal-Wallis test was used in lieu of an ANOVA although the ANOVA is a fairly robust test and copes well with reasonable departures from the assumptions of an ANOVA. The Kendall's τ test was used in lieu of parametric correlation analysis.

4.4. RESULTS

4.4.1. Stem and pith ratios

The 3 species comparison (stem ratios) showed there were significant differences in the 3 populations of long axis, short axis and ratio (Table 4.1). An analysis of the means, however, (Figure 4.2) showed that although there were significant differences in the means for long axis (Figure 4.2a) and short axis (Figure 4.2b) between the 3 species, there were no significant differences for ratio between *N. menziesii* and *N. solandri* var. *cliffortioides* (Figure 4.2c). The significant difference in the means between *N. fusca* and the other 2 species shows *N. fusca* was significantly more irregular in stem outline than either *N. menziesii* or *N. solandri* var. *cliffortioides*. As predicted, a species with aggregate rays (*N. fusca*) was shown to be more irregular in stem outline than a species lacking aggregate rays (*N. menziesii*). Since, however, there was no significant difference between the ratios of *N. menziesii* and *N. solandri* var. *cliffortioides* (which has aggregate rays), the significant F value, for the variable ratio, cannot be attributed to the presence of aggregate rays.

Table 4.1
Results of ANOVA for 3 species comparison (stem ratio)

variable	transformation	n	F value
long axis	log	62	45.19***
short axis	log	62	21.98***
stem ratio	log	62	16.81***

ns not significant, * P>0.05, ** P>0.01, *** P>0.0001

Figure 4.2.a
3 species comparison
(long axis)

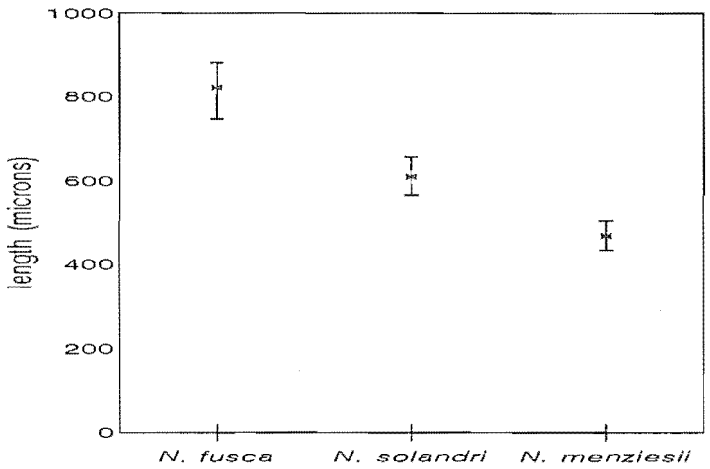

Figure 4.2.b
3 species comparison
(short axis)

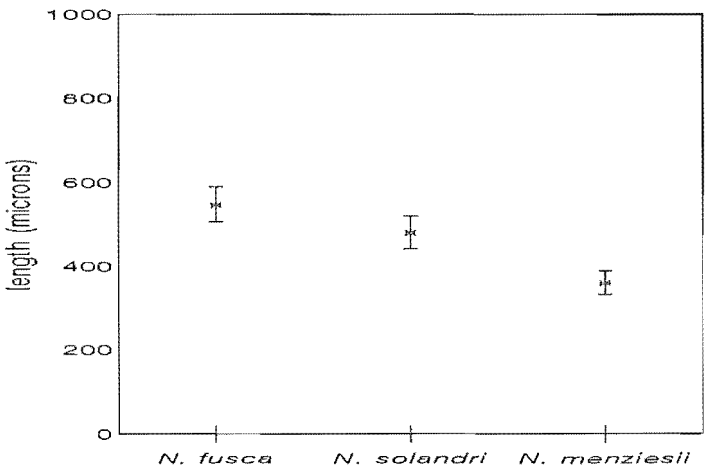

Figure 4.2.c
3 species comparison
(stem ratio)

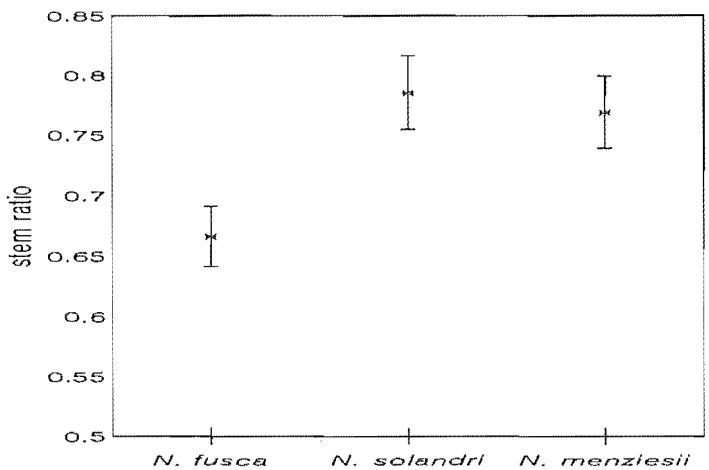

One source of error in the data above, was the relative maturity of the material examined. Although all the material was collected at the same time, and from roughly the same locality, this could not ensure that all the material was at an equivalent level of development. At the time the material was collected, buds of *N. menziesii* were fully expanded, whereas those of *N. fusca* and *N. solandri* var. *cliffortioides* were still in the process of expanding.

The results shown in Table 4.2 are from a more direct attempt to detect differences in stem ratio (2 species comparison [stem ratios]) between a species with aggregate rays and one without. Here the marker for the approximate level of development was the first appearance of phloem fibres, as stained with aniline sulphate. Again there are significant differences for the long and short axes but no significant differences for the ratio.

Table 4.2
Results of ANOVA for 2 species comparison (stem ratio)

variable	transformation	n	means		F value
			N. solandri	*N. menziesii*	
long axis	log	70	419 µm	523 µm	15.54**
short axis	log	70	327 µm	387 µm	10.68*
stem ratio	-	70	0.80	0.77	$2.71^{k,ns}$

^{k} Kruskal - Wallis test (χ^2 approximation), ^{ns} not significant, *P>0.05, **P>0.01, ***P>0.0001

A similar comparison of these 2 species (2 species comparison [pith ratio]), based on pith measurements, rather than whole stem measurements (and excluding attempts for equalisation of the level of development), does show a significant difference for the ratio (Table 4.3). There is, however, also a significant difference for the length of the internode, as the species with the most irregular pith outline (*N. solandri* var. *cliffortioides*) also has the longest internodes. This leaves open the possibility that the pith outline may be more a reflection of the length of the internode than an indication of the formation of aggregate rays. Correlation analysis[1] carried out for the entire dataset, however, showed no significant correlation of ratio with internode length.

1 Both parametric and non-parametric correlation analyses were performed, neither the Pearson coefficient of -0.1197 or the Kendall's τ of -0.095 ($P>\tau = 0.2006$) signifies any significant correlation between ratio and internode length.

Table 4.3

Results of ANOVA for 2 species comparison (pith ratio)

Variable	n	means		F value
		N. solandri	*N. menziesii*	
long axis	84	380 µm	350 µm	$0.73^{k,ns}$
short axis	84	221 µm	246 µm	$2.61^{k,ns}$
pith ratio	84	0.58	0.71	51.81***
internode length	84	6.9 mm	5.5 mm	5.66^{k}*

^{k} Kruskal - Wallis test (χ^2 approximation), ^{ns} not significant, * P>0.05, ** P>0.01, *** P>0.0001

Correlation analyses of the individual species (Tables 4.4 and 4.5) show strong correlations of long axis and short axis, with internode length for both *N. menziesii* and *N. solandri* var. *cliffortioides*, indicating an increase in the length of both axes with increasing internode length. Neither species shows a significant correlation of ratio with internode length, though a P>τ significance level of 0.097 for *N. solandri* var. *cliffortioides* (Table 4.4) is close enough to the 0.05 level to suspect there may be a correlation. Since, however, this correlation is positive (i.e. as internode length increases, ratio increases), it is extremely unlikely that the longer internodes of *N. solandri* var. *cliffortioides* are responsible for the more irregular pith outline in this species when compared to *N. menziesii.* This correlation can be attributed to short internodes where the irregular pith outline had been brought about by the close spacing of the leaves and departure of the leaf-traces.

Table 4.4

Non-parametric correlation of pith measurement variables versus internode length for *N. solandri* var. *cliffortioides*

variable	n	Kendall's τ	P>τ
long axis	42	0.496	0.0001
short axis	42	0.627	0.0001
pith ratio	42	0.178	0.0970

Table 4.5

Non-parametric correlation of pith measurement variables versus internode length for *N. menziesii*

variable	n	Kendall's τ	P>τ
long axis	42	0.473	0.0001
short axis	42	0.540	0.0001
pith ratio	42	-0.129	0.2302

Table 4.6 shows data from the *Nothofagus solandri* var. *cliffortioides* comparison. The data show that internodes collected under shade conditions tend to have smaller long and short axes, and more regular pith outlines than internodes collected under full sunlight conditions. Whether the trunk of the tree the internodes were collected from, was fluted or not, did not seem to be a significant feature in relation to the pith axes or the pith ratio, though a P>F of 0.0759 for the ratio is close enough to the P>F 0.0500 level to suggest a possibility that trees with fluted trunks have internodes with more irregular pith outlines. The figures for stem diameter are of particular interest here. It can be seen from this table that the largest trees tended to be: a) fluted and b) under the canopy[2]. In this instance stem diameter can be assumed to be a rough indicator of relative tree age. The age distribution of the trees among the 2 groups (fluting, shading) reflects 2 factors. The first factor is that the fluting associated with aggregate rays, tends not to appear as a feature of the external bark until after a few years growth. The second factor was that the stand of trees selected for this study, consisted of a central upper storey with seedlings and saplings beneath and further seedlings and saplings on the margins.

2 The internodes sampled from these trees were in shade conditions.

Table 4.6

Results of the Kruskal - Wallis test for *Nothofagus solandri* var. *cliffortioides* comparison

variable	means		$P>\chi^2$	means		$P>\chi^2$
	fluted n = 80	non fluted n = 76		in canopy n = 108	not in canopy n = 76	
long axis	286 µm	308 µm	0.7618	270 µm	357 µm	0.0002
short axis	199 µm	216 µm	0.1106	195 µm	234 µm	0.0023
pith ratio	0.70	0.73	0.0759	0.73	0.68	0.0117
stem diameter	124 mm	7 mm	0.0001	90 mm	15 mm	0.0001

Table 4.7 shows the correlation analysis for stem diameter verse pith ratio. The result for the total dataset (all the internodes examined) shows a significant negative correlation of pith ratio with stem diameter (as the stem diameter increases, the pith ratio tends to decrease - the stem outline becomes irregular). It would seem from this, that pith ratio may be a factor of tree age. When, however, the same correlation was performed with the data set split into 2 groups (shaded internodes and unshaded internodes), the shaded internodes produced the same correlation, increasing stem diameter relates to decreasing pith ratio (irregular pith outline). The unshaded internodes, however, do not show a significant correlation in this respect. It is beneficial, in this respect, to return to Table 4.5. Here the unshaded internodes have more irregular pith outlines than the shaded internodes, but tend to be from the younger trees. It would seem then that there are 2 factors (at least) effecting pith ratio: 1) the age of the tree and 2) an environmental feature or features, here represented by the degree of shading.

Table 4.7

Correlation of pith ratio with stem diameter (non-parametric) for *Nothofagus solandri* var. *cliffortioides* comparison

light conditions	Kendall's τ	n	$P>\tau$
shaded	-0.192	108	0.0022
not shaded	-0.102	48	0.3078
total	-0.125	156	0.0204

Tables 4.8.a and 4.8.b display data from the *N. fusca* comparison. Both the long and short axes show significant differences between fluted and non fluted branches for the recent growth, but show no significant differences for pith ratio. For basal growth, however, there are significant differences between fluted and non fluted branches for pith ratio. This provides further evidence that the presence of aggregate rays is related to an irregular pith outline, or that at the very least, an irregular pith outline is an indicator of the presence of aggregate rays. That the recent growth shows no significant differences between fluted and non fluted branches for pith ratio may indicate that aggregate ray are being formed in these areas[3].

Table 4.8.a

Results of ANOVA for *Nothofagus fusca* comparison (top growth)

variable	n	mean		F value
		fluted	non fluted	
long axis	60	549 µm	399 µm	36.08^{k***}
short axis	60	321 µm	244 µm	30.44^{k***}
pith ratio	60	0.56	0.59	1.94^{ns}

^{k} Kruskal - Wallis test (χ^2 approximation), ^{ns} not significant, * P>0.05, ** P>0.01, *** P>0.0001

Table 4.8.b

Results of ANOVA for *Nothofagus fusca* comparison (basal growth)

variable	n	mean		F value
		fluted	non fluted	
long axis	18	541 µm	351 µm	10.15^{k*}
short axis	18	250 µm	224 µm	$2.14^{k,ns}$
pith ratio	18	0.47	0.66	8.24^{k*}

^{k} Kruskal - Wallis test (χ^2 approximation), ^{ns} not significant, * P>0.05, ** P>0.01, *** P>0.0001

4.4.2. Application of plant growth substances

Tables 4.9.a and 4.9.b show the 3 treatments (IAA, GA3 and shading) had significant effects on long axis, short axis, pith ratio and internode length for *N. fusca*, and long

3 Aggregate rays are not clearly visible until after several years growth (Chapter 3).

axis and internode length for *N. menziesii.* A comparison of the mean pith ratios for the treatments (Figure 4.3) using Gabriel's comparison of means for unplanned comparisons, shows that none of the treatments is significantly different from the control for either species. It should, however, be noted that for *N. fusca* the GA3 treatment produced pith ratios significantly more irregular than both the IAA or shade treatments. For *N. menziesii* the only treatments that are significantly different from each other are GA3 and IAA.

Table 4.9.a

Results of ANOVA for the effects of plant growth regulators on *Nothofagus fusca* (class variable = treatment)

variable	n	F value	P>F
long axis	297	3.30	0.0207
short axis	297	3.16	0.0250
pith ratio	297	4.93	0.0023
internode length	297	32.93	0.0001

Table 4.9.b

Results of ANOVA for the effects of plant growth regulators on *Nothofagus menziesii* (class variable = treatment)

variable	n	F value	P>F
long axis	99	3.78	0.0130
short axis	99	0.86	0.4671
pith ratio	99	2.37	0.0752
internode length	99	12.77	0.0001

That the treatments also had an effect on internode length again raises the possibility there may be a correlation between internode length and pith ratio. Tables 4.10.a and 4.10.b show the figures for the correlation of internode length with pith ratio. For *N. fusca* there are significant correlations of internode length with pith ratio for GA3, IAA and shade, and for *N. menziesii* there is a significant correlation for GA3. Each of these correlations indicates that as internode length increases so does the pith ratio (the pith outline became more circular). The Gabriel comparison of means for internode length (Figure 4.4) indicated the GA3 treatments produced the longest

Figure 4.3.a
Nothofagus fusca
(pith ratio)

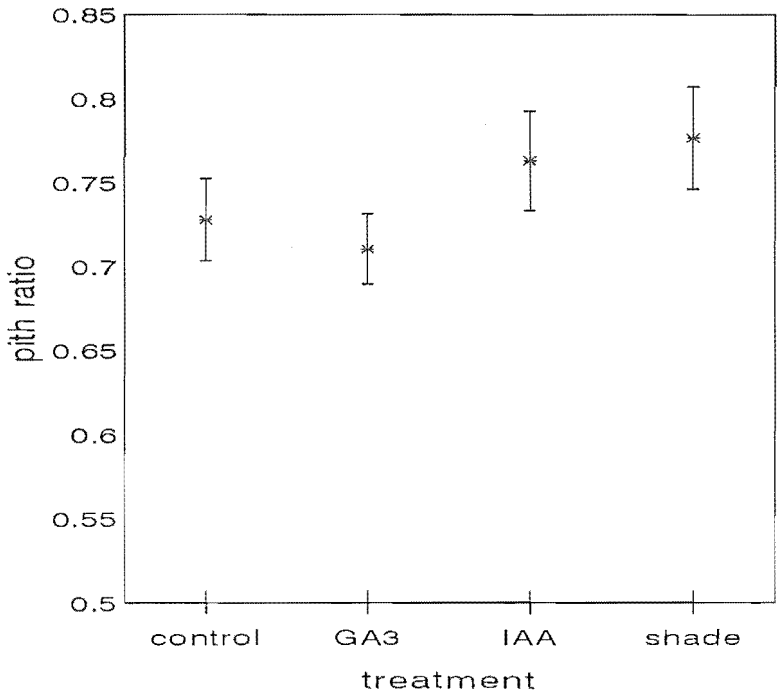

Figure 4.3.b
Nothofagus menziesii
(pith ratio)

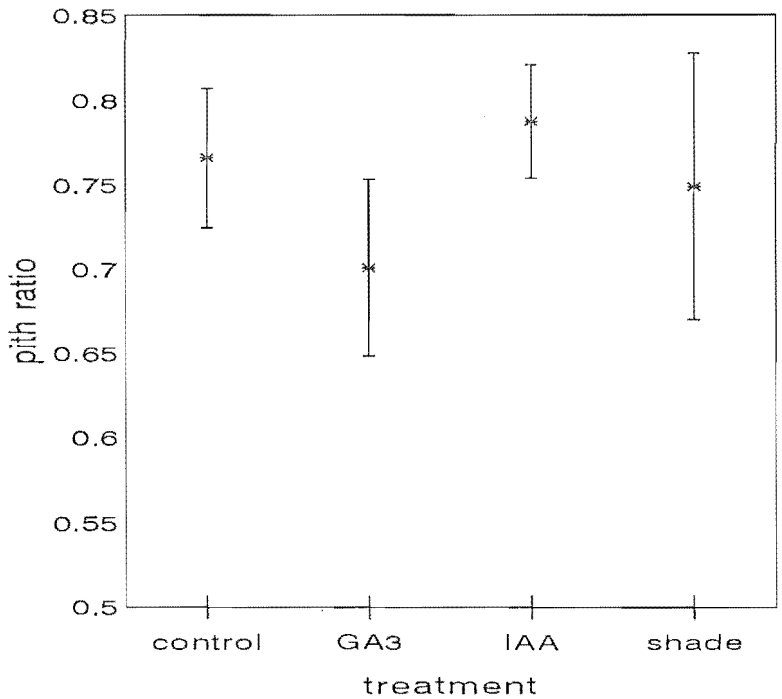

Figure 4.4.a
Nothofagus fusca
(internode length)

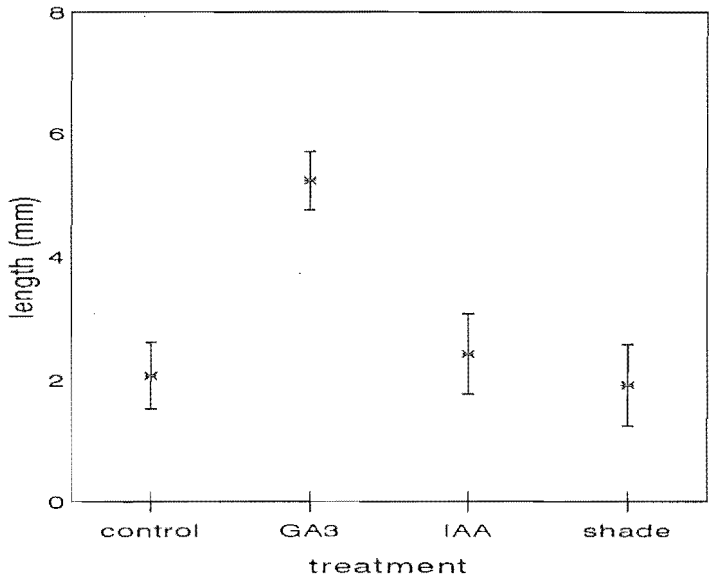

Figure 4.4.b
Nothofagus menziesii
(internode length)

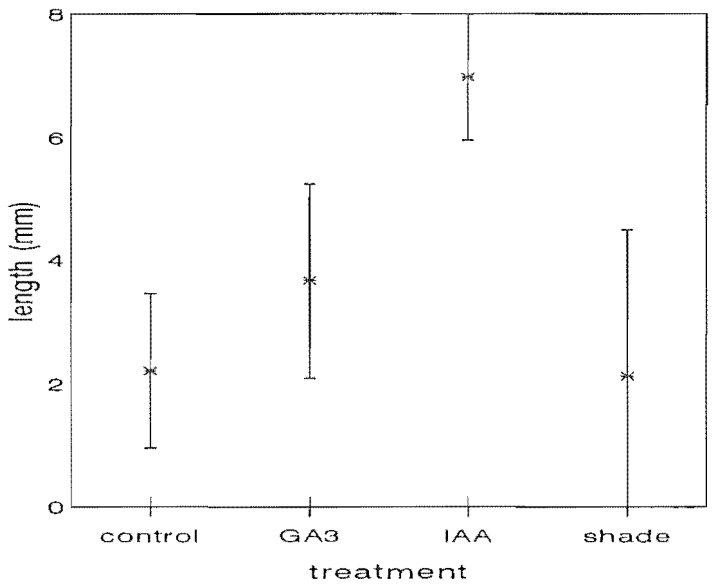

internodes for *N. fusca*, but this treatment also produced the most irregular pith outline. It is unlikely, therefore, that the differences in pith ratio between the treatments is a reflection of internode length. In fact internode length shows relatively little effect on pith ratio even though significant correlations were shown. The greatest R^2 shown for any of the correlations is 0.48398 for the GA3 treatment on *N. menziesii*, yet this figure means that approximately only 48% of the variation in pith ratio can be accounted for by the variation in internode length, or more importantly, that 52% of the variation in pith ratio cannot be accounted for by variation in internode length. It should also be noted from Figure 4.4 that although GA3 produced the most irregular pith outlines in *N. menziesii*, it is the IAA treatment that produced the longest internodes.

Table 4.10.a

The effect of applied plant growth substances on the correlation of internode length versus pith ratio (*Nothofagus fusca*)

treatment	n	coefficient	R^2	P>|R|
control	80	0.21914	0.04802	0.0508
GA_3	109	0.30499	0.09302	0.0013
IAA	55	0.31595	0.09982	0.0188
shade	53	0.43715	0.19110	0.0011

Table 4.10.b

The effect of applied plant growth substances on the correlation of internode length versus pith ratio (*Nothofagus menziesii*)

treatment	n	coefficient	R^2	P>|R|
control	29	0.18569	0.03448	0.3348
GA_3	18	0.69569	0.48398	0.0013
IAA	44	0.21713	0.04715	0.1568
shade	8	0.63074	0.39783	0.0936

Although much of these data showed significant differences when subjected to statistical tests, the data, especially for *N. menziesii*, should be regarded with caution. Five plants were used for each species, for each treatment, but a number of plants died during the experiment (possibly due to infestations). Since a maximum of 2

plants could be harvested for *N. menziesii* for each treatment (Table 4.11) the results are open to question. A minimum of 3 plants per treatment for *N. fusca* is probably acceptable, though more would have been desirable.

The application of exogenous IBA had no visible effect on existing aggregate rays.

Table 4.11

The number of plants and internodes harvested from each of the plant growth substance applications

treatment	*N. fusca*		*N. menziesii*	
	n (plants)	n (internodes)	n (plants)	n (internodes)
control	4	80	2	29
GA_3	3	109	1	18
IAA	3	55	2	44
shade	4	53	1	8

4.5. DISCUSSION

The correlation between an irregular pith outline and the formation of aggregate rays is supported by two lines of evidence. Firstly, both *N. fusca* and *N. solandri* var. *cliffortioides* (with aggregate rays) have pith outlines significantly more irregular than *N. menziesii* (without aggregate rays). Secondly, branches of *N. fusca* lacking significant aggregate rays, have significantly less irregular pith outlines than branches with significant aggregate rays. This evidence is, however, only circumstantial as no direct association could be found between an irregular stem outline and the presence of aggregate rays, associated with that internode. The reason for this is the difficulty in identifying aggregate rays within the first few growth rings, and the tendency for aggregate rays to become longitudinally extensive, anastomose with each other, and become far longer than the original internode (Chapter 3). The continuation of the IAA - GA3 application experiment could have provided this direct evidence, but this would have meant the maintenance of the experiment for at least 2 years, complete with frequent applications of the growth substances. This was not feasible for this study. Accepting the evidence is circumstantial, it still seems likely that an irregular pith outline tends to indicate the formation of aggregate rays.

The results of the *N. solandri* var. *cliffortioides* comparison show that in general terms the youngest plants have more circular pith outlines than older plants, and by extrapolation, are less likely to form aggregate rays. One of the noticeable features of natural stands of *Nothofagus* are the suppressed seedlings that occur under the closed canopy (the so called advance growth pool). With the opening of the canopy the suppression is released and the seedlings grow into mature trees, showing no negative effects of their previous suppression. Up to 70% of trees may have passed through this advanced growth stage. It is assumed that light is the controlling factor in the suppression of the seedlings though root competition for water and nutrients probably also plays a role (Wardle 1984).

Natural daylight contains approximately equal proportions of red (R) and far red (FR) light, but light within the leaf canopy contains a higher proportion of FR light. The highest proportion of the FR state of the photoreceptor phytochrome (P_{fr}) occurs in natural daylight, but there is a relationship between stem extension and the proportion of P_{fr}, with higher levels of FR light (i.e. shading) resulting in less stem extension (Waring and Phillips 1982). It is thought this response is related to the production of a growth substance active in stem extension, possibly a gibberellin (Morgan and Smith 1978).

Nothofagus solandri var. *cliffortioides* plants growing outside the canopy tend to have more irregular pith outlines than those growing inside the canopy, and this may reflect differences in the amount of growth occurring within these 2 light regimes. The more circular pith outlines of epicormic branches in *N. fusca* may also reflect a light differential. That the application of exogenous GA3 also produced significantly more irregular pith outlines than IAA for both *N. fusca* and *N. menziesii*, supports the hypothesis that gibberellins may be involved, to a large degree, in the stem extension of those plants not in state of suppressed growth (with irregular pith outlines), and are therefore more likely to produce aggregate rays. *Nothofagus menziesii* plants also go through this advanced growth stage followed by a 'release' with the opening of the canopy, yet they do not produce aggregate rays to any great extent. There are several features that may account for this. Firstly, *N. menziesii* tends to be more shade tolerant and slower growing than other New Zealand species of *Nothofagus* (Wardle 1984). Secondly, and more importantly, *N. menziesii* appears to have a different physiological response to GA3, than a species with aggregate rays (*N. fusca*). Although the application of GA3 produced significantly irregular pith outlines for both *N. menziesii* and *N. fusca*, there were different responses in terms of internode length, with GA3 producing internodes significantly longer than the control, or other

treatments, for *N. fusca*, but no significant increase in length for *N. menziesii*. For this species it was the application of IAA that produced the largest internodes.

The observations made on the variability of pith ratios in *N. solandri* var. *cliffortioides* takes on a greater significance when compared to the situation in *Alnus rubra* (Betulaceae) reported by Noskowiak (1978). Noskowiak noticed that within the lower half of the trunk of *A. rubra* there was often a cone shaped zone of juvenile wood, where aggregate rays were virtually absent. Juvenile and adult wood above, and adult wood surrounding this zone, however, contained aggregate rays. It would be expected from the relationships recorded above that internodes from seedlings and saplings of *A. rubra* would have more circular outlines than mature trees, mirroring the situation in *N. solandri* var. *cliffortioides*. *Alnus rubra*, however, unlike *Nothofagus*, does not go through an advanced growth pool stage. In fact *A. rubra* is quite the opposite, and is a vigorous pioneer with rapid juvenile growth which tapers off after 3 to 5 years (Newton, El Hassan and Zavitkovski 1968). Both *Nothofagus* (Wardle 1984) and *A. rubra* (Ruth 1968) prefer some shade for greater seedling survival, but *A. rubra* also shows a curvilinear relationship between seedling height and relative solar radiation (Ruth 1968). Seedling height increases with increasing solar radiation, until solar radiation reaches 30 to 40%, after which seedling height tends to decrease. It seems, therefore, that the rapid initial growth in *A. rubra* and the release from suppression in *Nothofagus* represent different responses to available light. What is clear from this, is that the physiology of stem elongation with respect to light availability warrants further investigation, especially in respect to the different responses exhibited by *N. menziesii* and *N. fusca* to IAA and GA3.

Due to the complex nature of the interactions of plant growth substances within any developmental tissue, it is difficult to speculate on how different levels of growth substance may be producing a particular outcome. A detailed study on the effects of various growth substances on the pith ratios' of plants would be necessary for any meaningful discussion on how this effect had been brought about.

Throughout this chapter, pith irregularity has been measured as a fraction of short pith axis over long axis. As the long axis becomes longer, in comparison to the short axis, the ratio decreases and the pith is regarded as being irregular. *Nothofagus* has an alternate phyllotaxis, with the long axis usually bisecting the medial leaf trace, and the short axis corresponding to the lateral leaf traces. The irregular pith outline induced by GA3 may relate to this phyllotaxis and the relative rate of cell elongation versus cell division in the elongating internode.

It seems likely that gibberellins may play a role in the formation of the aggregate rays of *Nothofagus*, and possible that the application of auxins may inhibit aggregate ray formation. That the introduction of exogenous IBA into stems seemed to have no effected on the aggregate rays in *Nothofagus solandri* var. *cliffortioides*, is at odds with Lev-Yadun and Aloni (1991a). These authors suggested that an increase in auxin induced by partial stem girdling, results in the dispersal of aggregate rays in *Quercus ithaburensis* and *Q. calliprinus,* by enhancing the differentiation of fusiform initials into vascular elements. There are 3 possible reasons for this discrepancy: 1) the IBA was not administered for long enough to elicit any noticeable response; 2) the results described by Lev-Yadun and Aloni (1991a) may be the result of other factors, and not just an increase in auxin; and 3) the aggregate rays of *Quercus* and *Nothofagus* are significantly different from each other to make a comparison meaningless. As shown in Chapter 2, the aggregate rays of *Quercus* tended to have a compound nature (entire aggregate rays) whereas *Nothofagus* has diffuse aggregate rays, and as such, may already represent the dispersed condition of the compound aggregate ray.

CHAPTER 5

THE ANALYSIS OF ELONGATION AND DIVISION IN THE CAMBIUM, BASED ON THE DISTRIBUTION OF CELL LENGTH DATA

5.1. INTRODUCTION

It is widely accepted that the lengths of fusiform initials are reflected in their derivatives, especially the tracheids in gymnosperms, and the vessel elements in dicotyledons. Fusiform initial length is governed by 2 variables: 1) the frequency of pseudotransverse anticlinal divisions; and 2) the rate of elongation of the daughter initials (Bannan 1957b, 1959, 1965, Cumbie 1967, Denne and Whitbread 1978, Philipson, Ward, Butterfield 1971).

In non-storeyed cambia, the walls dividing the parent cells in anticlinal divisions are pseudotransverse, whereas in storeyed cambia, they tend to be radial (Bailey 1923). High frequencies of pseudotransverse anticlinal divisions tend, therefore, to suppress the mean cell length, as the dividing fusiform initial produces 2 shorter daughter initials (Bannan 1957b, Cumbie 1967), whereas anticlinal divisions in storeyed cambia result in 2 daughter initials the same length as the parent.

High frequencies of pseudotransverse anticlinal division are accompanied by faster rates of cell elongation of the initials, reducing the extent to which mean cell length is suppressed (Bannan 1959). Although large numbers of initials are lost from the cambium (more daughter initials are produced than are actually required for an increase in girth - Bannan 1950b), the longest initials are more likely to survive with the very shortest being lost (Bannán and Bayly 1956). These processes, along with the tendency for pseudotransverse divisions to occur near the centre of the fusiform initials (Bannan 1951), would effectively result in a minimum length for fusiform initials.

Commonly in nature, frequency distributions for continuous variables (such as cell length) follow a normal distribution. This means that most of the observations are clustered around the mean value, with decreasingly fewer observations occupying the extremes (Figure 5.1.a). If the shortening of cambial initials by pseudotransverse

anticlinal divisions results in shorter daughter initials, and if, in turn, the very shortest daughter initials were less likely to survive (Figure 5.1.b), then this would result in a cambium where a sample of cambial initials would not show a normal distribution for their lengths, but would tend to be (+) skewed (right skewed - Figure 5.1.c).

In order to test this hypothesis, it was decided to investigate whether samples of wood element lengths were (+) skewed, where it was expected that high levels of pseudotransverse anticlinal divisions were occurring. The highest frequency of anticlinal divisions occur late in the growth increment (Bannan 1950b, Cumbie 1967, Evert 1961), this area would, therefore, be expected to have element length measurements that were (+) skewed. The derivatives of a storeyed cambium are also of interest, as here the anticlinal division of fusiform initials does not result in a decrease in length, and a significant trend for (+) skewed samples would not be expected.

If it could be shown that high levels of pseudotransverse anticlinal divisions were more likely to produce a (+) skewed distribution, then the distribution of a dataset may possibly be used as an indicator of relative cambial activity.

5.2. MATERIALS

All the specimens were obtained from the wood collection held by Dr. BG Butterfield at the University of Canterbury. All had been fixed in Formalin - Acetic - Alcohol (FAA) and stored in 70% alcohol. Table 5.1 lists the specimens used.

Figure 5.1

The effect of the loss of short fusiform initials on the data distribution

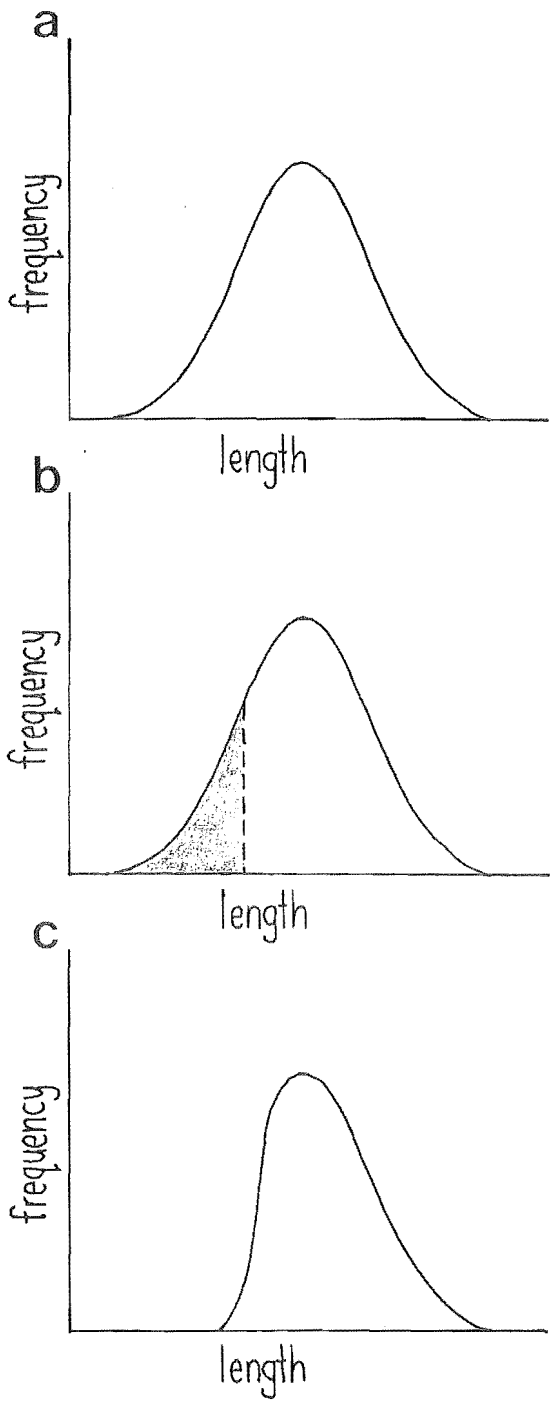

a. Normal distribution.
b. The shaded area represents fusiform initials that are too short and are lost from the cambium.
c. The resulting (+) skewed (right skewed) distribution.

Table 5.1

Specimens held in the wood collection of Dr. BG Butterfield and used in Chapter 5

specimen number	species
25	*Dacrycarpus dacrydioides*
384	*Dacrycarpus dacrydioides*
599	*Dacrycarpus dacrydioides*
142	*Hoheria angustifolia*
571	*Hoheria angustifolia*
572	*Hoheria angustifolia*
57	*Nothofagus menziesii*
66	*Nothofagus menziesii*
585	*Nothofagus menziesii*

5.3. METHODS

5.3.1. Sampling wood areas

For each specimen, a block of wood consisting of two full years' growth, was sampled. This block was approximately 1 to 2 mm wide (tangentially) and approximately 1 cm long (to minimise the effects of sampling near the cut surfaces).

Each years' growth was divided tangentially into 4 equal parts. The first quarter of each years' growth was designated as zone 1, the second quarter as zone 2, the third quarter as zone 3 and the fourth quarter as zone 4. For the purposes of graphical presentation the zones in the first growth (1 to 4) were designated as positions 1 to 4. The zones in the second growth ring were designated as positions 5 to 8.

5.3.2. Maceration of specimens

Each of the zones, from each specimen, were macerated in a 1:1 solution of hydrogen peroxide (50%) and glacial acetic acid, placed in a boiling tube and boiled in a water bath (Patel and Shand 1985). To ensure the complete separation and random dispersion of cells, with minimal damage, the macerates were agitated using a micropipette. Macerations were mounted on slides (2 per maceration), in glycerine gel.

5.3.3. Wood elements sampled

The wood elements sampled and measured for each species are shown on Table 5.2

Table 5.2

The wood elements sampled for each species

species	wood element
Dacrycarpus dacrydioides	tracheids
Hoheria angustifolia	fibres, vessels
Nothofagus menziesii	fibres, vessels

5.3.4. Method of sampling

Measurements were made on an Olympus BH2 light microscope, with an eye-piece graticle. The graticle was aligned vertically. Vertical 'sweeps' were made down each slide with a set distance between each 'sweep', that was considered to be greater than the maximum length of the wood elements being measured.

For the measurement of fibres and tracheids, an element was sampled when the 'tip' of the element[1] 'crossed' or 'touched' the graticle. This minimised the chances of obtaining a biased sample, as 'tips' of all elements had an equal chance of coming into contact with the graticle, regardless of their lengths.

All vessel elements that 'crossed' or 'touched' the graticle were sampled. This was done for two reasons: 1) there were generally far fewer vessel elements per slide than fibres; 2) vessel elements generally tended to be less variable than fibres and tracheids in length, and therefore less susceptible to sample bias.

To avoid sampling adjacent elements an element was not sampled until the previously sampled element was out of view. Twenty elements were sampled from each slide and the data from the 2 slides for each zone were pooled.

1 The tip of an element was specified as a length that was less than half of the probable length of the shortest element

Vessels of *H. angustifolia* were measured from the centres of the perforation plates to obtain an estimate of fusiform cambial initial length, as suggested by Philipson, Ward and Butterfield (1971).

5.3.5. The computer generation of elongating and dividing samples using SAS

Two algorithms were written using SAS. One algorithm represented the elongation of fusiform cambial initials, and the elongation of elements differentiating from those initials. The second algorithm represented anticlinal divisions of the cambial initials. Both algorithms made use of the same base population. Both algorithms are described below in a slightly stylised format that accurately represents the intent and function of the algorithms. A number of the steps involved in SAS programs are implicit in the SAS system, therefore, some of the datasets generated do not have to be named in the algorithm, but have been included in the descriptions for the sake of clarity. The actual programs are contained in Appendix 2.

5.3.5.1. The base population

A base population of 20 observations was generated by random number generator. Each observation represented the length of a fusiform cambial initial. The population was normally distributed, and had a mean length of 100 (actual units are immaterial) and a skew approaching zero.

5.3.5.2. Elongation algorithm with two stages of elongation

Each length measurement (variable name = **LENGTH**) in the base population was increased by an elongation factor (variable = **EF**) with the resulting length being a variable named **LENGTH1**. This represents the elongation of fusiform cambial initials. The resulting dataset (INITIALS), consisting of 20 observations, was copied to a dataset designated as CAMBIUM. The INITIALS dataset was then increased by **EF** (further elongation during the differentiation of the initials into xylem elements), with the resulting length being a variable named **LENGTH2**, in a dataset designated INITIALS2. This was copied to a dataset designated as DERIVATIVES. INITIALS then became the base population and the above process was executed a further 9 times. At each run, the datasets CAMBIUM and DERIVATIVES were increased by 20 observations, each having 200 observations after 10 executions. The base population was always kept at 20 observations. This algorithm is represented by Figure 5.2.

Figure 5.2

Elongation algorithm with 2 stages of elongation

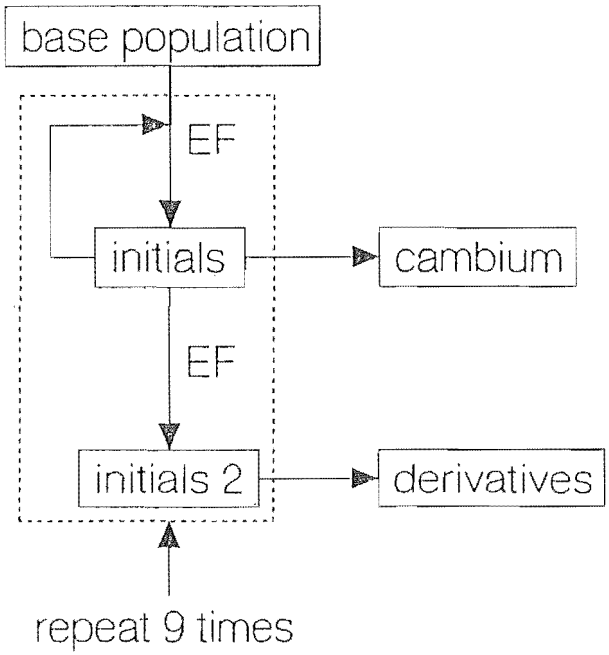

(see text for details).

Figure 5.3

The angle of the division plane in the cambial initial

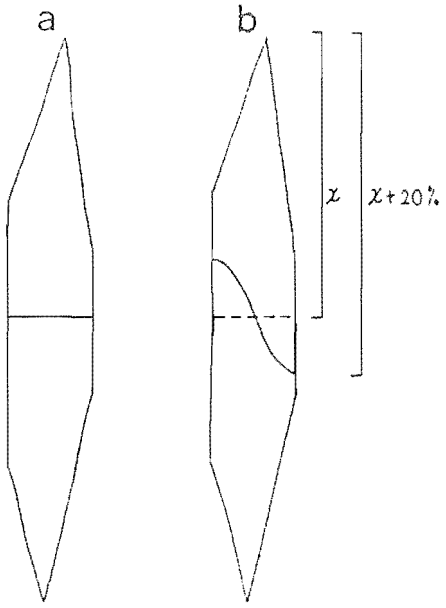

(see text for details).

a. PT = 0 (transverse).

b. PT = 0.2 (pseudotransverse anticlinal).

The overall intention of this algorithm is to represent a set of fusiform cambial initials (INITIALS), which elongate over a period of time and produce derivatives arising by further elongation during differentiation into xylem elements. The dataset CAMBIUM represents the increasing length of the initials over a period of time. The dataset DERIVATIVES, however, represents the length of the derivatives (derived from CAMBIUM) over a period of time, and thus incorporates 2 periods of elongation.

Elongation was performed in 3 ways (Table 5.3). Elongation equation 1 assumes the amount of elongation is proportional to **LENGTH** (long cells elongate more than short cells). Elongation equation 2 assumes the amount of elongation is fixed and not proportional to **LENGTH** (short cells can elongate as much as long cells). Elongation equation 3 assumes the amount of elongation is proportional to **LENGTH**, but that once a maximum length is reached, no further elongation will take place (long cells elongate more than short cells, but only to a maximum length).

Table 5.3

Elongation equations used in the elongation algorithm with 2 stages of elongation

equation number	elongation equation
1	length = length + (length * EF)
2	length = length + EF
3	length = length + (length * EF)
	LENMAX = 175

Three values of **EF** were used, and were based on 5%, 10% and 15% of the mean cell length of the base population.

5.3.5.3. Division algorithm

Each observation in the base population was assigned a random value (variable name = **DIVIDE**) between 0 and 1. This variable was generated in such a way that 50 percent of the population received a value of 0.5 or greater, 30% of 0.7 or greater, 10% of 0.9 or greater. Only those observations that exceeded a minimum value of **DIVIDE**, were permitted to undergo anticlinal/transverse division (if **DIVIDE** = 0.1

then 90% of the observations were permitted to divide). Allowable values of **DIVIDE** ranged from 0.1 (90% of the sample) to 0.99 (1% of the sample).
A minimum length of an initial that was allowed to divide (**LENMIN1**), was set. The value for **LENMIN1** determined the distribution, from which the minimum length for an initial before it could divide, was sampled. The base population had a mean of 100, if **LENMIN1** was 90, then the minimum length for division was sampled from a population with a mean of 90. This would include most of the base population. If **LENMIN1** was 110, then the minimum length for division was sampled from a population with a mean of 110 and would include, mostly, only the very longest initials in the base population. Values of **LENMIN1** ranged from 90 to 110. Both **DIVIDE** and **LENMIN1** determined whether a fusiform initial was to divide.

If a fusiform initial was to divide, the position of the division was determined by another random number with a mean value of 0.5 (most of the dividing walls were centred on a position half way up the length of the initials and most of the initials would divide in half). Another random variable (variable name = **PT**), determined the angle of the division. If **PT** = 0 the division was transverse. Increasingly greater values of **PT** signify increasingly greater degrees of pseudotransverse divisions (Figure 5.3). Values of **PT** ranged from 0 to 0.9.

If the resulting cells were less than a minimum length (variable name = **LENMIN2**), they were deleted from the dataset. Two values of **LENMIN2** were used, 10 and 20 (10% and 20% respectively of the mean length of the observations in the base population). Cells were elongated by a mean elongation factor (variable name = **EF**). Two values of **EF** were selected, 0.00 (0% increase) and 0.02 (2% increase). Those initials that were not selected to divide were simply elongated by **EF**.

All initials were assigned an extinction value (variable name = **EXTINCT**) between 0 and 1. If 10% of initials were to be lost from the dataset then **EXTINCT** was set at 0.90, if 1% were to be lost then **EXTINCT** was set at 0.99.

The resulting dataset was appended to the original base population, resulting in an output dataset with the number of observations depending on **DIVIDE**, **LENMIN1**, **LENMIN2** and **EXTINCT**. The divided and elongated dataset was put through the same process again (Figure 5.4), as with the elongation algorithm.

The overall intention of this algorithm, is to represent a set of fusiform cambial initials that are undergoing a continuous period of anticlinal division. Elongation is also a

Figure 5.4

Division algorithm

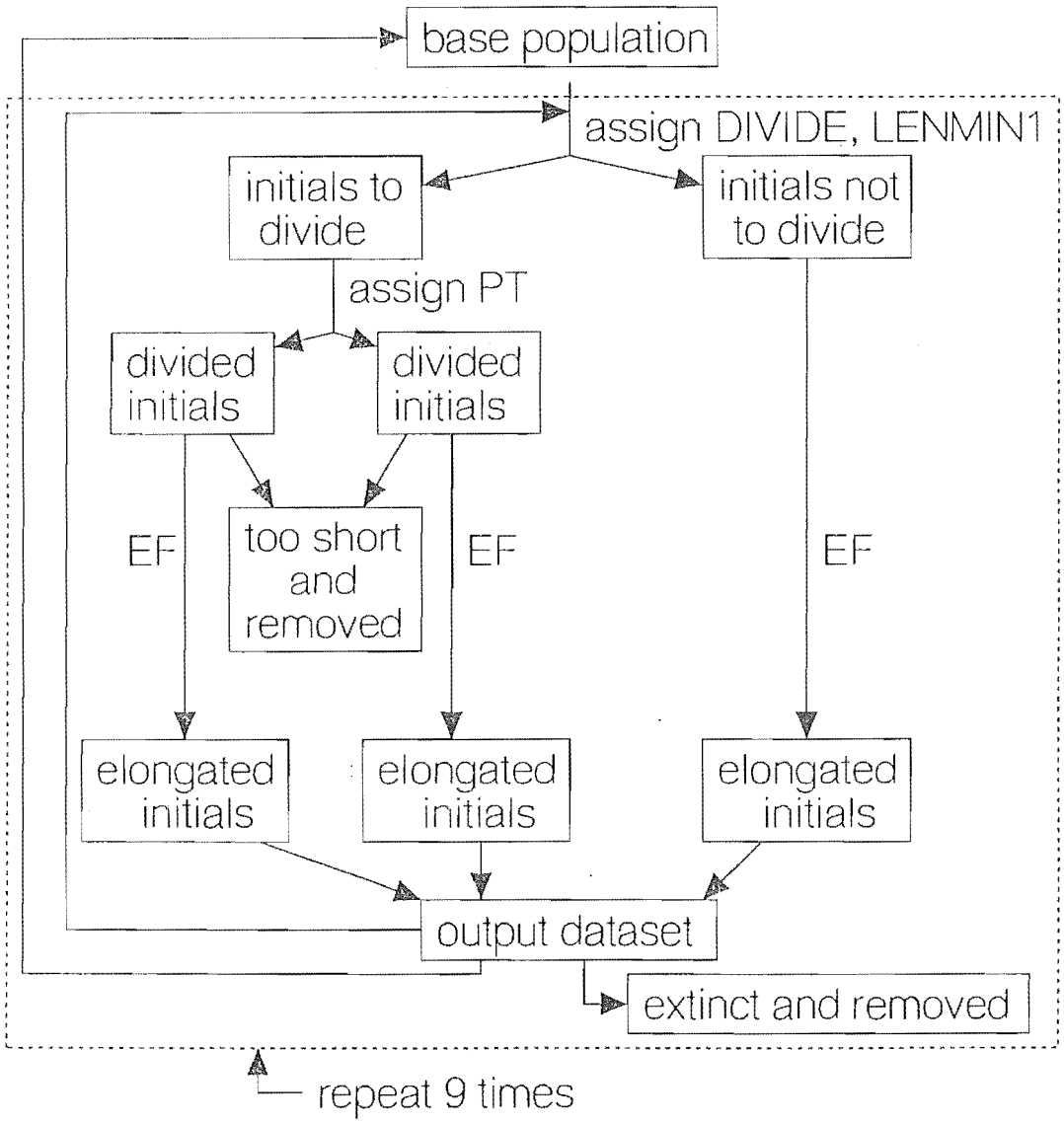

(see text for details).

factor in the algorithm, and it should be noted that new initials are elongated in the same fashion as existing initials. The most important variable (in terms of its effect on the skew of the final dataset) is **LENMIN1**. This variable sets a theoretical lower limit, below which fusiform initials ceased to function as fusiform initials, and declined or became ray initials.

5.3.6. Analysis of wood element length and output from algorithms

The skews of the length measurements were calculated using SAS. The significance of each skew was calculated by a method for small sample sizes (D'Agostino and Tietjen 1973).

5.4. Results

5.4.1. Measurement of wood elements

Aggregated skew data for each zone, and each species, is shown in Table 5.4. Tables 5.5.a to 5.5.c show the zone data aggregated for each species, and analysed using χ^2 analysis.

Table 5.4

Aggregated skew data for each species

species	elements	position							
		1		2		3		4	
		skew		skew		skew		skew	
		+	-	+	-	+	-	+	-
Dacrycarpus dacrydioides	tracheid	3	3	2	4 (2)	4	2	2	4
Nothofagus menziesii	fibre	2	4	4	2	2	4	2	4
	vessel	5	1	1	5	3	3 (1)	4	2
Hoheria angustifolia	fibre	1	5 (3)	3 (1)	3 (1)	0	6 (1)	0	6 (2)
	vessel	0	6 (3)	0	6 (1)	3 (1)	3	1	3 (2)

numbers in brackets represent the number of samples showing a significant value for skew

The samples of tracheids, of *D. dacrydioides*, have a slightly greater tendency to be (-) skewed than (+) skewed. The difference is, however, not significant (Table 5.5.a) The samples from *N. menziesii* show fibres tending to be (-) skewed, and vessels (+)

skewed. However these differences are again not significant (Table 5.5.b). There are, however, significant differences shown for the samples from *H. angustifolia*. From Table 5.5.c it is clear that samples tend to be (-) skewed, and relatively few are (+) skewed. Both fibres and vessels show this tendency and there are no significant differences between them.

Table 5.5.a

Skew data recorded for *Dacrycarpus dacrydioides*

element	(+) skew	(-) skew	χ^2
tracheids	11	13	0.16^{ns}

^{ns} not significant, * P>0.05, ** P>0.01, *** P>0.0001

Table 5.5.b

Skew data recorded for *Nothofagus menziesii*

element	(+) skew	(-) skew	χ^2
fibres	10	14	
vessels	13	11	$0.76^{t,ns}$

$^{t}\chi^2$ for entire table, ^{ns} not significant, * P>0.05, ** P>0.01, *** P>0.0001

Table 5.5.c

Skew data recorded for *Hoheria angustifolia*

element	(+) skew	(-) skew	χ^2
fibres	4	20	7.20^{s**}
vessels	4	20	$0.00^{t,ns}$

$^{t}\chi^2$ for entire table, $^{s}\chi^2$ for 1 comparison of (+) and (-) skews, ^{ns} not significant, * P>0.05, **P>0.01, *** P>0.0001

Tables 5.6.a to 5.6.e show the data rearranged in such a way that early wood and late wood (zones 1 and 4), are grouped together, and compared with the centre of the growth increment (zones 2 and 3).

For *D. dacrydioides* there are no significant differences in the skew of the samples, based on the position in the growth increment (Table 5.6.a). This is also the case for the fibres of *N. menziesii* (Table 5.6.b). There is, however, a greater tendency for the samples of fibres in the early/late wood to be (-) skewed. The vessel elements of *N. menziesii* however, do show significant differences (Table 5.6.c), there being a greater tendency for (+) skews in the early/late wood, and for (-) skews in the centre of the growth increment. It would appear, therefore, that there is a difference between vessels elements and fibres based on their position in the growth increment.

Table 5.6.a

Skew data recorded for *Dacrycarpus dacrydioides* tracheids based on the position in the growth increment

skew	early/late wood	centre of growth ring	χ^2
(+)	5	6	
(-)	7	6	$0.17^{t,ns}$

$^{t}\chi^2$ for entire table, $^{s}\chi^2$ for 1 comparison of (+) and (-) skews, ^{ns} not significant, * P>0.05, ** P>0.01, *** P>0.0001

Table 5.6.b

Skew data recorded for *Nothofagus menziesii* fibres based on the position in the growth increment

skew	early/late wood	centre of growth ring	χ^2
(+)	4	8	
(-)	8	6	$0.69^{t,ns}$

$^{t}\chi^2$ for entire table, $^{s}\chi^2$ for 1 comparison of (+) and (-) skews, ^{ns} not significant, * P>0.05, ** P>0.01, *** P>0.0001

Table 5.6.c

Skew data recorded for *Nothofagus menziesii* vessel elements based on the position in the growth increment

skew	early/late wood	centre of growth ring	χ^2
(+)	9	3	
(-)	4	8	4.20^{t*}

$^{t}\chi^2$ for entire table, $^{s}\chi^2$ for 1 comparison of (+) and (-) skews, ^{ns} not significant, * P>0.05, ** P>0.01, *** P>0.0001

Table 5.6.d

Skew data recorded for *Hoheria angustifolia* fibres based on the position in the growth increment

skew	early/late wood	centre of growth ring	χ^2
(+)	1	3	
(-)	11	9	$1.20^{t,ns}$

$^{t}\chi^2$ for entire table, $^{s}\chi^2$ for 1 comparison of (+) and (-) skews, ^{ns} not significant, * P>0.05, ** P>0.01, *** P>0.0001

Table 5.6.e

Skew data recorded for *Hoheria angustifolia* vessel elements based on the position in the growth increment

skew	early/late wood	centre of growth ring	χ^2
(+)	1	3	
(-)	11	9	$1.20^{t,ns}$

$^{t}\chi^2$ for entire table, $^{s}\chi^2$ for 1 comparison of (+) and (-) skews, ^{ns} not significant, * P>0.05, ** P>0.001, *** P>0.0001

There are no significant differences for *H. angustifolia* based on the position in the growth increment for either fibres (Table 5.6.d), or vessels elements (Table 5.6.e).

The tables referred to above show all the skew data. It was hoped that only significant skews would be used for this analysis, however, there were generally too few significantly skewed samples to indicate any significant differences in skew.

Aggregated kurtosis data for each zone, and each species, is shown in Table 5.7. Results of note here are those for the vessel elements of *H. angustifolia.* These samples show a significant tendency (χ^2 = 4.17, P>χ^2 = 0.05) to be (+) kurtosed, indicating that the data tends to be relatively tightly aggregated around the mean value. The fibres of *H. angustifolia* also show this tendency for the significantly kurtosed samples, with 9 samples (+) kurtosed and only 1 sample (-) kurtosed (χ^2 = 6.4, P>χ^2= 0.025). The samples of *N. menziesii* vessel elements, showed a tendency to be (-) kurtosed, however, the χ^2 value of 2.67 for this is just below a significant value at the 10% level. This indicates that the data tends to be relatively loosely aggregated around the mean value. Also of note are the samples of *D. dacrydioides* tracheids, where a significant kurtosis was recorded. These showed a significant

tendency to be (+) kurtosed in the centre of the growth increment, and (-) kurtosed at the ring boundary ($\chi^2 = 4.44$, $P>\chi^2 = 0.05$). This provides circumstantial evidence that elongation tends to produce length data more tightly aggregated than pseudotransverse anticlinal divisions, which tend to produce loosely aggregated data.

Table 5.7

Aggregated kurtosis data for each species

species	elements	position							
		1		2		3		4	
		kurtosis		kurtosis		kurtosis		kurtosis	
		+	-	+	-	+	-	+	-
Dacrycarpus dacrydioides	tracheid	3	3 (2)	5 (4)	1	2 (1)	4 (1)	2	4
Nothofagus menziesii	fibre	4	2	3 (1)	3	1	5	3	3 (1)
	vessel	2 (1)	4	2	4 (1)	3	3	1	5
Hoheria angustifolia	fibre	3 (3)	3	3 (3)	3 (1)	4 (2)	2	4 (1)	2
	vessel	3 (3)	3 (1)	6 (2)	0	3 (2)	3 (2)	5 (3)	1

numbers in brackets represent the number of samples showing a significant value for kurtosis

Figures 5.5 to 5.7 illustrate the mean lengths of elements for each of the 3 species. From these graphs it can be seen that the lengths of the elements tend to display the expected pattern throughout the growth ring (they have a maximum length towards the centre of the growth increment, and a minimum length at the ring boundary).

5.4.2. The computer generation of elongating and dividing samples using SAS

5.4.2.1. Elongation algorithm with two stages of elongation

From Table 5.8 it can be seen that simple elongation of the dataset results in a sample that is either (+) skewed ,or does not change in skew. The skew only becomes (-) when a maximum length (equation 3) is specified. If this simulation was continued for higher levels of **EF**, without changing the maximum obtainable length, a minimum value for skew (a greater negative value) would be reached, after which skews would begin to approach 0, as all measurements reached the maximum value. Or to put it another way, the data would become more tightly aggregated, until all observations were the same length, and measurements of skew became meaningless.

Figure 5.5.a
Dacrycarpus dacrydioides
specimen 25

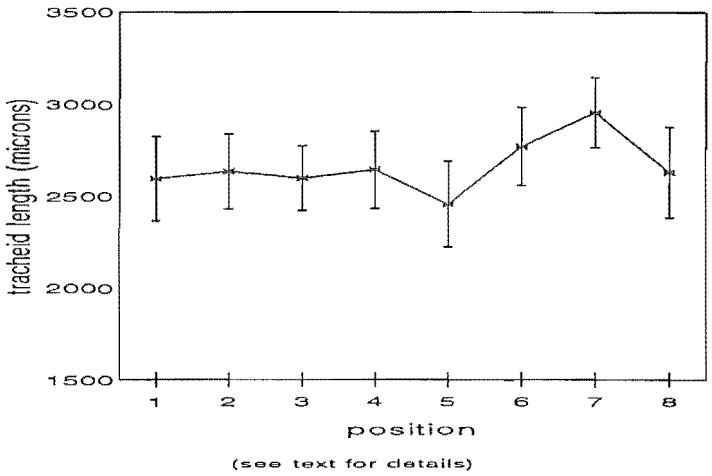

(see text for details)

Figure 5.5.b
Dacrycarpus dacrydioides
specimen 384

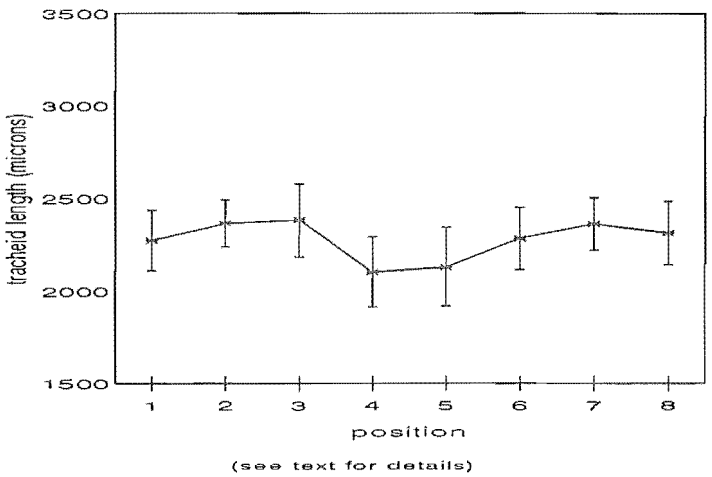

(see text for details)

Figure 5.5.c
Dacrycarpus dacrydioides
specimen 599

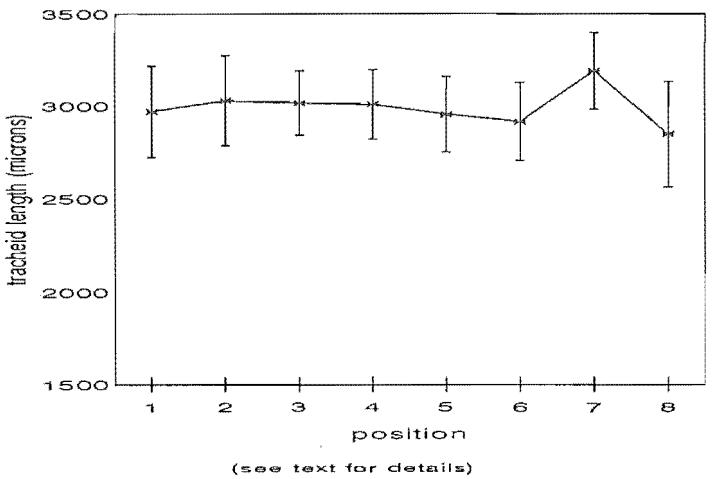

(see text for details)

Figure 5.6.a
Hoheria angustifolia
specimen 142

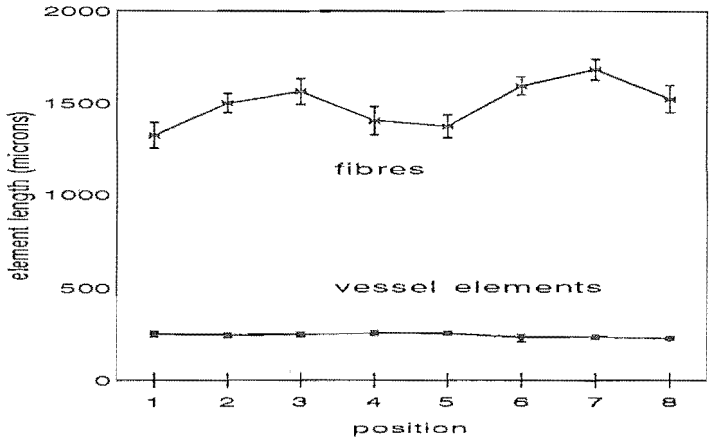

(see text for details)

Figure 5.6.b
Hoheria angustifolia
specimen 571

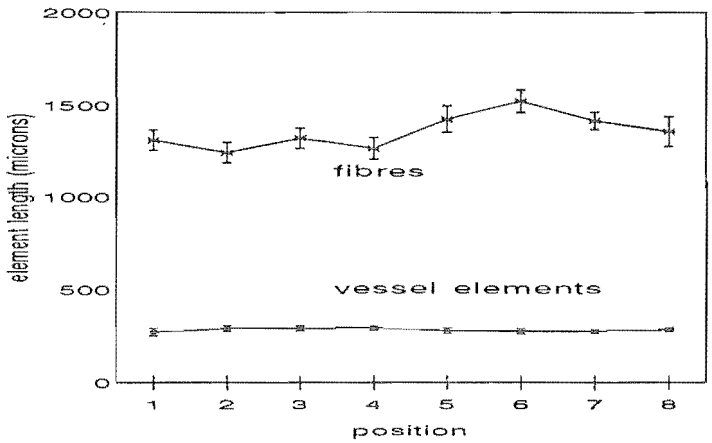

(see text for details)

Figure 5.6.c
Hoheria angustifolia
specimen 572

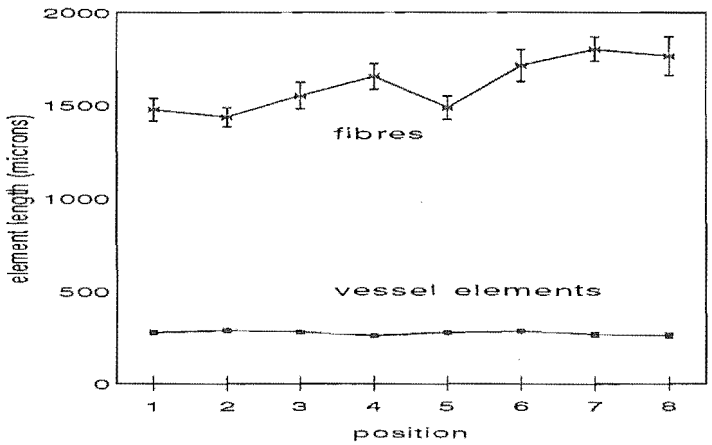

(see text for details)

Figure 5.7.a
Nothofagus menziesii
specimen 57

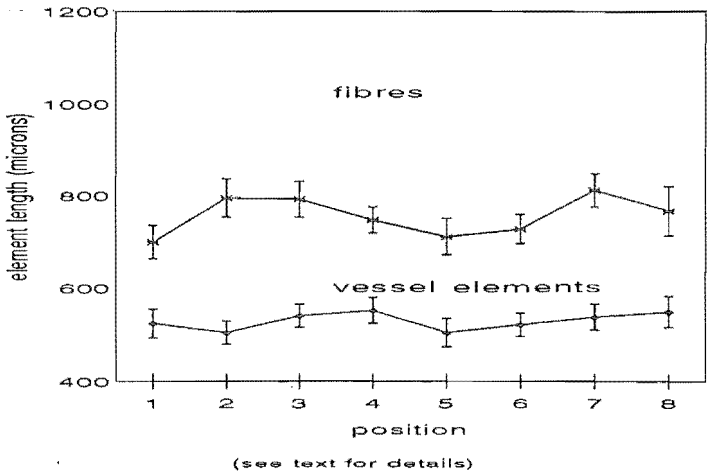

Figure 5.7.b
Nothofagus menziesii
specimen 66

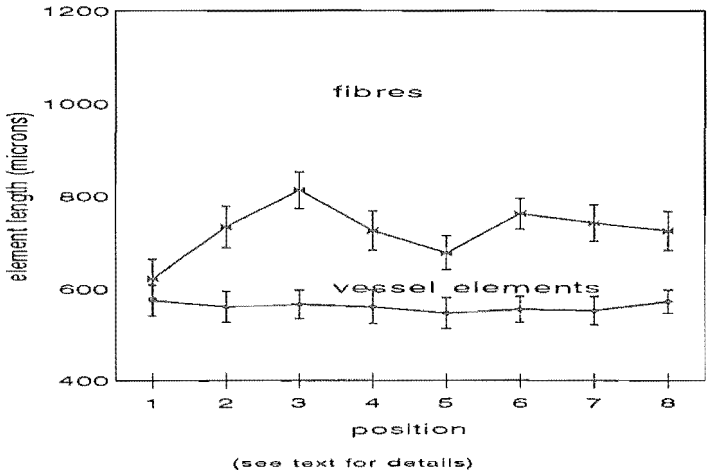

Figure 5.7.c
Nothofagus menziesii
specimen 585

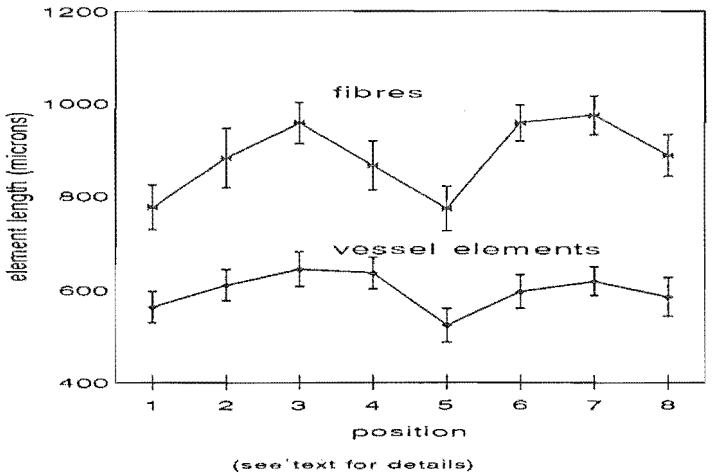

Table 5.8

Output from elongation algorithm with 2 stages of elongation

cambium equation	derivative equation	cambium EF	derivative EF	cambium skew	derivative skew
1	1	0.05	0.05	+ 0.20	+ 0.20
1	1	0.05	0.10	+ 0.20	+ 0.20
1	1	0.05	0.15	+ 0.20	+ 0.20
1	1	0.10	0.05	+ 0.34	+ 0.34
1	1	0.10	0.10	+ 0.34	+ 0.34
1	1	0.10	0.15	+ 0.34	+ 0.34
1	1	0.15	0.05	+ 0.48	+ 0.48
1	1	0.15	0.10	+ 0.48	+ 0.48
1	1	0.15	0.15	+ 0.48	+ 0.48
1	2	0.05	5.00	+ 0.20	+ 0.20
1	2	0.05	10.00	+ 0.20	+ 0.20
1	2	0.05	15.00	+ 0.20	+ 0.20
1	2	0.10	5.00	+ 0.34	+ 0.34
1	2	0.10	10.00	+ 0.34	+ 0.34
1	2	0.10	15.00	+ 0.34	+ 0.34
1	2	0.15	5.00	+ 0.48	+ 0.48
1	2	0.15	10.00	+ 0.48	+ 0.48
1	2	0.15	15.00	+ 0.48	+ 0.48
1	3	0.05	0.05	+ 0.20	+ 0.16
1	3	0.05	0.10	+ 0.20	+ 0.04
1	3	0.05	0.15	+ 0.20	- 0.13
1	3	0.10	0.05	+ 0.34	- 0.88
1	3	0.10	0.10	+ 0.34	- 1.06
1	3	0.10	0.15	+ 0.34	- 1.24
1	3	0.15	0.05	+ 0.48	- 1.53
1	3	0.15	0.10	+ 0.48	- 1.72
1	3	0.15	0.15	+ 0.48	- 1.92
2	1	5.00	0.05	+ 0.00	+ 0.00
2	1	5.00	0.10	+ 0.00	+ 0.00
2	1	5.00	0.15	+ 0.00	+ 0.00
2	1	10.00	0.05	+ 0.00	+ 0.00
2	1	10.00	0.10	+ 0.00	+ 0.00
2	1	10.00	0.15	+ 0.00	+ 0.00
2	1	15.00	0.05	+ 0.00	+ 0.00
2	1	15.00	0.10	+ 0.00	+ 0.00
2	1	15.00	0.15	+ 0.00	+ 0.00
2	2	5.00	5.00	+ 0.00	+ 0.00
2	2	5.00	10.00	+ 0.00	+ 0.00
2	2	5.00	15.00	+ 0.00	+ 0.00
2	2	10.00	5.00	+ 0.00	+ 0.00
2	2	10.00	10.00	+ 0.00	+ 0.00
2	2	10.00	15.00	+ 0.00	+ 0.00
2	2	15.00	5.00	+ 0.00	+ 0.00
2	2	15.00	10.00	+ 0.00	+ 0.00
2	2	15.00	15.00	+ 0.00	+ 0.00
2	3	5.00	0.05	+ 0.00	+ 0.00
2	3	5.00	0.10	+ 0.00	+ 0.00
2	3	5.00	0.15	+ 0.00	- 0.03

2	3	10.00	0.05	+ 0.00	- 0.63
2	3	10.00	0.10	+ 0.00	- 0.83
2	3	10.00	0.15	+ 0.00	- 1.04
2	3	15.00	0.05	+ 0.00	- 1.29
2	3	15.00	0.10	+ 0.00	- 1.50
2	3	15.00	0.15	+ 0.00	- 1.72
3	1	0.05	0.05	+ 0.20	+ 0.20
3	1	0.05	0.10	+ 0.20	+ 0.20
3	1	0.05	0.15	+ 0.20	+ 0.20
3	1	0.10	0.05	- 0.72	- 0.72
3	1	0.10	0.10	- 0.72	- 0.72
3	1	0.10	0.15	- 0.72	- 0.72
3	1	0.15	0.05	- 1.36	- 1.36
3	1	0.15	0.10	- 1.36	- 1.36
3	1	0.15	0.15	- 1.36	- 1.36
3	2	0.05	5.00	+ 0.20	+ 0.20
3	2	0.05	10.00	+ 0.20	+ 0.20
3	2	0.05	15.00	+ 0.20	+ 0.20
3	2	0.10	5.00	- 0.72	- 0.72
3	2	0.10	10.00	- 0.72	- 0.72
3	2	0.10	15.00	- 0.72	- 0.72
3	2	0.15	5.00	- 1.36	- 1.36
3	2	0.15	10.00	- 1.36	- 1.36
3	2	0.15	15.00	- 1.36	- 1.36
3	3	0.05	0.05	+ 0.20	+ 0.16
3	3	0.05	0.10	+ 0.20	+ 0.04
3	3	0.05	0.15	+ 0.20	- 0.13
3	3	0.10	0.05	- 0.72	- 0.88
3	3	0.10	0.10	- 0.72	- 1.06
3	3	0.10	0.15	- 0.72	- 1.24
3	3	0.15	0.05	- 1.36	- 1.53
3	3	0.15	0.10	- 1.36	- 1.72
3	3	0.15	0.15	- 1.36	- 1.92

5.4.2.2. Division algorithm

The results here are represented in Table 5.9 which is sorted in order of decreasing skew. The simulations of most interest are those which resulted in significantly (+) skewed populations with a reduced mean length. Five simulations show this result, all had pseudotransverse anticlinal divisions, a high number of cells dividing (90%), and most, if not all, cells eligible to divide (**LENMIN1** = 90 in Table 5.9). There was also a tendency for there to be little or no elongation. Also of interest are those simulations resulting in the opposite effect (significantly (-) skew with an increased mean cell length). There were 9 simulations with this result, all were elongated and had a low number of cells dividing.

Table 5.9

Output from division algorithm

EF	PT	Lenmin 2	Divide %	Lenmin 1	Extinct %	Sign of skew	Skew	Mean
0.00	0.5	10	90	90	1	+	3.22 *	93@
0.00	0.5	10	1	90	10	+	3.13 *	101
0.02	0.5	10	90	90	10	+	3.08 *	93@
0.02	0.5	20	90	99	1	+	2.88 *	102
0.00	0.5	20	90	90	10	+	2.59 *	82@
0.02	0.5	10	90	110	1	+	2.57 *	108
0.02	0.5	10	90	90	1	+	2.52 *	105
0.00	0.5	20	90	90	1	+	2.36 *	95@
0.02	0.5	20	90	90	10	+	2.10 *	100
0.00	0.5	10	90	90	10	+	1.99 *	94@
0.02	0.5	10	90	110	10	+	1.95 *	102
0.02	0.5	10	10	110	1	+	1.59 *	111
0.02	0.0	10	1	100	10	+	0.46 *	112
0.02	0.5	20	10	90	10	+	0.40 *	115
0.02	0.5	10	1	110	10	+	0.35	114
0.00	0.1	10	90	90	0	+	0.19	52
0.02	0.5	10	10	90	10	+	0.19	103
0.00	0.0	10	90	90	0	+	0.15	52
0.00	0.0	10	10	105	0	+	0.08	100
0.00	0.1	10	90	95	0	+	0.06	56
0.02	0.0	10	90	100	10	+	0.05	59
0.00	0.0	10	90	95	0	+	0.02	54
0.02	0.0	10	90	90	10	+	0.01	58
0.00	0.5	20	10	90	10	+	0.01	94
0.00	0.0	10	90	110	0	+	0.00	100
0.00	0.0	10	10	110	0	+	0.00	100
0.00	0.1	10	90	110	0	+	0.00	100
0.00	0.1	10	10	110	0	+	0.00	100
0.02	0.0	10	90	90	1	-	0.00	59
0.02	0.5	10	10	90	1	-	0.02	107
0.02	0.0	10	90	100	1	-	0.06	60
0.00	0.5	10	90	110	10	-	0.06	100
0.00	0.0	10	10	90	0	-	0.12	64
0.00	0.5	20	1	90	10	-	0.14	100
0.00	0.0	10	90	98	0	-	0.15	62
0.02	0.5	20	10	90	10	-	0.22	106
0.00	0.5	20	10	90	1	-	0.36 *	88
0.00	0.0	10	90	100	0	-	0.38 *	66
0.00	0.1	10	90	100	0	-	0.38 *	68
0.02	0.5	10	1	90	1	-	0.47 *	113^
0.00	0.5	10	10	90	1	-	0.48 *	90
0.02	0.0	10	10	90	10	-	0.56 *	88
0.02	0.5	20	10	90	1	-	0.56 *	109^
0.00	0.5	10	10	90	10	-	0.64 *	91
0.02	0.0	10	10	90	1	-	0.65 *	88
0.00	0.0	10	10	95	0	-	0.68 *	75
0.02	0.0	10	10	100	1	-	0.82 *	88
0.02	0.0	10	10	100	10	-	0.83 *	88
0.00	0.0	10	10	98	0	-	0.99 *	80
0.00	0.1	10	10	90	0	-	1.00 *	77
0.00	0.1	10	10	95	0	-	1.30 *	86
0.00	0.0	10	90	102	0	-	1.32 *	80
0.00	0.0	10	90	105	0	-	1.32 *	83
0.00	0.1	10	90	105	0	-	1.44 *	83
0.02	0.5	10	1	110	1	-	1.46 *	115^
0.02	0.5	10	10	110	10	-	1.46 *	103^
0.02	0.5	10	1	90	10	-	1.56 *	112^
0.00	0.1	10	10	100	0	-	1.84 *	87
0.02	0.5	10	1	90	10	-	1.97 *	109^
0.00	0.0	10	10	100	0	-	2.06 *	88
0.02	0.5	20	1	90	1	-	2.09 *	113^
0.00	0.0	10	10	102	0	-	2.18 *	93
0.02	0.0	10	1	90	10	-	2.22 *	109^
0.00	0.5	10	1	90	1	-	2.26 *	95
0.02	0.0	10	1	100	1	-	2.76 *	114^
0.00	0.1	10	10	105	0	-	3.55 *	97
0.00	0.5	20	1	90	1	-	5.40 *	99

* significantly skewed sample (P>0.05), @ significant (+) skewed sample with a reduced mean length, ^ significant (-) skewed sample with an increased mean length

5.5. DISCUSSION.

The data tend to suggest that (+) and (-) skews could be used as rough indicators of cambial activity. The best support for this is the data from the vessel elements of *N. menziesii*, where assumed areas of high rates of pseudotransverse anticlinal divisions produced (+) skewed samples. Areas of maximum element length (the centre of the growth increment) tend to show (-) skews. The fibres of *N. menziesii* and the tracheids of *D. dacrydioides*, however, offer no evidence in support.

It is generally accepted that dicotyledonous fibres elongate considerably, and tracheids 5 to 10% after periclinal division (Bailey 1920), vessel elements elongate less. The lack of a significant result for the fibres of *N. menziesii* and the tracheids of *D. dacrydioides* could, therefore, be attributed to the distribution being obscured by the subsequent elongation of the derivatives. Another factor may be the rapid elongation of new fusiform initials. As Evert (1961) showed in *Pyrus communis*, the greatest elongation of new fusiform initials occurred in the period between anticlinal division, and the cambium becoming actively involved in the production of derivatives. This situation also occurs in gymnosperms (Bannan 1959), where high levels of anticlinal division are accompanied by faster rates of elongation of initials.

It seems likely that the (+) skew of the vessel elements in *N. menziesii*, during, and just after, a period of anticlinal division, may be retained due to the minimal elongation of these derivatives. Bailey (1920) noted a shortening of some specialised vessel elements. Over a period of time, however, a positive elongation (increase in length) is going to produce the same distribution as a negative elongation (decrease in length by the shortening of elements not brought about by pseudotransverse anticlinal divisions), unless there is a restriction in the degree to which this elongation can occur (as shown by the elongation algorithm).

Elongating populations tended to have more long than short elements, and to have relatively tightly aggregated data. Wenham and Cusick (1975) have shown intrusive growth as a process occurring at the tips of elongating elements, and dependant on the radial expansion of neighbouring cells, as well as the position of the tip in relation to their tangential and radial walls. If these were the sole processes in operation, then the areas of greatest radial expansion would generally have the longest derivatives, all being able to elongate in this way depending on how their tips were positioned, independent of their lengths. One possible cause for a maximum obtainable length would be if the longer a derivative got, the less favourable the position of its tip. This

seems unlikely, because as derivatives get longer, the greater the chances of coming into contact with other elongating derivatives, offering more opportunities to obtain favourable tip positions. A more likely possibility to explain a maximum obtainable length may be a maximum tip to tip distance for the elongating cell.

It was not expected that samples of *H. angustifolia* would show any significant trend in skew, and this species was included as a control for pseudotransverse anticlinal divisions. It is of some interest, therefore, to notice samples tend to be (-) skewed. This may indicate that the effect of the elongation of derivatives (even if that elongation is only very slight, as is the case with vessel elements) may be a dominant feature in determining the skew of a sample, especially if there is a maximum length for the derivatives. Since, however, this prevalence of (-) skews is consistent for both vessel elements and fibres, it is possible this may be a true reflection of the distribution of the cambial initials. This situation could occur in a storeyed cambium if anticlinal divisions were more prevalent in the longest fusiform initials, resulting in more long initials than short initials.

Cumbie (1967) suggests that in *Leitneria floridana*, generally only the longer fusiform initials underwent anticlinal division. However, he does not present any convincing figures in support of this. It could also be suggested that if elongation of initials was set to maximum length, resulting in a (-) skewed population, then it could well appear that longer initials were undergoing more anticlinal divisions, as there would be more long initials in the population. Also of note in this respect, are the results of the division algorithm. Although this represents an artificial system, it is interesting to note those simulations that had the expected result (+ skew and reduced mean) had no restriction on the lengths of initials undergoing anticlinal division.

Overall it would seem that elongation produces (-) skewed samples and pseudotransverse anticlinal divisions produce (+) skewed samples. Generally the results were not as clear cut as had been hoped for and may have benefited from a greatly increased number of samples and observations. This could have made an analysis much easier. As it is, the main conclusions of this chapter must be made on trends and indications of the data, rather than on hard and fast statistical analyses.

CHAPTER 6

CHARACTERISTICS OF THE FLUTED REGIONS IN *NOTHOFAGUS*

6.1. INTRODUCTION

The most obvious feature of the aggregate rays of *Nothofagus*, are the indentations in the growth rings associated with their presence. Similar indentations are also associated with aggregate rays in other angiosperm woods (Holdheide 1955, Kucera, Bosshard and Katz 1980, Ziegler and Merz 1961). Indentations also occur in gymnosperms, some with aggregate ray like structures (Sugawa and Fujii 1993) and others without (Bannan 1957a, Imamura 1978 and Ohtani, Fukuzawa and Fukumorita 1987).

The axial elements in these fluted regions (indentations) tend to be shorter than those in non-fluted regions (Bannan 1957a, Schultze-Dewitz and Gotze 1986). Bannan (1957a) and Ohtani *et al* (1987), have shown that in gymnosperms without aggregate rays, the cambium in the fluted regions also has an increase in the frequency of anticlinal divisions compared to the non-fluted regions. In Chapter 5 it was suggested that the skew of the length measurements, from a sample of fibres, can be used to indicate the presence of high frequencies of pseudotransverse anticlinal divisions in the cambium. Therefore, if there was a significant decrease in mean fibre length in the fluted zone, then (+) skewness of samples would indicate this had most likely been brought about by pseudotransverse anticlinal divisions. If, on the other hand, samples were (-) skewed, this would indicate differences in the amount of elongation occurring in the flutes.

As well as having a greater frequency of pseudotransverse anticlinal divisions, fluted regions also tend to show an accumulation of ray material, though individual rays tend to show a reduction in height (Ziegler and Merz 1961). Holdheide (1955) and Ohtani *et al* (1987) show it is often the sides of the flutes, rather than the centres, where the greatest such activity occurs.

Although the flutes of *Nothofagus* are related to the aggregate rays, it is the flutes themselves and the processes occurring within them that are of interest in this chapter.

Therefore, the fluted regions of *Nothofagus*, will generally be regarded as analogous to the fluted regions of other woods in the literature, whether or not they are described as having aggregate rays. The aggregate rays of *Nothofagus* will consequently be referred to as fluted areas.

6.2. MATERIAL

Four specimens were used. Two were of *Nothofagus truncata* (specimens 113 and 114 - Chapter 2) and two of *N. solandri* var. *cliffortioides* (specimens c02 and c03), collected from the Cass region of the Southern Alps. All were from mature, straight stemmed trees.

6.3. METHODS

6.3.1. Fluted and non-fluted regions - a comparison of skews

Growth rings were reconstructed from serial tangential sections, as specified in Appendix 3. Fibres were measured if they occurred at the grid and section co-ordinates sampled in PROGRAM 4B, but only if those co-ordinates corresponded to minimum or maximum turning points (if they were in the middle of a fluted region, or on a ridge). Individual measurements were assigned to a sample number, depending on their weights (positions) in the growth increment. If the weighting was 1 (1st quarter of the growth increment) in the inner growth increment it was assigned to sample 1, 0.66 (2nd quarter of the growth increment) to sample 2, 0.34 (3rd quarter of the growth increment) to sample 3, 0 (4th quarter of the growth increment) to sample 4. If the weighting was 1 in the next growth increment it was assigned to sample 5, 0.66 to sample 6 *et cetera.*

Significant differences in means between fluted (minimum turning points), and non-fluted regions (maximum turning points), were calculated using the Kruskal-Wallis test for non-parametric samples. Skews were analysed as in Chapter 5. All statistical analyses were performed using SAS.

6.3.2. Deformation in relation to flute angle

Only specimens 113 and 114 were used for this section.

Safranin stained transverse sections of the material were photographed with a camera mounted on an Olympus BH2 microscope. Three growth ring boundaries showing fluted configurations were selected from each specimen. Working from the micrographs, each of the growth ring boundaries was dissected into a number of zones, each being 5 radial files of cells wide (including ray cells). These 5 cells determined the tangential length. Each of the zones had a radial length of 5 cells (2 in the late wood and 3 in the early wood) determined by the middle radial file in each zone. Thus each zone represented 5X5 cells (Figure 6.1.a). The inclusion of ray cells in the zones would not be expected to have any effect on the outcome of the analysis as there was at most 1 ray per zone.

The angle of the growth ring boundary was determined by taking a straight line from the boundary at the 1st radial file of each zone, and extending it to the 5th radial file. The angle measured was the deviation of this line from a line perpendicular to the main trend of the radial files (Figure 6.1.b). Zones were categorised into 4 areas (Figure 6.1.c). The in-flute area consisted of the 4 zones in the middle of the flute. The side area consisted of the zone with the greatest angle, and those zones on either side of this zone (unless 1 of these zones was also in the in-flute area). The non-fluted area consisted of all those zones outside the side area. The other area consisted of any zone occurring between the fluted and side zones. Length and width measurements were collected and correlated with the angle of the growth ring boundary for each zone using SAS. An ANOVA was performed on the four areas.

6.3.3. Length of fibres in growth rings

One reconstructed growth ring (from section 6.3.1. above) was selected from each specimen. Measurements of fibres were made on every second slide, at the columns where the growth ring crossed every second row (rows 2, 4, 6 and 8).

6.3.4. Activity of individual ray initials

One ray from each column, of each specimen, was selected. Where possible, a ray was selected that was in the middle of a column, and crossed a line of the grid. The number of ray cells in the ray was recorded. Rays were followed through the serial

Figure 6.1

Deformation in relation to the flute

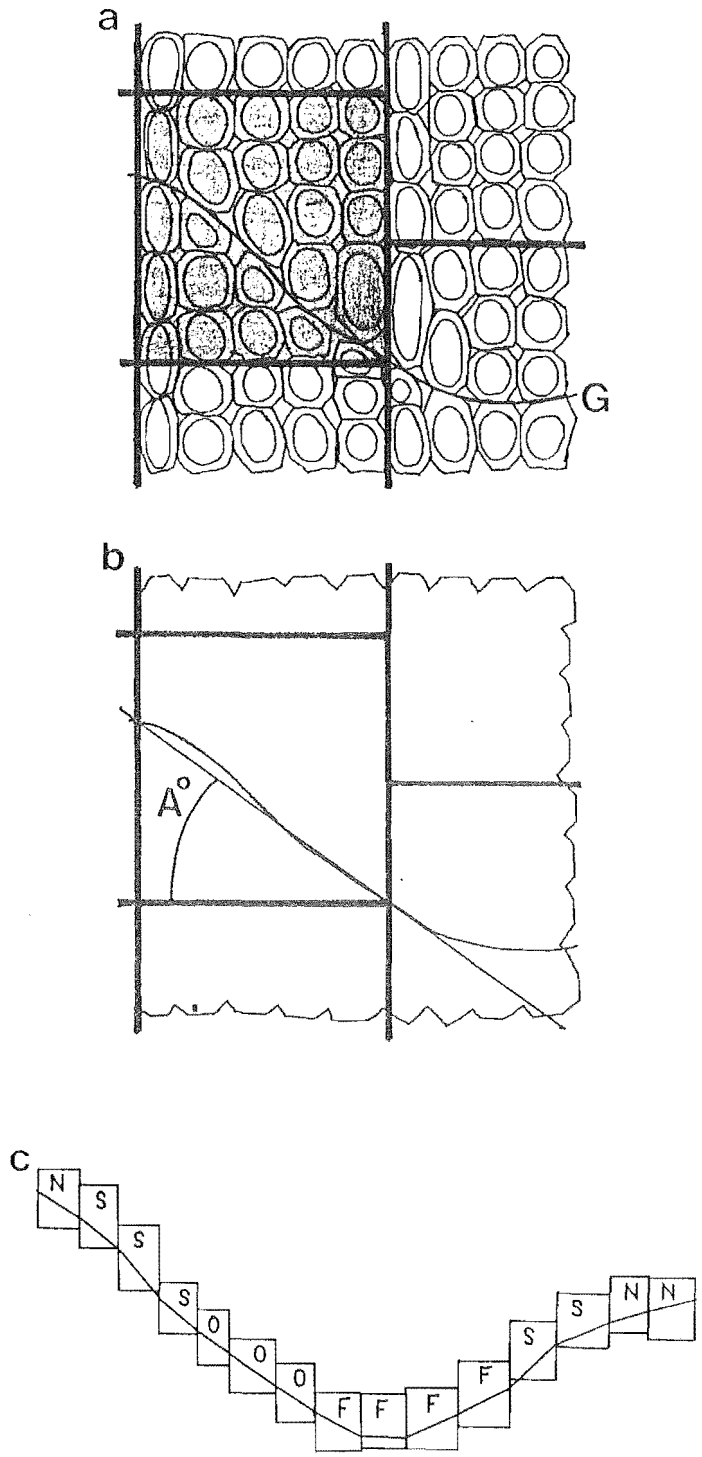

(see text for details).

a. 5x5 cell zone (shaded). Growth ring (G).

b. As above with cell detail removed. Angle of growth ring (A^{o}).

c. Individual zones labelled in their appropriate areas. Non-fluted (N). In-flute (F). Side (S). Other (O).

sections, and the number of vertical ray cells recorded periodically. Changes in the number of ray cells in a ray were only recorded if that change was consistent over a number of sections. This was done as cells were often obscured by vessels. There was also evidence of transverse division of ray cells after they had been cut off from the cambial initials. Where the increase in the number of cells in a ray was achieved as the result of the fusion of 2 or more rays then this was not regarded as an increase in ray number.

Individual rays were followed until they were completely lost from the cambium, moved out of section, or became incorporated into aggregations of ray material so extensive that individual rays become indistinguishable.

The rays were categorised depending on whether the columns they occurred within had minimum turning points, maximum turning points, or no turning points (i.e. inside the flute, outside the flute or on the sides of the flute).

6.4. RESULTS

6.4.1. Fluted and non-fluted regions - a comparison of skews

Specimen c03 appears to exhibit an unusual pattern of growth, with fibre length apparently decreasing with increasing distance from the pith (Figure 6.2.d). This is, however, due to the fibres becoming increasingly oblique and, as a consequence, appearing shorter in tangential section. If the fibres had become too oblique the comparison between the fluted and non-fluted regions would have been effected. This did not seem to be the case.

In nearly all cases the mean fibre length of the samples from the fluted regions is shorter than those for the non-fluted regions. Where there is a significant difference in fibre length, based on the results of the Kruskal-Wallis test, the samples from the fluted regions are always shorter.

In general terms, there are no differences in the skew of samples based on whether they were in fluted on non-fluted regions. Table 6.1 shows that in total there tend to be slightly more (-) skewed samples in the fluted regions, indicating a possible slight prevalence of elongation factors. Table 6.1 also shows, that when this is further broken down into 2 categories, depending on whether there was any significant difference in fibre length, between fluted and non-fluted regions, there is a slight

tendency for significantly shorter samples in the fluted region to be (+) skewed. It is possible then, that these represent areas of pseudotransverse anticlinal division, especially as the overall trend for all samples seems to be one of elongation. Where the samples show no significant difference in fibre length there is a significant trend for the samples in the fluted region to have (-) skews. From this analysis the only significant trend is one suggesting that fluted regions, where fibres are not significantly shortened, tend to be areas that have undergone a relatively high degree of elongation.

Table 6.1

Sample skews recorded for fluted and non-fluted regions

difference in means between samples	non-fluted region		fluted region	
	skew		skew	
	+	-	+	-
significant	8 (1)	10 (4)	10 (0)	8 (0)
not significant	21 (2)	29 (0)	15 (3)	35 (5)
total	29 (3)	39 (4)	25 (3)	43 (5)

numbers in brackets represent the number of samples showing a significant value for skew

There are, however, other factors to be considered. One is the degree of ray aggregation occurring in the fluted regions. The fluted regions mostly had morphologies consistent with diffuse aggregate rays (Chapter 2), but occasionally there were fasciculate aggregate rays, consistent with disruption zones (Chapter 2). These areas of higher aggregation, in the fluted regions, showed a significant tendency to be (+) skewed, when the mean fibre length was significantly shorter than in the non-fluted regions, and (-) skewed when not significantly shorter (Table 6.2). When the disruption zones were not present there appeared to be no significant differences based on whether the sample was from a fluted, or non-fluted region. It would seem that within these areas of aggregation, there is a relatively high number of pseudotransverse anticlinal divisions (though not necessarily in the cambial initials), resulting in a depressed cell length. It would also seem that within other parts of the disruption zones, there is an increase in the elongation of derivatives and/or cambial initials, resulting in cell which are not significantly shorter than expected.

Table 6.2

Sample skews recorded for areas of aggregation

difference in means between samples	(+) skew	(-) skew
significant	4	1
not significant	1	6

χ^2 = 5.08 with 1 degree of freedom, indicating a significant difference

Only 2 of the 4 specimens had disruption zones in the fluted region (Figure 6.2.a to 6.2.d). These were specimens c03 and 113. From these 2 specimens there were 5 samples where aggregated zones had fibres significantly shorter than the corresponding samples from the non-fluted region. In all cases these samples had a higher value for the skew (though the skews were not always (+)), than the corresponding non-fluted regions. This is consistent with the disruption zones being regions where a relatively large number of pseudotransverse anticlinal divisions are occurring in the cambial initials.

6.4.2. Deformation in relation to flute angle

There were several significant correlations of zone characteristics with the angle of the flute, and these are shown on Table 6.3. There was a highly significant positive correlation of radial length of the zone, with the flute angle (as the angle got greater the radial length increased). However, an R^2 of only 0.2023 indicates a relatively loose aggregation of data, with only 20% of the variation in radial length being accounted for by the angle of the flute. The tangential length shows the opposite correlation. As the angle of the flute increases, the tangential length decreases. Here the R^2 was 0.2530, meaning 25% of the variation could be accounted for by the angle of the flute. The ratio of radial length:tangential length defines the shape of the 5X5 cell zone. This ratio is generally greater than 1, with the radial length being larger than the tangential length. This may well be the case in normal situations, with cells usually being wider in their radial dimensions than their tangential dimensions (Patel 1965). This ratio also shows a significant correlation with flute angle, with radial length increasing with respect to tangential length as the flute angle increases. With increasing flute angle the zones tend to be elongated radially (or compressed tangentially). The R^2 of 0.3963, however, still indicates a relatively loose distribution of the data, with approximately only 40% of the variation in the ratio being accounted for by flute angle. Although it appears that the shape of the zones was related to the

Figure 6.2.a
fibre lengths and sample skews
specimen 113

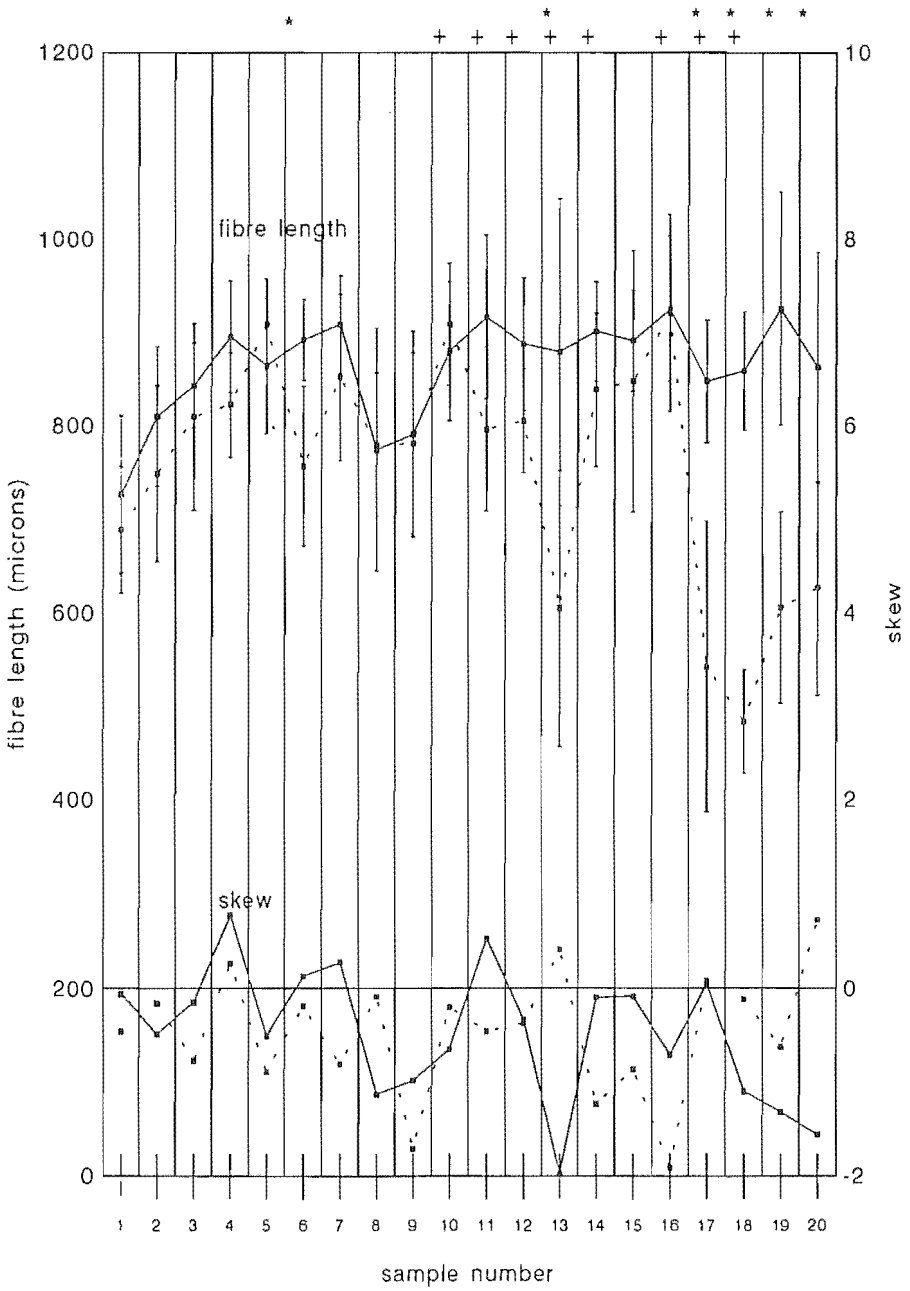

non-fluted fluted

* significant difference between fluted and non-fluted
\+ disruption zones present

(see text for details)

Figure 6.2.b
fibre lengths and sample skews
specimen 114

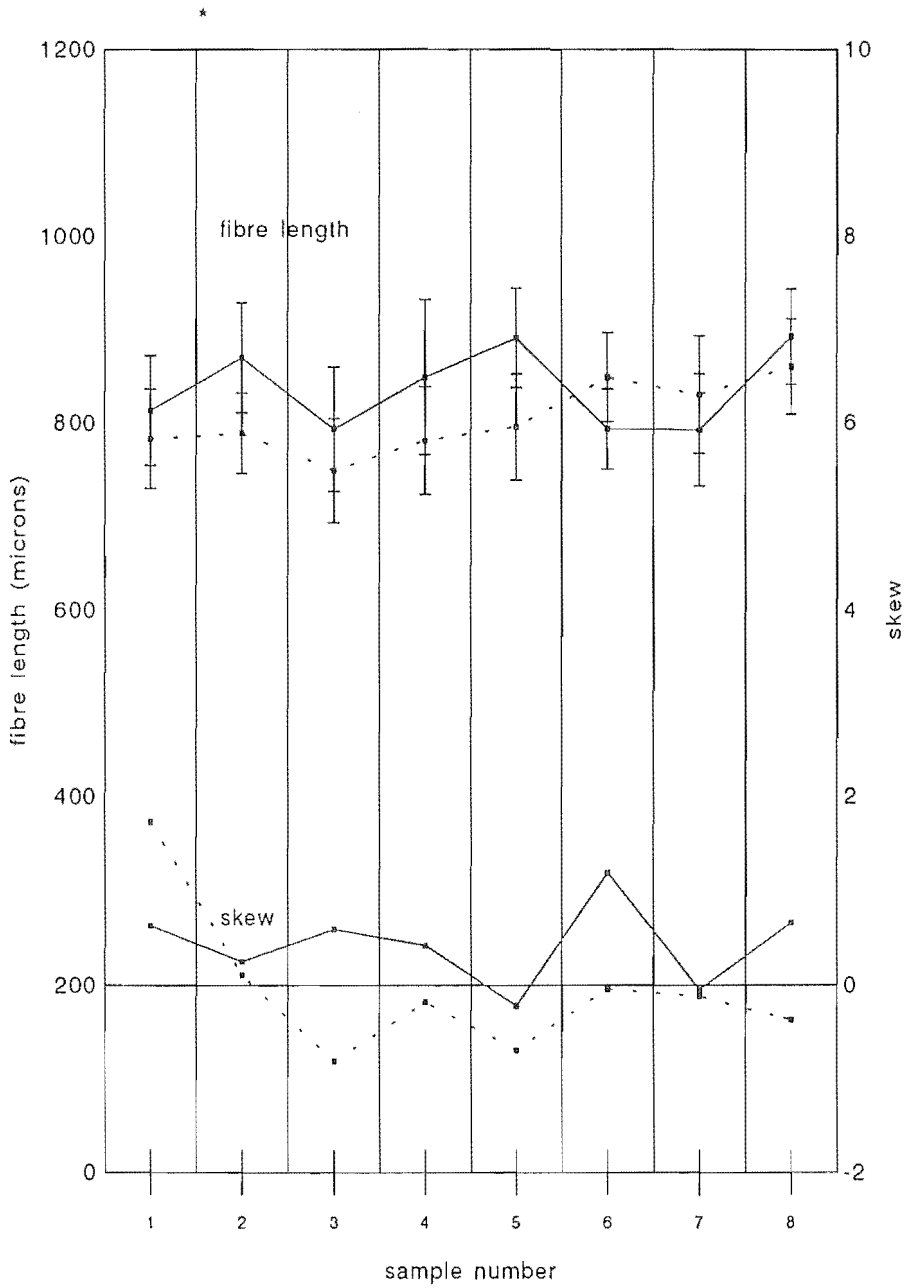

fluted non-fluted

* significant difference between fluted and non-fluted
+ disruption zones present

(see text for details)

Figure 6.2.c
fibre lengths and sample skews
specimen c02

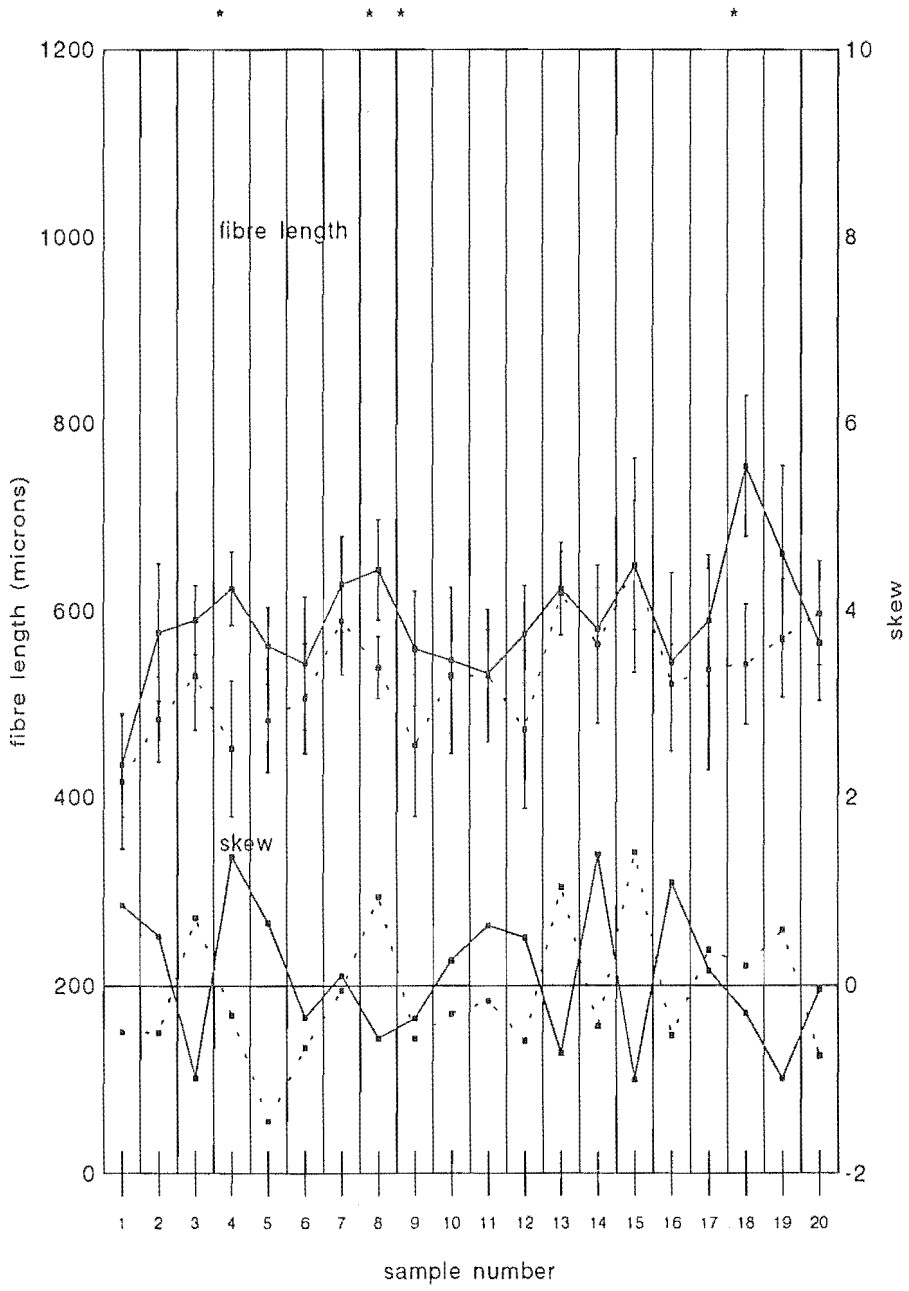

fluted non-fluted

* significant difference between fluted and non-fluted
+ disruption zones present

(see text for details)

Figure 6.2.d
fibre length and sample skews
specimen c03

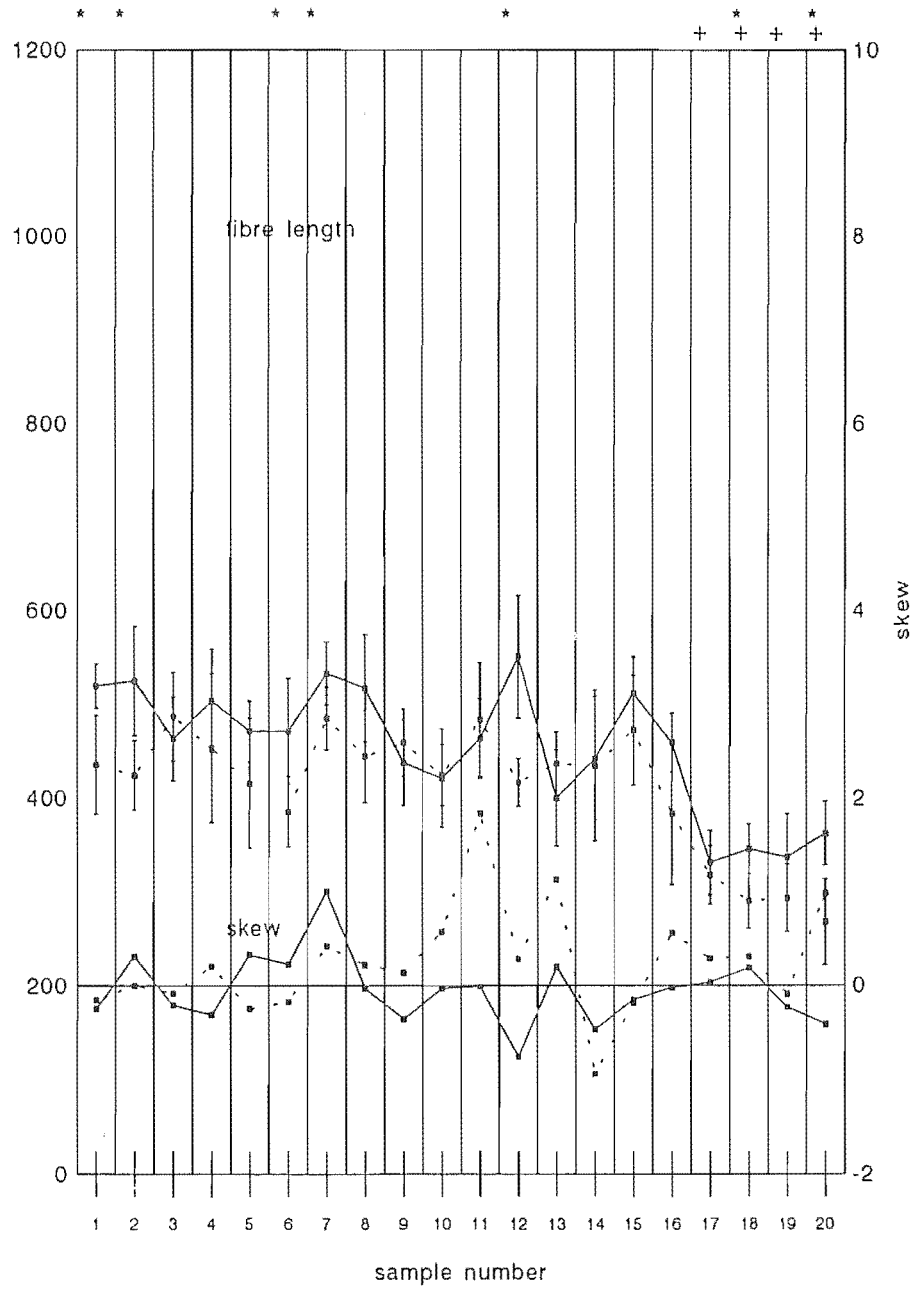

non-fluted fluted

* significant difference between fluted and non-fluted
+ disruption zone present

(see text for details)

angle of the flute, the actual area of the zones seems to be unaffected. Here an R^2 value of 0.0049 indicates none of the variation in the area of the zone could be accounted for by the angle of the flute.

Table 6.3

Correlation of 5X5 cell zone dimensions with flute angle

cell zone dimension	coefficient	R^2	P>|R|
radial length	0.4498	0.2023	0.0001
tangential length	-0.5029	0.2530	0.0001
ratio	0.6300	0.3963	0.0001
area	-0.0670	0.0049	0.5198

Table 6.4

Results of ANOVA showing the variability of 5X5 cell zone dimensions based on area within the flute

cell zone dimension	df	F value	P>F
radial length	86	4.37	0.0066
tangential length	86	2.68	0.0522
ratio	86	5.39	0.0019
area	86	0.80	0.4950

When the various regions that make up the flutes (non-fluted, side, in-flute, other) are analysed, there are significant differences for the radial length, and the ratio of the individual zones, and very close to a significant difference for tangential length. There are no significant differences for the areas of the zones however (Table 6.4). From Figure 6.3.a it can be seen that the greatest radial lengths occur within the in-flute areas, or at the sides of the flutes. The only means for the tangential length of the zones that are significantly different from each other, are those recorded for the non-fluted areas, and the sides of the flutes (Figure 6.3.b), with the non-fluted areas having the longest tangential lengths. However, it is the ratio of the radial to the tangential length that gives the most significant result. Again, the greatest differences are between the sides of the flutes and the non-fluted areas, with the sides of the flutes showing the greatest 'deformation' of the 5X5 cell zone (Figure 6.3.c). The in-flute

Figure 6.3.a
radial length of 5x5 cell zone

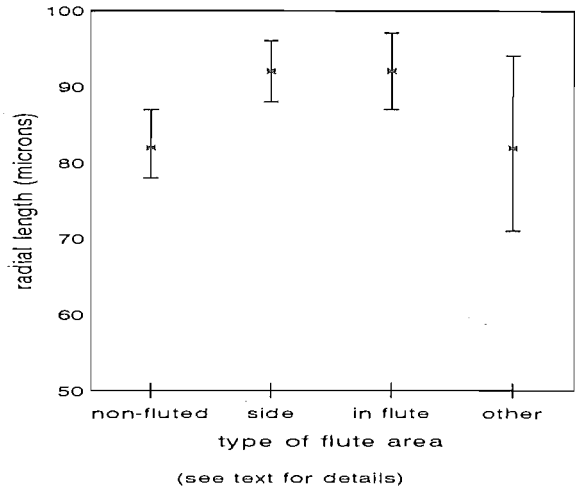

(see text for details)

Figure 6.3.b
tangential length of 5x5 cell zone

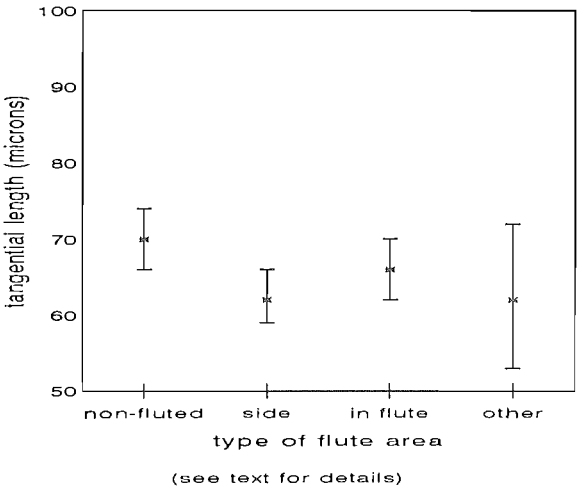

(see text for details)

Figure 6.3.c
ratio of radial/tangential length of 5x5 cell zone

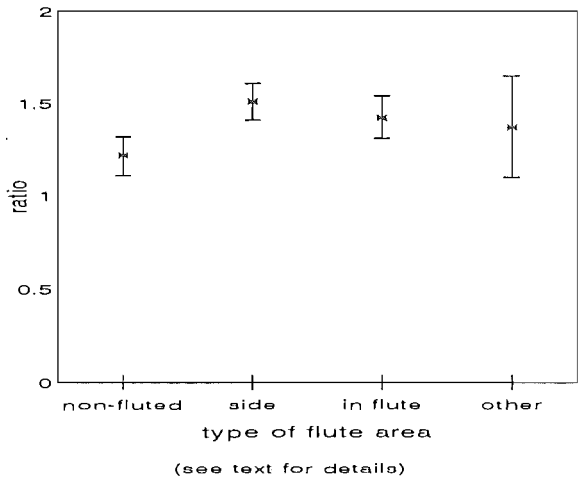

(see text for details)

areas are near to being significantly different from the non-fluted areas but are not significantly different from the sides of the flute. From this it seems clear that the greatest 'deformation' (the greatest difference between the radial and tangential lengths) of the 5X5 cell zones occurs at the sides of the flutes, with the in-flute areas experiencing slightly less 'deformation'.

6.4.3. Length of fibres in the growth ring

Graphs for the four specimens (Figures 6.4.a to 6.4.d) generally show a decrease in fibre length from the non-fluted area (max) to the fluted area (min). The areas in between (the sides of the flutes) generally follow this trend. Only for sample c03 (columns G and H) is there any significant deviation from this, with column H having fibres shorter than expected, or perhaps more correctly, column G having fibres longer than expected.

6.4.4 Activity of individual ray initials.

The combined results are presented in Table 6.5. It is clear that outside the flutes (top of the flute), there are far more increases in cell number than there are decreases. On the sides of the flutes, there are approximately equal numbers of increases and decreases, and in the centre of the flutes (bottom of the flute), there are far more decreases in cell number, than increases. The difference between the 3 categories is highly significant. Table 6.6 shows the number of fusions and splits of rays occurring in each category. There are not enough of these to draw any conclusions. Generally ray splitting was facilitated by the intruded tips of surrounding fibres. Occasionally rays were 'squeezed' into 2 parts by the fusiform derivatives on either side.

Table 6.5

Changes in the number of ray cells in rays within a flute

position	no. of increases in cell number	no. of decreases in cell number
top of flute	20	8
side of flute	22	26
bottom of flute	8	35

χ^2 = 19.69 with 2 degrees of freedom, indicating a highly significant difference

Figure 6.4.a
length of fibres in growth ring
specimen 113

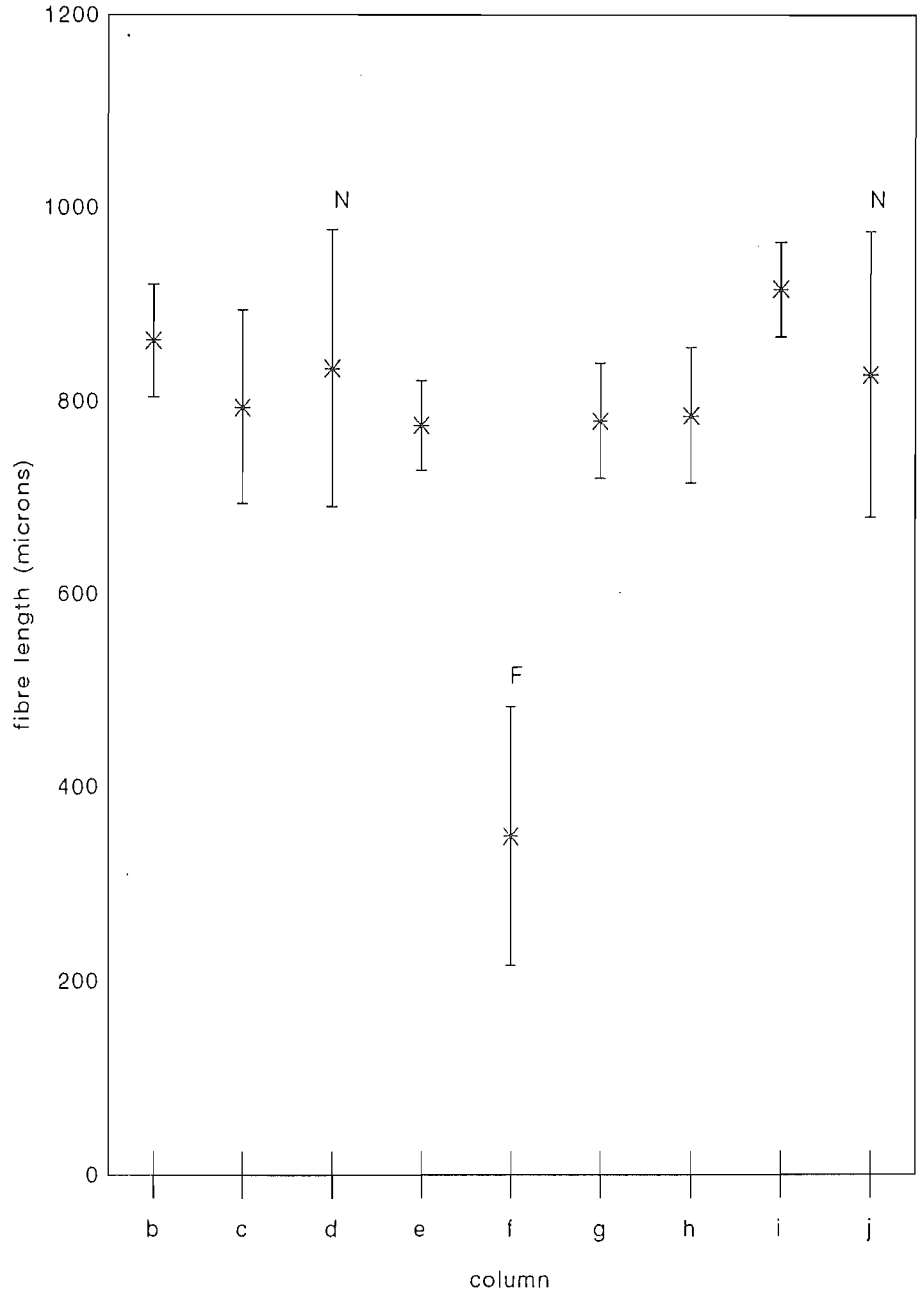

F = fluted
N = non-fluted

(see text for details)

Figure 6.4.b
length of fibres in growth ring
specimen 114

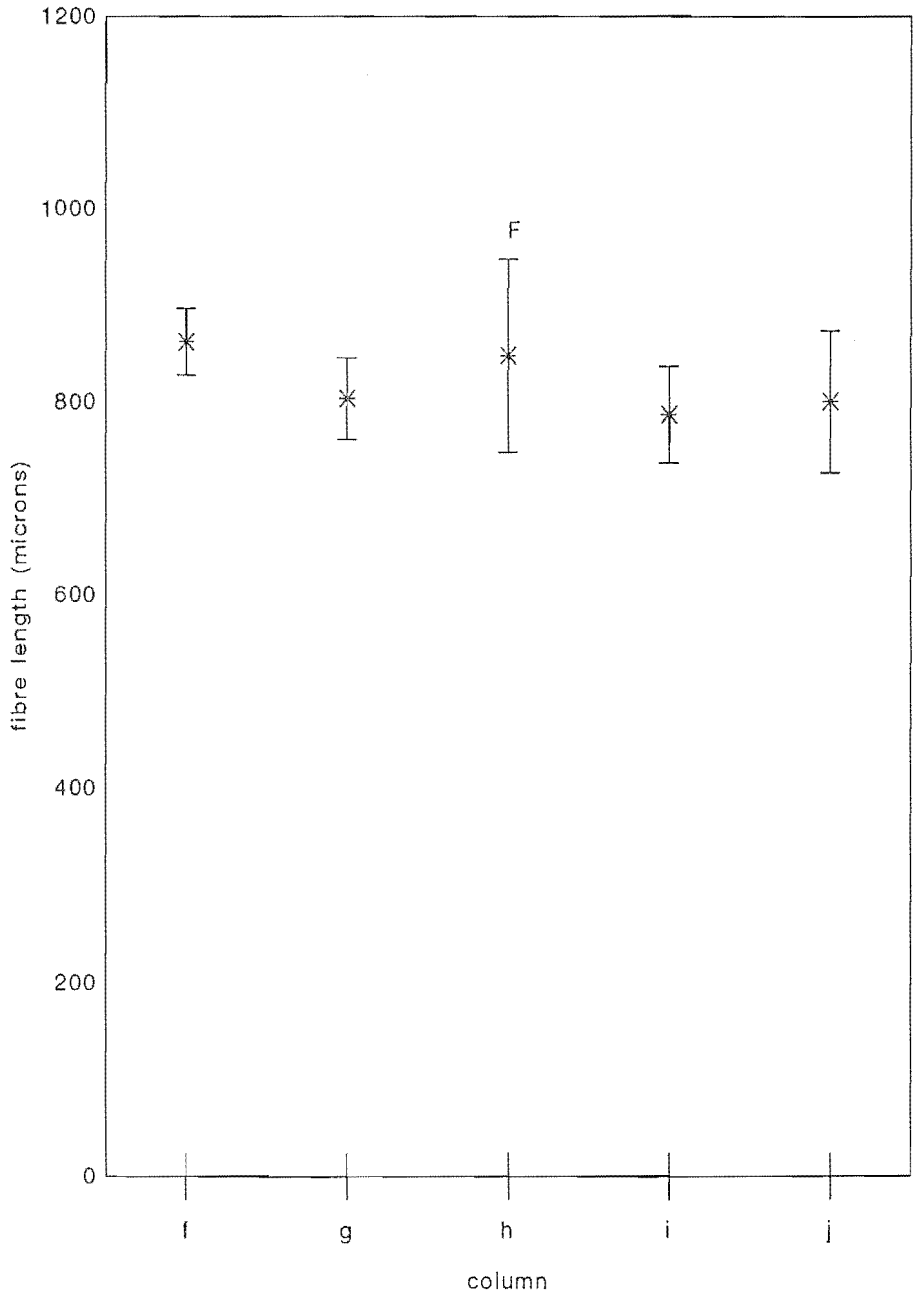

F = fluted
N = non-fluted

(see text for details)

Figure 6.4.c
length of fibres in growth ring
specimen c02

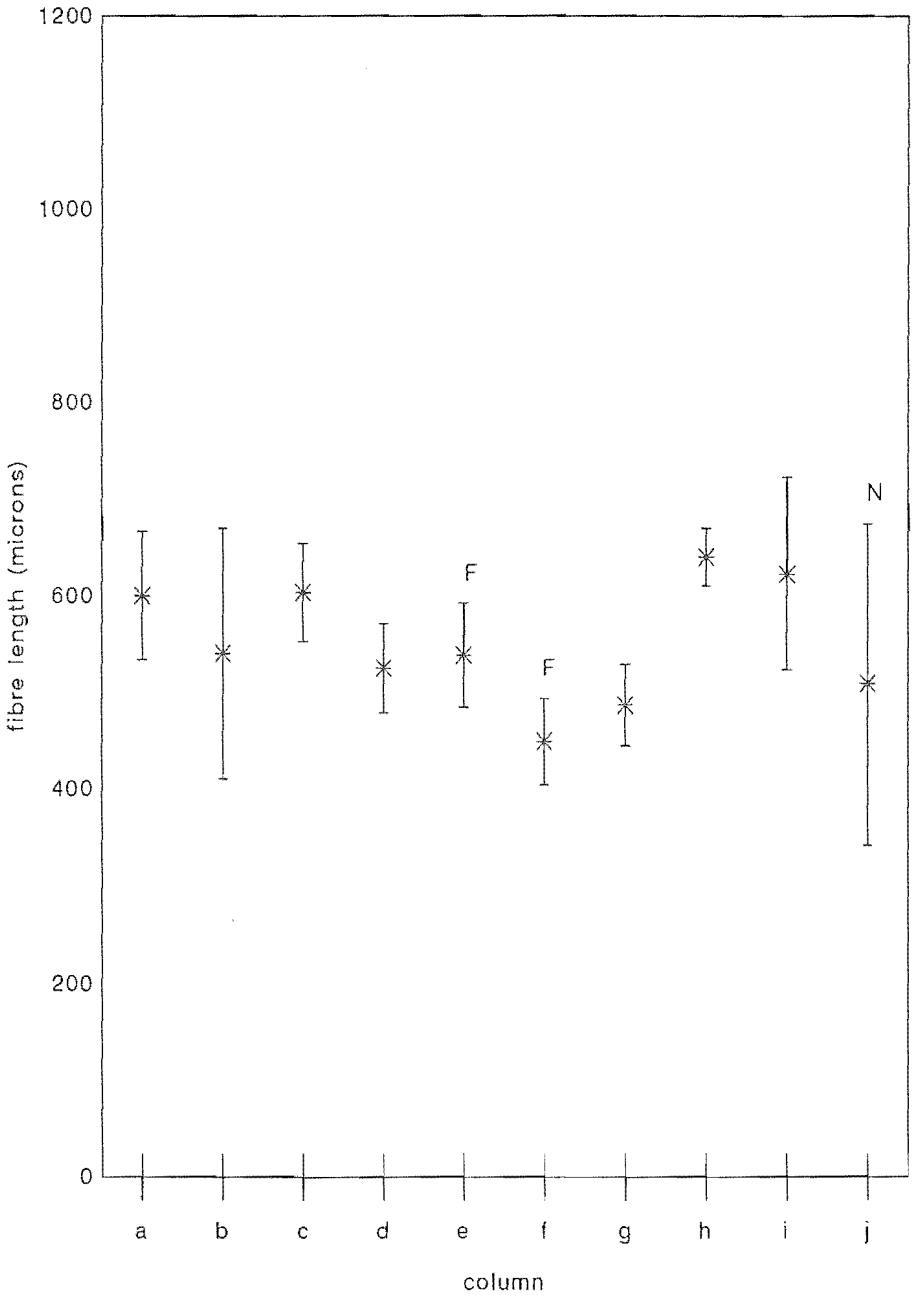

F = fluted
N = non-fluted

(see text for details)

Figure 6.4.d
length of fibres in growth ring
specimen c03

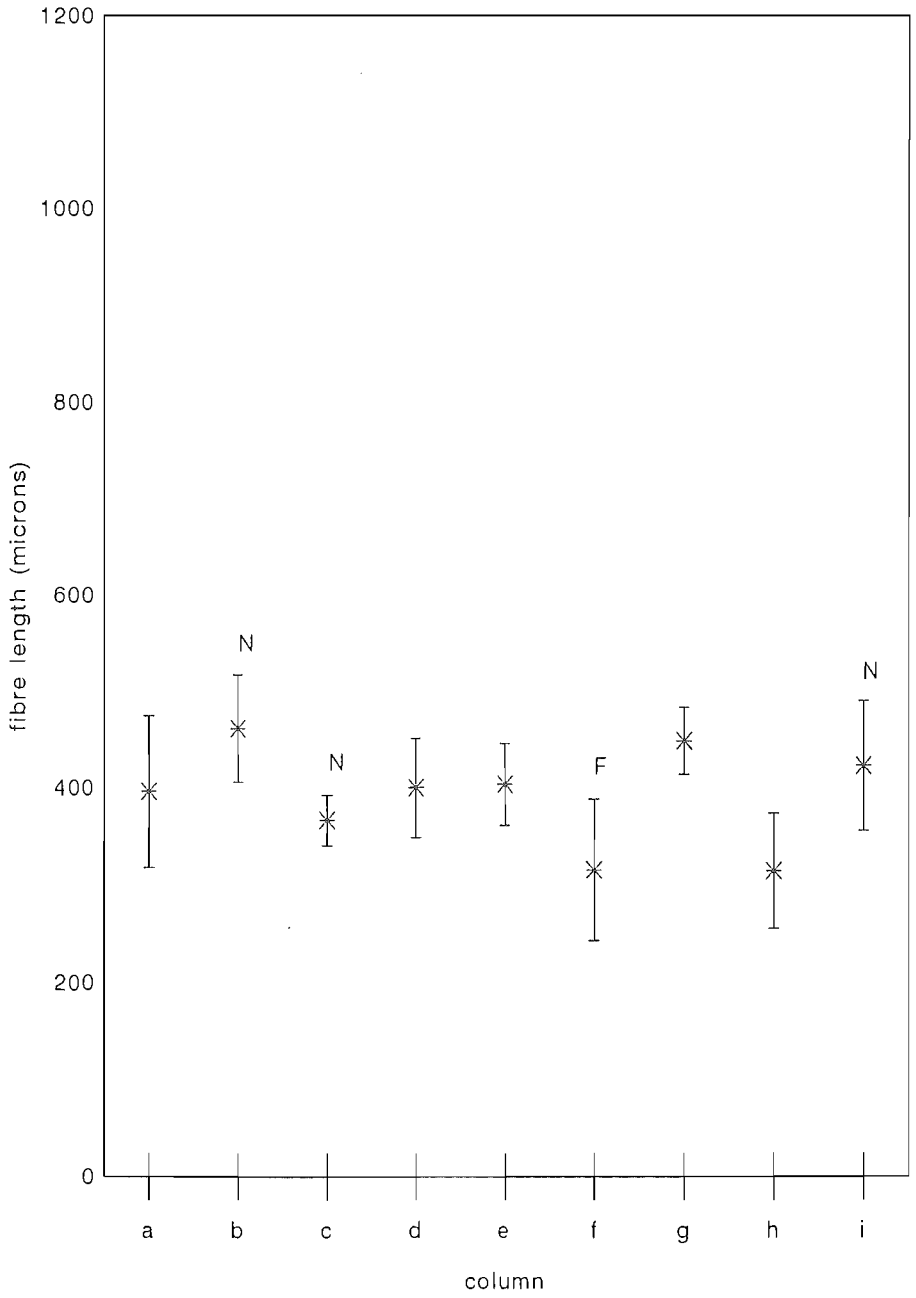

F = fluted
N = non-fluted

(see text for details)

Table 6.6

The number of fusions and splits of rays within the flute

position	no. of splits	no. of fusions
top of flute	1	0
side of flute	7	1
bottom of flute	7	3

Occasionally the fusiform initial between 2 adjacent rays, was lost from the cambium, resulting in a temporary biseriate ray. Biseriate rays formed in this way tended eventually to become uniseriate again over a period of time as the ray cell initials were 'squeezed' together. Where these rays did remain biseriate they tended to correspond to disruption zones.

6.5. DISCUSSION

The prevalence of (+) skews suggests that the decreased length of the fibres in the fluted regions of *Nothofagus* may be a consequence of increased frequencies of anticlinal divisions. This is consistent with the observations of Bannan (1957a) who showed tracheids are shorter, and the frequency of pseudotransverse anticlinal divisions greater, in the fluted regions of *Thuja occidentalis* than in non-fluted regions. This is also in agreement with Schultze-Dewitz and Gotze (1986) who noted that fluted areas have a few very long fibres (longer than in the normal wood), and numerous shorter fibres. Figure 3 page 7 of Schultze-Dewitz *et al* (1986) shows a frequency distribution of fibre lengths for a fluted region, that appears to be (+) skewed, whereas the normal wood is apparently normally distributed.

Bannan (1957a) also stated, that as fluted areas show a 156% increase in frequency of pseudotransverse divisions over non-fluted areas but only show a 19% drop in cell length, that higher rates of pseudotransverse division are accompanied by increased rates of cell elongation between divisions. It is not possible from the results presented here to say that this is also the case with the fluted regions of *Nothofagus*. In chapter 5 it was pointed out that a (-) skewed sample of element lengths, tends to indicate elongation factors. However, this is only the case if a maximum length has been obtained. The 2 daughter initials resulting from a pseudotransverse anticlinal division tend to be shorter than the parent, therefore they can elongate to a greater extent before a maximum obtainable length is reached. If the daughter initials elongated

without reaching a maximum obtainable length, then the distribution of the data would not be effected, and the sample would remain (+) skewed. Although no evidence could be produced showing that pseudotransverse anticlinal divisions are accompanied by increased rates of cell elongation, there is evidence of increased rates of cell elongation after a period of rapid pseudotransverse anticlinal divisions, especially in the disruption zones.

Bannan (1957a) suggested that an increased frequency of pseudotransverse anticlinal divisions and a decreased frequency of periclinal divisions in *Thuja*, results from an increase in radial and tangential pressure within the fluted regions. Wardrop (1948) recorded a decrease in tracheid length as a result of applied radial pressure in *Pseudotsuga* and suggested this was due to increased transverse divisions in the cambium. In contrast to this, applied radial pressure has also been shown to decrease cambial activity (Brown and Sax 1961, Makino, Kuroda and Shimaji 1983). This suppression, however, was in relation to explants, where pressure had been removed, and divisions were frequent and unordered. Lintilhac and Vesecky (1981) found increased radial pressure has no apparent suppressing effect on cell proliferation. Mechanical pressure applied by gentle rubbing has some effect on primary development (Jaffe 1973) and may result in increased development of xylem (Biro and Jaffe 1984). However, these responses relate to temporary stimuli and as such may need to be viewed with caution when compared to long-term application of pressure.

The consensus would suggest that pressure does play some role in the activity occurring within fluted regions, and applied radial pressure can induce these flutes in some situations (Imamura 1978). However, the greatest amount of deformation occurs at the sides of the flutes in *Nothofagus*. This is also the case with the indented rings of *Picea sitchensis* (Ohtani, Fukuzawa and Fukumorita 1987). Here there are abnormal tracheids on the sides of the flutes, whereas the centres of the flutes appear similar to the normal wood. Ohtani *et al* (1987) also suggested that there are higher frequencies of pseudotransverse divisions on the sides of the flutes as well as disordered periclinal divisions of cambial initials or xylem mother cells. It is the sides of the flutes where the shear stresses are the greatest, and as new cell walls tend to orient themselves perpendicular to the direction of greatest pressure (Lintilhac and Vesecky 1981) this results in cambial walls inclined to the surface in fluted areas (Bannan 1957a, Newman 1956).

Although it appears there may be more deformation at the sides of the flutes than in the middle, it is in the middle of the flutes in *Nothofagus* where the aggregation of

parenchyma is most pronounced, and where fibre lengths are significantly shorter than elsewhere. Wenham and Cusick (1975) have suggested that tensile stress across the tangential middle lamellae is required for intrusive growth of derivatives. Hejnowicz (1980) has illustrated these tangential stresses, and shown there are also tensile stresses across the radial middle lamellae.

With every successive periclinal division in a non-fluted cambium, the tensile stress across the radial middle lamellae of the cambial initials would be increased. A certain amount of this stress would be dissipated by cell enlargement (tangentially), and cell elongation, as well as by anticlinal divisions. In the fluted regions, every successive periclinal division would decrease the tensile stress across the radial middle lamellae of the cambial initials. Eventually, with further divisions, this tensile stress would be converted to compression stress. This compression stress could be dissipated by a decrease in cambial cell lengths[1], or width, or by increasing the number of cell initials lost from the cambium. In this situation the shorter lengths may be a consequence of increased pseudotransverse anticlinal divisions and decreased cell elongation. The elongation aspect of this decreased cell length would not necessarily show up in the skew of the sample, as the resulting axial lengths would have been brought about by a decreased amount of elongation, not by the cells obtaining a maximum length, beyond which further elongation is not possible.

The compression acting on the cambial initials, within the fluted regions, would also be acting on the xylem derivatives of those initials. This would tend to restrict the diameter of these derivatives, and inhibit the formation of vessel elements. Where vessel elements are present, however, this may lead to an increase in the lengths of neighbouring fibres, as their increased radial width would produce a localised increase in tensile stress across the tangential middle lamellae (Wenham and Cusick 1975). This would result in the few very long fibres in the flutes, noted by Schultze-Dewitz and Gotze (1986). If this was the case, then it throws the use of the (+) skew, for the determination of cambial activity, into doubt, as a few very long fibres would also produce this distribution.

In the fluted areas of *Alnus, Carpinus* and *Corylus*, individual parenchyma rays tend to be lost more on the sides of the flutes than in the middle (Holdheide 1955). This situation apparently also exists in *Picea* (Ohtani *et al* 1987). Although rays tend to

---

1 The significant reduction in the number of ray cells per ray, in the fluted regions, may indicate such a process. Ziegler and Merz (1961) also record a reduction in the number of cells per ray in fluted regions.

converge at the sides of the flutes in *Nothofagus*, there was no evidence that this leads to the loss of rays, or ray initials, at a greater rate than occurs in the centre of the flutes.

Bosshard (1976) relates the presence of indented rings, and aggregate rays, to the functional properties of wood. In his theory of functional tropism, the structure of the wood relates to the processes of transportation and assimilation. He suggests indented stems and aggregate rays are caused by concentrations of slower growing radial storage tissue. These woods, therefore, have a dominance of assimilation over water transportation, and as such exhibit negative functional tropism. This negative functional tropism may be a factor in *Fagus* and others with a similar structure. The aggregation of rays in the flutes of *Nothofagus* is, by comparison, a more haphazard process. The convergence of rays in the fluted areas does not result in the build up of ray tissue, as biseriate or multiseriate rays built-up in this way tend to be reduced back to uniseriate rays, with further cambial development. The shortening of rays within the fluted areas is another example of this. To the contrary, the build-up of parenchyma is achieved largely by the loss or dissection of axial elements, and the ray material built-up in this way is again reduced by further cambial development (Chapter 2). Activity such as this is far more suggestive of conditions within the fluted regions, than it is of some holistic condition of the plant where assimilation is dominant to water transportation.

Holdheide (1955) suggested the large rays of *Quercus*, and those of *Alnus*; *Carpinus*; and *Corylus* (with a similarity to those of *Nothofagus*) are probably different, but relates the formation of all fluted areas to nutrient deficiency in the phloem. Lev-Yadun and Aloni (1991b) showed that flutes can be initiated by wounding that apparently restricts the auxin flow, and existing aggregate rays can be dissipated by an apparent increase in auxin (Lev-Yadun and Aloni 1991a). That the phloem in the fluted regions of *Nothofagus* seems to have a deficit of sieve tube elements lends support to this idea.

A dominant feature of the development of the diffuse aggregate ray in *N. fusca* is the prominent indentation under the leaf-trace (Chapter 3). It may be that the diffuse aggregate ray in this species, is a feature of the flute, rather than the other way around. Certain features of the diffuse aggregate rays of *Nothofagus*, such as: reduced axial length; the general lack of vessels; a reduction in the number of individual rays and the disruption zones, can be accounted for by the constraining influence of the flute on the cambium. However, the leaf-trace of *N. menziesii* is also

subtended by a prominent indentation, but this fails to develop into an aggregate ray (Chapter 3). However, it was shown in Chapter 4 that *N. menziesii* and *N. fusca* seedlings have different responses to applied growth substances, especially auxin.

The physical features of the flutes, in addition to the possible restrictions in auxin flow (or other growth substance flows), may account for the presence of these diffuse aggregate rays. If such is the case, then the diffuse aggregate ray of *Nothofagus* can be regarded as an artefact produced by a set of circumstances, and not a discrete morphological feature for which a purpose or function must be found.

CHAPTER 7

CONCLUSIONS

The term 'aggregate ray' encompasses a wide variety of structures, ranging from the very high and wide multiseriate rays characteristic of some species of *Quercus* and *Casuarina*, to the radially extensive zones characterised by a general absence of vessels and a close association of individual rays, characteristic of some species of *Nothofagus* and *Alnus*. Although it was recognised that the aggregate ray represents a continuum of structures, it was convenient to break this continuum up into 3 separate groups:

Entire aggregate rays. The broad and high rays, commonly designated as compound, with only a few signs of dissections or fusions;

Fasciculate aggregate rays. Closely associated uniseriate, biseriate and multiseriate rays;

Diffuse aggregate rays. Morphologically indistinct zones, consisting of closely associated uniseriate or biseriate rays, and marked by the general absence of vessels.

The term 'aggregate ray' is in some ways unfortunate. The word 'aggregate' implies a collection of associated individuals, and when it is used to describe structures, here defined as 'entire aggregate rays', suggests a particular ontogeny. The word 'ray' is also unfortunate in some ways, as it tends to define a discrete structure. The diffuse aggregate ray is not a discrete structure, but is to the contrary, an indistinct zone. Despite the problems with the terminology, the term 'aggregate ray' has been retained as it is the accepted term in the literature.

The entire aggregate ray of *Fagus sylvatica* is essentially a continuation of the 'leaf-gap', that shows signs of dissection by axial elements at the margins. The fasciculate aggregate rays of *Dracophyllum pronum* and *D. uniflorum* are also extensions of the 'leaf-gaps', but become continuous with tissue below the leaf-trace, after it has ruptured. The tissue under the leaf-trace consists of ray parenchyma that has become closely associated (aggregated) due to the 'arching over' of the leaf-trace, and its confining effect on cambial activity. The diffuse aggregate ray of *Nothofagus* also relates back to the leaf,

where there is some aggregated tissue below the leaf-trace. However, this aggregated tissue dissipates quickly and no direct connection could be found between it, and the full development of the diffuse aggregate ray structure. There is apparently evidence for both the 'synthetic' and 'dissection' theories of aggregate ray origin, depending on the species and the relative point of observation. Most sections from above the leaf-trace will show evidence for the 'dissection' theory, and most sections below the leaf-trace will show evidence for the 'synthetic' theory.

The presence of aggregate rays can be correlated with an irregular pith outline (not circular). An irregular pith outline can, in turn, be correlated with increased light availability, and the application of gibberellin. It is suggested that the presence of aggregate rays in some species of *Nothofagus*, relates to the extension of the internode and the development of the leaf-trace, especially with respect to the relative proportions of cell elongation and division within the procambium, and the early vascular cambium.

Certain characteristics of the diffuse aggregate rays of *Nothofagus*, such as: reduced axial element length; the general lack of vessels; reduction in the number of individual ray cells and the disruption zones, can be accounted for by the constraining influence of the flute on the cambium. The influence of the flute, plus the response to the presence (or lack) of various growth substances, during both juvenile and mature growth, may account for the presence of diffuse aggregate rays in *Nothofagus*. As such, these structures may represent artefacts of growth activity, rather than functional features of the plant.

APPENDIX 1

METHODS USED IN PARAFFIN EMBEDDING, AND SECTION STAINING

A1.1. SPECIMEN PREPARATION AND SECTIONING

Formalin - Acetic acid - Alcohol (FAA) vacuum fixed specimens, were softened in a 10% aqueous solution of diaminoethane (ethylenediamine - Carlquist 1982) for periods up to 5 days, or more, depending on the size and hardness of the sample. Samples were then rinsed in water and dehydrated in a Tertiary Butyl Alcohol (TBA) series (Johansen 1940), with the samples being left in each grade of the series for 24 hours. Samples were then infiltrated with Paraplast Plus[1] paraffin wax, via a liquid paraffin intermediary. Samples were placed in a vacuum oven during the paraffin wax infiltration. Samples were mounted in paraffin wax, and the face to be cut was trimmed until the surface of the sample was exposed. The embedded blocks were then placed in water until the water had infiltrated the entire sample (approximately 1 day for each 1mm of tissue beyond the cut surface for woody samples). Sections were cut on a Reichert-Jung Autocut microtome with a steel knife, making sure at all times that the cut surface was not allowed to dry out. Sections were affixed to slides with an gelatin adhesive (Bissing 1974).

A1.2. SAFRANIN - FAST GREEN DOUBLE STAINING

Slides were dewaxed in xylene and double stained according to the standard procedure (Johansen 1940).

A1.3. BRILLIANT CRESYL BLUE STAINING

Slides were dewaxed in xylene and rehydrated in an ethanol series for 1 minute in each of 100; 90; 80 and 70 % grades. They were then stained in a 0.01% aqueous solution of Brilliant cresyl blue for 5 minutes, and then dehydrated in an ethanol series, with 5 seconds in each of 60; 70; 80; 95 and 100% grades, and placed in xylene (3 changes). Slides were mounted in Depex[2].

---

1 Lancer Division of Sherwood Medical.
2 BDH Limited Poole England.

This staining method resulted in dark blue primary (unlignified) walls and pale green-blue secondary (lignified) walls. Phenolics in the bark were yellow-orange to yellow-brown, as were some of the intercellular spaces in the xylem (Figure A1.1). The stain was particularly good for septate fibres, bordered pits and perforation plates. Reaction wood also stained well, the gelatinous layer staining dark blue. To achieve this level of staining the sections appeared to require the diaminoethane pretreatment.

Figure A1.1

Section stained with brilliant cresyl blue with a diaminoethane pretreatment (*Fagus sylvatica* TS)

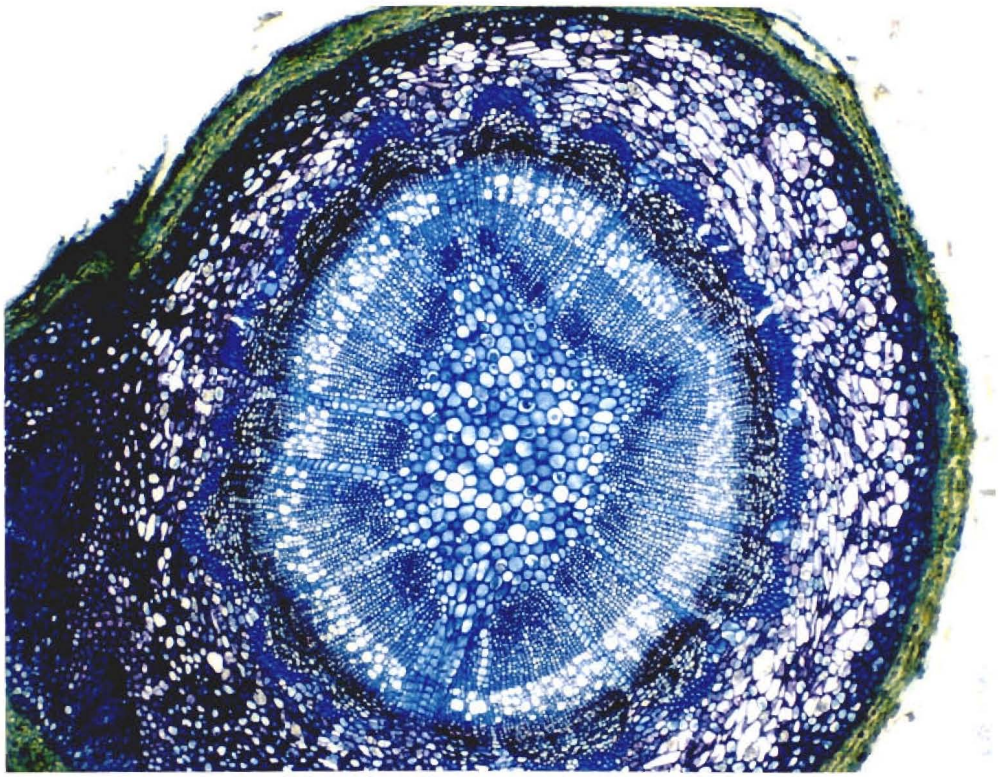

APPENDIX 2

SAS PROGRAMS USED FOR THE CELL ELONGATION AND DIVISION ALGORITHMS

A2.1. ELONGATION ALGORITHM WITH 2 STAGES OF ELONGATION

```
options pagesize = 50;

%macro increase;

%do efs = 02 %to 002 %by 02;

data a (drop = LENGTH);
set a;
EF = 15.00;
length1 = LENGTH+(EF);
lenmax = 1000175;
if length1 > lenmax then length1 = lenmax;

data a (drop = length1 );
set a;
LENGTH = length1;

data b (drop = LENGTH);
set a;
EF = 15.00;
length1 = LENGTH+(EF);
lenmax = 1000175;
if length1 > lenmax then length1 = lenmax;

data b (drop = length1 );
set b;
LENGTH = length1;

proc append base = record.cam data = a;
proc append base = record.der data = b;

%end;

%mend increase;

libname record 'c:\sas\altemp\';

data a ;
 set record.longbase;
 EF = .;

%increase;
```

```
proc univariate noprint data = record.cam;
id EF;
var LENGTH;
output out = skewscam mean = mean n = n skewness = skewness kurtosis = kurtosis;

data skewscam (keep = EF n mean skewness probs kurtosis probk);
set skewscam;

sk = 3*(((n**2)+(27*n)-70)*(n+1)*(n+3))/((n-2)*(n+5)*(n+7)*(n+9));
v1 = ((4*sk)-6)/(sk-3);
v2 = (v1)/(v1-2);
    if v2 lt 0 then v2 = v2*(-1);
v3 = v2**0.5;
vs = sqrt((6*(n-2))/((n+1)*(n+3)));
ts = abs((skewness*v3)/vs);
tk = abs((kurtosis*v3)/vs);
df = round(v1,1);
probs = (1 - probt(abs(ts),v1))*2;
probk = (1 - probt(abs(tk),v1))*2;

proc append base = record.e32clong data = skewscam;

proc print data = record.e32clong;
title 'cambium';

proc univariate noprint data = record.der;
id EF;
var LENGTH;
output out = skewsder mean = mean n = n skewness = skewness kurtosis = kurtosis;

data skewsder (keep = EF n mean skewness probs kurtosis probk);
set skewsder;

sk = 3*(((n**2)+(27*n)-70)*(n+1)*(n+3))/((n-2)*(n+5)*(n+7)*(n+9));
v1 = ((4*sk)-6)/(sk-3);
v2 = (v1)/(v1-2);
    if v2 lt 0 then v2 = v2*(-1);
v3 = v2**0.5;
vs = sqrt((6*(n-2))/((n+1)*(n+3)));
ts = abs((skewness*v3)/vs);
tk = abs((kurtosis*v3)/vs);
df = round(v1,1);
probs = (1 - probt(abs(ts),v1))*2;
probk = (1 - probt(abs(tk),v1))*2;

proc append base = record.e32dlong data = skewsder;

proc print data = record.e32dlong;
title 'derivatives';

run;
```

A2.2. DIVISION ALGORITHM

```
options pagesize = 50;

%macro increase;

%do efs = 02 %to 020 %by 02;

data a ;
set d;
if divlen = 1;
div1 = ranuni(0);
div2 = 1 - div1;

data b (drop = length1 length2);
set a;
EF = 0.02;
PT = 0.50;
ef1 = ranuni(0)*EF+EF;
LENMIN2 = normal(0)+20;
length_p = (LENGTH*div1);
length1 = length_p+(length_p*PT);
if length1 < LENMIN2 then delete;
length2 = length1+(length1*ef1);
LENGTH = length2;

data c (drop = length1 length2 length_p);
set a;
EF = 0.02;
PT = 0.50;
ef1 = ranuni(0)*EF+EF;
LENMIN2 = normal(0)+20;
length_p = (LENGTH*div2);
length1 = length_p+(length_p*pt);
if length1 < LENMIN2 then delete;
length2 = length1+(length1*ef1);
LENGTH = length2;

data e (drop = length2);
set d;
if divlen = 0;
EF = 0.02;
ef1 = ranuni(0)*EF+EF;
length2 = LENGTH+(length*ef1);
LENGTH = length2;

data d (drop = div1 div2 LENMIN2 EXTINCT LENMIN1);
set b c e;
DIVIDE = uniform(0);
EXTINCT = uniform(0);
if EXTINCT > .99 then delete;
LENMIN1 = 090;
lenmin = normal(0)+LENMIN1;
if LENGTH >= lenmin and DIVIDE > .99 then divlen=1;
else divlen=0;
```

```
proc append base = record.out data = d;

%end;

%mend increase;

libname record 'c:\sas\altemp';

data d (drop =lenmin);
 set record.longbase;
    EF = .;
    DIVIDE = uniform(0);
    lenmin = normal(0) + 090;
if LENGTH >= lenmin and DIVIDE > .99 then divlen=1;
else divlen=0;

proc append base = record.out data = d;

%increase;

proc univariate noprint data = record.out;
id EF;
var LENGTH;
output out = skews mean = mean n = n skewness = skewness kurtosis = kurtosis;

data skews (keep = n mean skewness probs kurtosis probk);
set skews;

sk = 3*(((n**2)+(27*n)-70)*(n+1)*(n+3))/((n-2)*(n+5)*(n+7)*(n+9));
v1 = ((4*sk)-6)/(sk-3);
v2 = (v1)/(v1-2);
    if v2 lt 0 then v2 = v2*(-1);
v3 = v2**0.5;
vs = sqrt((6*(n-2))/((n+1)*(n+3)));
ts = abs((skewness*v3)/vs);
tk = abs((kurtosis*v3)/vs);
df = round(v1,1);
probs = (1 - probt(abs(ts),v1))*2;
probk = (1 - probt(abs(tk),v1))*2;

proc append base = record.e22long data = skews;

proc print data = record.e22long;

run;
```

APPENDIX 3.A

THE RECONSTRUCTION OF GROWTH RINGS FROM SERIAL LONGITUDINAL SECTIONS

A3.A.1. INTRODUCTION

This method takes a set of serial tangential longitudinal sections, and by using a set of co-ordinates, enables the reconstruction of growth rings in 3 dimensions. Having done so, any point, on any section within the series of sections, can have its position identified relative to any other point in the series. From this it is possible to take any fibre from a section within the series, and locate its position in the growth increment (i.e. its relativity to the growth rings). For this method to be successful it must be possible to locate growth rings in tangential section (i.e. the sections cannot be perfectly tangential). Programs were constructed using SAS.

A3.A.2. METHOD

Serial tangential sections, of a known thickness were cut, mounted, and stained in the normal manner (Appendix 1). An eye-piece grid was used with 10X10 squares. The grid size was calibrated for the magnification used. The grid was placed over each section on a fixed reference corner, and the position of the growth ring recorded in grid co-ordinates (Figure A3.1).

For each series of sections there were a number of growth rings, each ring was numbered beginning from the cambium (0 if present in series). The co-ordinates for each section were incorporated into PROGRAM 1.

Variables that are explicitly stated in the programs summaries below are capitalised, Those that are implicit are italicised. The actual programs are contained in Appendix 3b.

PROGRAM 1 (format.sas) incorporates raw data of growth rings collected from serial sections. Rows and columns of the grid are recognised. The data is formatted in such a way that individual rows are represented as variables. The output of this program was then fed into PROGRAM 2.

Figure A3.1

Recording growth ring position in grid co-ordinates

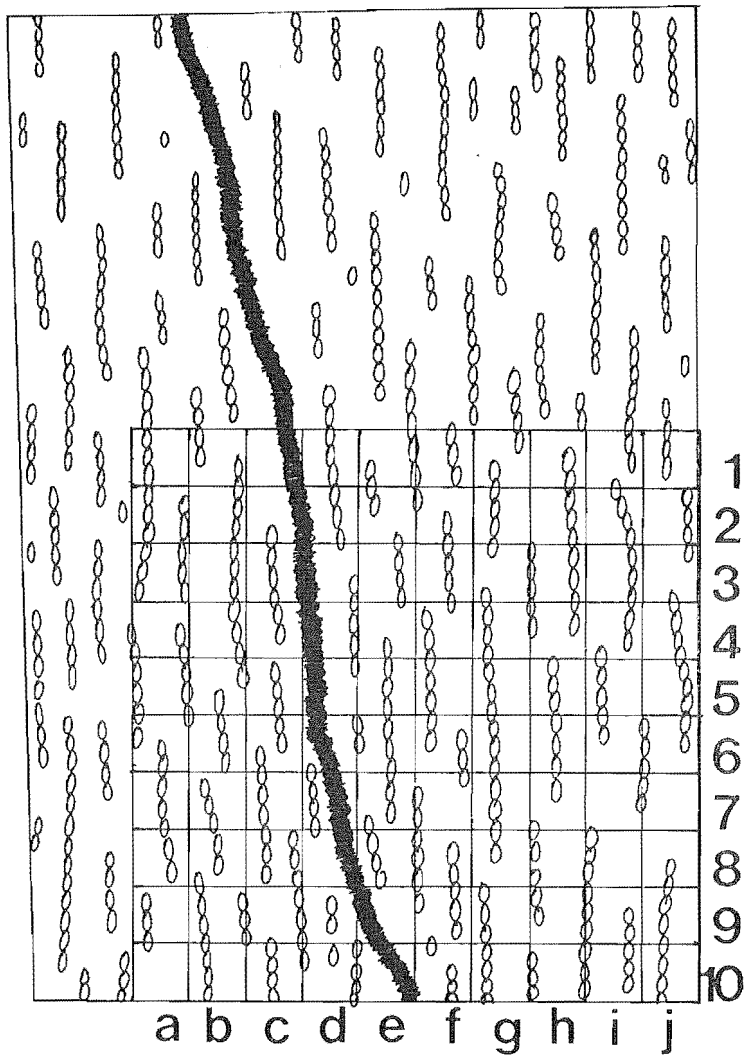

A 10x10 grid with rows 1 to 10, and columns a to j, is placed on a TLS (here the fixed point is at j10, but may be on any of the 4 corners). The thick black line represents the growth ring, its co-ordinates are c1,c2,d3 to d8,e9,e10.

PROGRAM 2 (printts.sas) takes the output of PROGRAM 1, which is still in the form of a serial tangential dataset, and transposes it to a serial transverse dataset. The variables **SLIDE** and **SECT_NUM** are modified depending on the sample. The result of PROGRAM 2 was a printed output showing a serial transverse section for each growth ring at each row of the grid (Figure A3.2).

From this printout it was possible to pin-point where the growth ring crossed columns. As the growth rings were indented, it was also noted whether each column contained a minimum turning point (concave growth ring = flute) or a maximum turning point (convex growth ring). These co-ordinates were recorded and incorporated into PROGRAM 3.

PROGRAM 3 (coordraw.sas) incorporates the raw data from the printout. From this a gradient of the growth ring for each column was calculated on section thickness, grid width, and where the growth ring crossed columns. If a minimum or maximum turning point was in the column then the gradient was set to zero (Figure A3.3). A slide (X_REF) was identified where the growth ring occurred in the middle of the column (Figure A3.3).

This was done for each row of the grid, for each growth ring. The result of this was each growth ring being represented as a surface defined by 3 axes, **SLIDE**, **ROW** and *column* (Figure A3.4).

PROGRAM 4A (radtrans.sas) takes the output dataset from PROGRAM 3 and transposes it into a serial radial dataset, with individual growth rings represented as variables.

PROGRAM 4B (samplgen.sas) generates a sample file based on the number of slides in the series. This sample is in random grid co-ordinates on random slides. These co-ordinates may occur anywhere in the growth increment.

PROGRAM 5 (samerge1.sas) merges the output from PROGRAM 4A, with that from PROGRAM 4B. It also transposes the sample file into a form where rows are represented as variables.

PROGRAM 6A (rowfora1.sas) takes the merged file output from PROGRAM 5 and expands it for ring position and gradient variables. It also remerges the transposed

Figure A3.2
A portion of printed output from PROGRAM 2 (printts.sas)

ring	slide	section	column									
			a	b	c	d	e	f	g	h	i	j
5	1774	6					1	1				
5	1774	8					1	1				
5	1774	10			MX		1	1				
4	1772	18		1	1							
4	1772	20	1		1							
4	1772	22	1			1						
4	1772	24				1						
4	1773	2				1						
4	1773	4				1				MX		
4	1773	6					1		1	1		
4	1773	8					1		1		1	
4	1773	10					1		1			1
4	1773	12					1	1				1
4	1773	14					1	1				1
4	1773	16					1	1				
3	1771	22		1	1			MN				
3	1771	24	1		1							
3	1772	2				1						

This printout shows the growth ring data in its transverse aspect. In the example above the complete growth ring for the first row (row 1) of the 4th growth ring is shown (portions of rings 3 and 5 are also shown). The number 1 indicates that the growth ring is present in that column on that slide and section. From this it is possible to pin-point where growth rings crossed columns (*). MX indicates the maximum turning points (non-fluted regions) and MN indicates the minimum turning point (fluted region).

Figure A3.3

The calculation of gradients and the positioning of X_REF

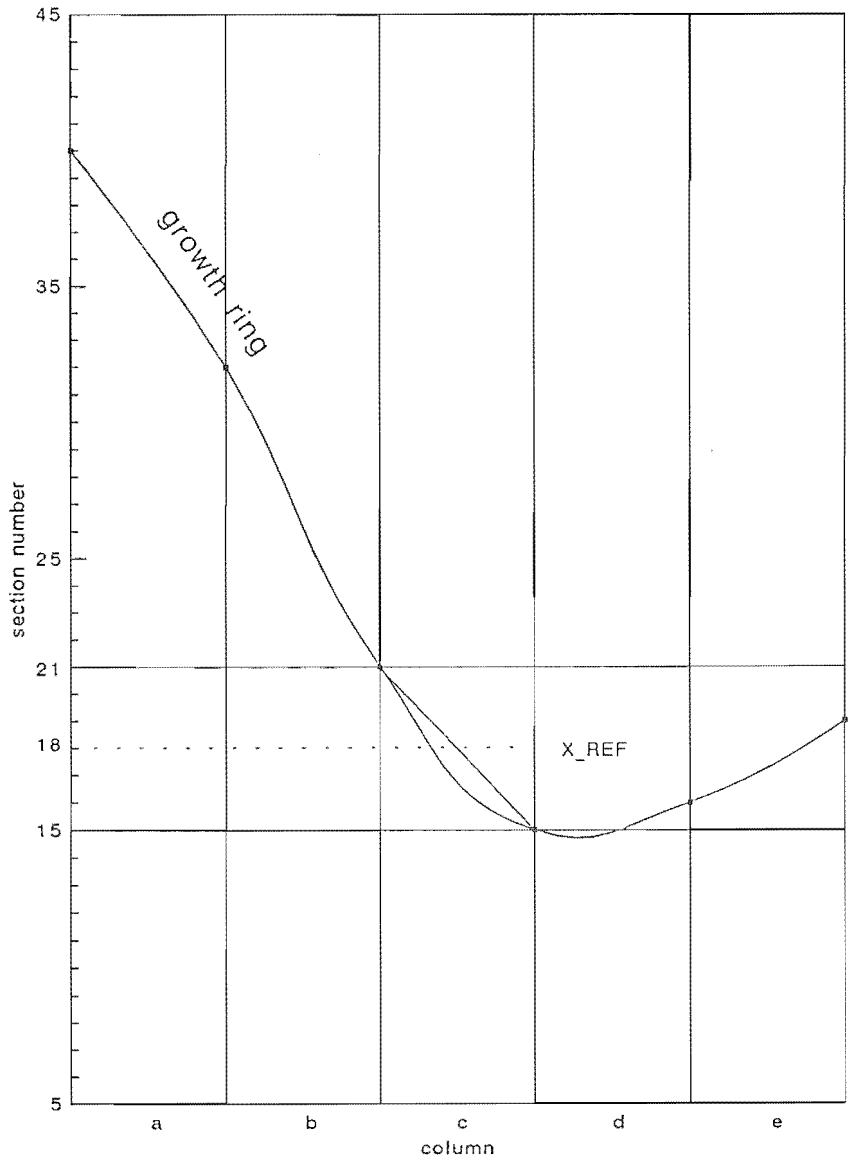

As the columns have a known, fixed, width, the gradient of the growth ring can be calculated if the thickness of the sections is also known. The growth ring crosses from column b into column c at section number 21, and passes from column c into column d at section number 15. The gradient is calculated as ((21-15)*X)/Y, where X = the thickness of the sections, and Y = the width of the column. The variable X_REF represents where the growth ring (as a straight line) crosses the middle of the column. In this case the X_REF for column c (C_REF) is at section 18.

sample file with the dataset. PROGRAM 6B (rowforb1.sas) does the same as PROGRAM 6B, for the turning point variables.

PROGRAM 7 calculates where observations in the sample file occur in relation to the growth rings, depending on their co-ordinates. The relative position of an observation, in the sample file, to the growth rings is calculated as in Figure A3.5. The value for the relative position ranged from 0 to 1. A value close to 0 represents a position close to the inner growth ring, and a value close to 1 represents a position close to the outer growth ring. If the relative position was less than 0.25 a weighting variable was given to the value of 1. For relative positions from 0.25 to 0.50 the weighting value was 0.66, from 0.50 to 0.75 it was 0.34 and from 0.75 to 1.00 it was 0. The gradient of the cambium, when it was at the position of the observation in the sample file, was estimated based on the gradients of the growth rings on either side, adjusted by the weighting value. Whether an observation from the sample file had a turning point was estimated based on the growth rings on either side. If a turning point was present, for that row and column, on either of those growth rings, then the observation was given that turning point.

Figure A3.4

The reconstruction of growth rings for specimen 113

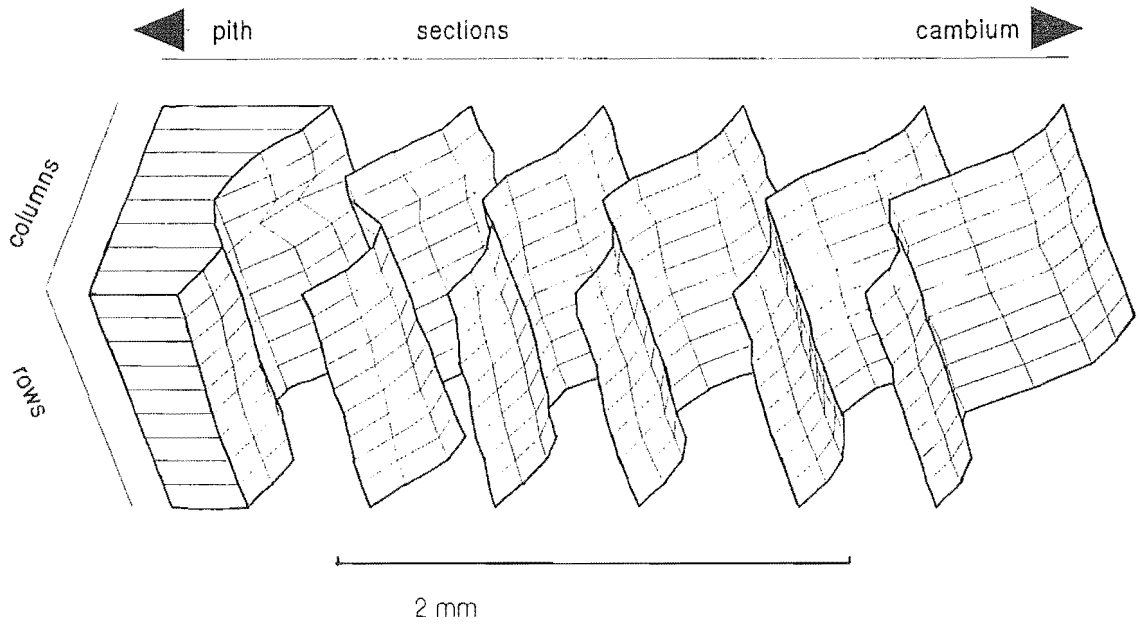

Each growth ring is represented as a 3 dimensional surface. The axis labelled as rows also represents the long axis of the stem.

Figure A3.5

The calculation of the position of an observation from the sample file relative to the growth rings

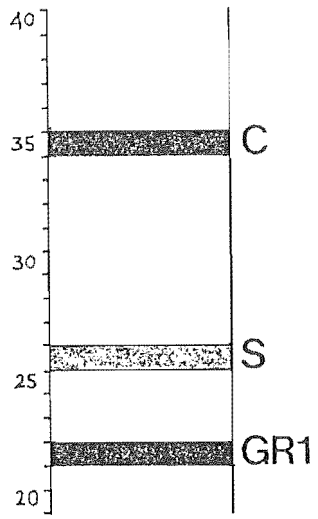

This figure represents a column with the cambium (C) present at section 35 and growth ring 1 (GR1) at section 22. The observation from the sample file (S) is at section 26. The relative position of (S) is calculated as (26-23)/(35-23) = 0.25.

APPENDIX 3.B

SAS PROGRAMS USED FOR THE RECONSTRUCTION OF GROWTH RINGS FROM SERIAL LONGITUDINAL SECTIONS

A3.B.1. PROGRAM 1

```
/*****************************************************;
 * TITLE.            format.sas                      *
 *                                                   *
 * INPUT FILE.       grwthrng.dat                    *
 *                                                   *
 * OUTPUT FILE.      ordered.ssd                     *
 *                                                   *
 *****************************************************/;

libname ringdata 'f:\sas\alan\ringtran\working';
 options obs = max;

filename grwthrng
'f:\sas\alan\ringtran\working\grth3rng.dat';
data form;
 infile grwthrng missover;
 input ring slide section col $ row01 - row10;
run;

proc sort data = form;
 by ring slide section col;

proc transpose data = form out = rows;
 by ring slide section col;
 var row01 - row10;
 run;

 data change (drop = _name_) ;
  set work.rows;
  if col1 ne .;
  length across $ 5;
  if col1 = 01 then across = 'row01';
  if col1 = 02 then across = 'row02';
  if col1 = 03 then across = 'row03';
  if col1 = 04 then across = 'row04';
  if col1 = 05 then across = 'row05';
  if col1 = 06 then across = 'row06';
  if col1 = 07 then across = 'row07';
  if col1 = 08 then across = 'row08';
  if col1 = 09 then across = 'row09';
  if col1 = 10 then across = 'row10';
run;

proc transpose data = change out = ringdata.ordered;
```

```
by ring slide section col;
id across;
run;

proc print;
var ring slide section col row01 - row10;
run;
```

A3.B.2. PROGRAM 2

```
/*******************************************************;
 * TITLE.            printts.sas                       *
 *                                                     *
 * INPUT FILE.       ordered.ssd                       *
 *                                                     *
 * OUTPUT FILE.   printts.lst (manual output)          *
 *                                                     *
 *******************************************************/;

libname ringdata 'f:\sas\alan\ringtran\working';
 options pagesize = 66;

data a;
 set ringdata.ordered;

proc transpose data = a out = a;
 by ring slide section col;

data b;
 set a;
 if col1 ne .;
 if ring = 0 then rank = 6;
 if ring = 1 then rank = 5;
 if ring = 2 then rank = 4;
 if ring = 3 then rank = 3;
 if ring = 4 then rank = 2;
 if ring = 5 then rank = 1;

 proc sort data = b;
 by _name_ rank slide section col1 ring ;

proc transpose data = b out = b;
 by _name_ rank slide section ring;
 id col;

data c;
set b;
 if a>. or b>. or c>. or d>. or e>. or f>. or g>. or h>. or i>. or j>.;
 if slide = 1766 then sect_num = 0 + section;
 if slide = 1767 then sect_num = 24 + section;
 if slide = 1768 then sect_num = 48 + section;
 if slide = 1769 then sect_num = 72 + section;
 if slide = 1770 then sect_num = 96 + section;
 if slide = 1771 then sect_num = 120 + section;
 if slide = 1772 then sect_num = 144 + section;
```

```
if slide = 1773 then sect_num = 168 + section;
if slide = 1774 then sect_num = 192 + section;

proc print data = c noobs;
var ring sect_num slide section a b c d e f g h i j;
run;
```

A3.B.3. PROGRAM 3

```
/*****************************************************;
* TITLE.            coordraw.prg                      *
*                                                     *
* INPUT FILE.       rngord01.dat                      *
*                                                     *
* OUTPUT FILE.      interdat.ssd                      *
*                                                     *
******************************************************/;

libname ordout01 'f:\sas\alan\ringtran\working';

filename coords 'f:\sas\alan\ringtran\working\rngord3.dat';

data raw;
 infile coords missover;
 input ring 2. row 2. s_sli 4. s_sec 2. s_max 1. s_min 1.
      a_sli 4. a_sec 2. a_max 1. a_min 1.
      b_sli 4. b_sec 2. b_max 1. b_min 1.
      c_sli 4. c_sec 2. c_max 1. c_min 1.
      d_sli 4. d_sec 2. d_max 1. d_min 1.
      e_sli 4. e_sec 2. e_max 1. e_min 1.
      f_sli 4. f_sec 2. f_max 1. f_min 1.
      g_sli 4. g_sec 2. g_max 1. g_min 1.
      h_sli 4. h_sec 2. h_max 1. h_min 1.
      i_sli 4. i_sec 2. i_max 1. i_min 1.
      j_sli 4. j_sec 2. j_max 1. j_min 1.;
run;

data a;
 set raw;
  array slide {11} s_sli a_sli b_sli c_sli d_sli e_sli f_sli g_sli h_sli i_sli j_sli;
  array section {11} s_sec a_sec b_sec c_sec d_sec e_sec f_sec g_sec h_sec i_sec j_sec;
  array number {11} s_num a_num b_num c_num d_num e_num f_num g_num h_num i_num
j_num;
  do i = 1 to 11;
   if slide {i} = 1766 then number {i} = 0 + section {i};
   if slide {i} = 1767 then number {i} =24 + section {i};
   if slide {i} = 1768 then number {i} =48 + section {i};
   if slide {i} = 1769 then number {i} =72 + section {i};
   if slide {i} = 1770 then number {i} =96 + section {i};
   if slide {i} = 1771 then number {i} =120 + section {i};
   if slide {i} = 1772 then number {i} =144 + section {i};
   if slide {i} = 1773 then number {i} =168 + section {i};
   if slide {i} = 1774 then number {i} =192 + section {i};
   end;
run;
```

```
data b;
 set a;
 array grad {10} grad_a grad_b grad_c grad_d grad_e grad_f grad_g grad_h grad_i grad_j;
 array num1 {10} s_num a_num b_num c_num d_num e_num f_num g_num h_num i_num;
 array num2 {10} a_num b_num c_num d_num e_num f_num g_num h_num i_num j_num;
 array reff {10} a_ref b_ref c_ref d_ref e_ref f_ref g_ref h_ref i_ref j_ref;
  do i = 1 to 10;
    grad {i} = round(((abs(num1 {i} - num2 {i})*16)/111.11),.01);
    if num1 {i} le num2 {i} then do;
      reff {i} = num2 {i} - (round(((num2 {i} - num1 {i})/2),1));
      end;
    if num1 {i} gt num2 {i} then do;
      reff {i} = num1 {i} - (round(((num1 {i} - num2 {i})/2),1));
      end;
   end;
run;

data ordout01.interdat;
 set b;
 length a_tp $ 3;
 length b_tp $ 3;
 length c_tp $ 3;
 length d_tp $ 3;
 length e_tp $ 3;
 length f_tp $ 3;
 length g_tp $ 3;
 length h_tp $ 3;
 length i_tp $ 3;
 length j_tp $ 3;

 array max1 {10} s_max a_max b_max c_max d_max e_max f_max g_max h_max i_max;
 array max2 {10} a_max b_max c_max d_max e_max f_max g_max h_max i_max j_max;
 array min1 {10} s_min a_min b_min c_min d_min e_min f_min g_min h_min i_min;
 array min2 {10} a_min b_min c_min d_min e_min f_min g_min h_min i_min j_min;
 array grad {10} grad_a grad_b grad_c grad_d grad_e grad_f grad_g grad_h grad_i grad_j;
 array turn {10} a_tp b_tp c_tp d_tp e_tp f_tp g_tp h_tp i_tp j_tp;
  do i = 1 to 10;
    if max1 {i} = 1 and max2 {i} = 1 then do;
      grad {i} = 0;
      turn {i} = "+";
     end;
    if min1 {i} = 1 and min2 {i} = 1 then do;
      grad {i} = 0;
      turn {i} = "-";
    end;
  end;
run;

proc print;
run;
```

A3.B.4. PROGRAM 4A

```
/*******************************************************;
 * TITLE.            radtrans.prg                      *
 *                                                     *
 * INPUT FILE.       interdat.ssd                      *
 *                                                     *
 * OUTPUT FILE.      raddat01.ssd                      *
 *                                                     *
 *******************************************************/;

libname ordout01 'f:\sas\alan\ringtran\working';

data in (keep = ring row a_ref b_ref c_ref d_ref e_ref f_ref g_ref h_ref i_ref j_ref
       a_tp b_tp c_tp d_tp e_tp f_tp g_tp h_tp i_tp j_tp
       grad_a grad_b grad_c grad_d grad_e grad_f grad_g grad_h grad_i grad_j);
 set ordout01.interdat;
run;

data ref;
 set in;
  a = a_ref;
  b = b_ref;
  c = c_ref;
  d = d_ref;
  e = e_ref;
  f = f_ref;
  g = g_ref;
  h = h_ref;
  i = i_ref;
  j = j_ref;
run;

proc sort;
 by ring row;
run;

proc transpose out = tref name = col prefix = ref;
 var a b c d e f g h i j;
 by ring row;
run;

proc sort;
 by row col;
run;

data cam (drop = ring ref1);
 set tref;
 if ring = 0 ;
 ring0 = ref1;
 run;

data r1 (drop = ring ref1);
 set tref;
 if ring = 1 ;
 ring1 = ref1;
 run;
```

```
data r2 (drop = ring ref1);
 set tref;
 if ring = 2 ;
 ring2 = ref1;
 run;

data r3 (drop = ring ref1);
 set tref;
 if ring = 3 ;
 ring3 = ref1;
 run;

data r4 (drop = ring ref1);
 set tref;
 if ring = 4 ;
 ring4 = ref1;
 run;

data r5 (drop = ring ref1);
 set tref;
 if ring = 5 ;
 ring5 = ref1;
 run;

data rings;
 merge cam r1 r2 r3 r4 r5;
 by row col;
run;

data tp;
 set in;
  a = a_tp;
  b = b_tp;
  c = c_tp;
  d = d_tp;
  e = e_tp;
  f = f_tp;
  g = g_tp;
  h = h_tp;
  i = i_tp;
  j = j_tp;
run;

proc sort;
 by ring row;
run;

proc transpose out = ttp name = col prefix = tp;
 var a b c d e f g h i j;
 by ring row;
run;

proc sort;
 by row col;
run;

data ctp (drop = ring tp1);
```

```
 set ttp;
 if ring = 0 ;
 camtp = tp1;
 run;

data r1tp (drop = ring tp1);
 set ttp;
 if ring = 1 ;
 rtp1 = tp1;
 run;

data r2tp (drop = ring tp1);
 set ttp;
 if ring = 2 ;
 rtp2 = tp1;
 run;

data r3tp (drop = ring tp1);
 set ttp;
 if ring = 3 ;
 rtp3 = tp1;
 run;

data r4tp (drop = ring tp1);
 set ttp;
 if ring = 4 ;
 rtp4 = tp1;
 run;

data r5tp (drop = ring tp1);
 set ttp;
 if ring = 5 ;
 rtp5 = tp1;
 run;

data turns;
 merge ctp r1tp r2tp r3tp r4tp r5tp;
 by row col;
run;

data grad;
 set in;
  a = grad_a;
  b = grad_b;
  c = grad_c;
  d = grad_d;
  e = grad_e;
  f = grad_f;
  g = grad_g;
  h = grad_h;
  i = grad_i;
  j = grad_j;
run;

proc sort;
 by ring row;
run;
```

```
proc transpose out = tgrad name = col prefix = grad;
 var a b c d e f g h i j;
 by ring row;
run;

proc sort;
 by row col;
run;

data cgrad (drop = ring grad1);
 set tgrad;
 if ring = 0 ;
 camgrad = grad1;
 run;

data r1grad (drop = ring grad1);
 set tgrad;
 if ring = 1 ;
 rgrad1 = grad1;
 run;

data r2grad (drop = ring grad1);
 set tgrad;
 if ring = 2 ;
 rgrad2 = grad1;
 run;

data r3grad (drop = ring grad1);
 set tgrad;
 if ring = 3 ;
 rgrad3 = grad1;
 run;

data r4grad (drop = ring grad1);
 set tgrad;
 if ring = 4 ;
 rgrad4 = grad1;
 run;

data r5grad (drop = ring grad1);
 set tgrad;
 if ring = 5 ;
 rgrad5 = grad1;
 run;

data grads;
 merge cgrad r1grad r2grad r3grad r4grad r5grad;
 by row col;
run;

data ordout01.raddat01;
 merge rings turns grads;
 by row col;
run;

proc print;
run;
```

A3.B.5.PROGRAM 4B

```
/*****************************************************;
 * TITLE.          samplgen.prg                      *
*                                                     *
 * INPUT FILE.     none                              *
 *                                                   *
 * OUTPUT FILE.    samfile.ssd                       *
 *                                                   *
 *****************************************************/;

libname output 'F:\SAS\ALAN\RINGTRAN\working';

data rannum01 ;
  do i = 1 to 2000;
    val = (round(uniform(-1),0.001));
 output;
  end;
 run;

data rslide (drop = val i);
set rannum01;
 if val <= 0.100 then slide = 1766;
 if 0.100 < val <= 0.200 then slide = 1766;
 if 0.200 < val <= 0.300 then slide = 1767;
 if 0.300 < val <= 0.400 then slide = 1768;
 if 0.400 < val <= 0.500 then slide = 1769;
 if 0.500 < val <= 0.600 then slide = 1770;
 if 0.600 < val <= 0.700 then slide = 1771;
 if 0.700 < val <= 0.800 then slide = 1772;
 if 0.800 < val <= 0.900 then slide = 1773;
 if val > 0.900 then slide = 1774;
 rank = i;
 run;

data rannum02 ;
  do i = 1 to 2000;
    section = (round((uniform(-1)*24),1));
 output;
  end;
 run;

data rsection (drop = i);
 set rannum02;
 if section = 0 then section = 24;
 rank = i;
 run;

data rannum03 ;
  do i = 1 to 2000;
    row = (round((uniform(0)*8),1));
 output;
  end;
 run;

data rline (drop = i);
 set rannum03;
```

```
if row = 0 then row = 8;
rank = i;
run;

data rannum04 ;
  do i = 1 to 2000;
     val = (round((uniform(0)*9),1));
 output;
  end;
run;

data rcolumn (drop = val i);
 set rannum04;
 if val = 0 then col = 'A';
 if val = 1 then col = 'B';
 if val = 2 then col = 'C';
 if val = 3 then col = 'D';
 if val = 4 then col = 'E';
 if val = 5 then col = 'F';
 if val = 6 then col = 'G';
 if val = 7 then col = 'H';
 if val = 8 then col = 'I';
 if val = 9 then col = 'J';
 rank = i;
 run;

data samfile;
 merge rslide rsection rline rcolumn;
 by rank;
 run;

data output.samfile;
 set samfile;
   if slide = 1766 then number = 0 + section ;
   if slide = 1767 then number =24 + section ;
   if slide = 1768 then number =48 + section ;
   if slide = 1769 then number =72 + section ;
   if slide = 1770 then number =96 + section ;
   if slide = 1771 then number =120 + section ;
   if slide = 1772 then number =144 + section ;
   if slide = 1773 then number =168 + section ;
   if slide = 1774 then number =192 + section ;
run;

proc sort;
 by row col slide section;

proc print ;
 var slide section number col row rank;
run;
```

A3.B.6.PROGRAM 5

```
/*****************************************************.
 * TITLE.            samerge1.sas                     *
 *                                                    *
 * INPUT FILE.       raddat01.ssd                      *
 *                   samfile.ssd                      *
 *                                                    *
 * OUTPUT FILE.      formsam.ssd                      *
 *                                                    *
 *****************************************************/;

libname input 'f:\sas\alan\ringtran\working';
libname output 'f:\sas\alan\ringtran\working';

data sample;
 set input.samfile;
run;

proc sort;
 by rank;
run;

data output.svyfile1;
 set sample ;
 if row = 1 then row1 = 1;
 if row = 2 then row2 = 1;
 if row = 3 then row3 = 1;
 if row = 4 then row4 = 1;
 if row = 5 then row5 = 1;
 if row = 6 then row6 = 1;
 if row = 7 then row7 = 1;
 if row = 8 then row8 = 1;
 if row = 9 then row9 = 1;
 if row = 10 then row10 = 1;
run;

data collect2 (keep = row1 row2 row3 row4 row5 row6 row7 row8 row9 row10
          col row rank);
 set output.svyfile1;
run;

proc sort;
 by row col rank;
run;

proc transpose out = tcollect;
 var row1 row2 row3 row4 row5 row6 row7 row8 row9 row10;
 by row col rank;
 run;

data change (drop = _name_ col1);
 set tcollect;
 if col1 ne 1 then delete;
 if _name_ = 'ROW1' then rtie = 1;
 if _name_ = 'ROW2' then rtie = 2;
 if _name_ = 'ROW3' then rtie = 3;
```

```
if _name_ = 'ROW4' then rtie = 4;
if _name_ = 'ROW5' then rtie = 5;
if _name_ = 'ROW6' then rtie = 6;
if _name_ = 'ROW7' then rtie = 7;
if _name_ = 'ROW8' then rtie = 8;
if _name_ = 'ROW9' then rtie = 9;
if _name_ = 'ROW10' then rtie = 10;
run;

proc sort;
 by rtie col;
run;

data table ;
 set input.raddat01;
 rename row = rtie;
run;

data join ;
 merge change (in = a) table;
  by rtie col;
  if a;
 run;

proc sort data = join out = output.formsam;
 by row col rank;
run;

proc print ;
title 'formsam.ssd';
run;
```

A3.B.7. PROGRAM 6A

```
/*********************************************************;
 * TITLE.            rowfora1.sas                        *
 *                                                       *
 * INPUT FILE.       formsam.ssd                         *
 *                   svyfile1.ssd                        *
 *                                                       *
 * OUTPUT FILE.      rowform.ssd                         *
 *                                                       *
 *********************************************************/;

libname input 'f:\sas\alan\ringtran\working';
libname output 'f:\sas\alan\ringtran\working';

data include;
 set input.formsam;
run;

data argn (drop = i rtie ring0 ring1 ring2 ring3 ring4 ring5
        camgrad rgrad1 rgrad2 rgrad3 rgrad4 rgrad5);
 set include;
 if rtie = 1 ;
```

```
 array oldring {6} ring0 ring1 ring2 ring3 ring4 ring5;
 array newring {6} aring0 aring1 aring2 aring3 aring4 aring5;
 array oldgrad {6} camgrad rgrad1 rgrad2 rgrad3 rgrad4 rgrad5;
 array newgrad {6} acagrad argrad1 argrad2 argrad3 argrad4 argrad5;
  do i = 1 to 6;
   newring {i} = oldring {i};
   newgrad {i} = oldgrad {i};
  end;
run;

data brgn (drop = i rtie ring0 ring1 ring2 ring3 ring4 ring5
       camgrad rgrad1 rgrad2 rgrad3 rgrad4 rgrad5);
 set include;
 if rtie = 2 ;
 array oldring {6} ring0 ring1 ring2 ring3 ring4 ring5;
 array newring {6} bring0 bring1 bring2 bring3 bring4 bring5;
 array oldgrad {6} camgrad rgrad1 rgrad2 rgrad3 rgrad4 rgrad5;
 array newgrad {6} bcagrad brgrad1 brgrad2 brgrad3 brgrad4 brgrad5;
  do i = 1 to 6;
   newring {i} = oldring {i};
   newgrad {i} = oldgrad {i};
  end;
run;

data crgn (drop = i rtie ring0 ring1 ring2 ring3 ring4 ring5
       camgrad rgrad1 rgrad2 rgrad3 rgrad4 rgrad5);
 set include;
 if rtie = 3 ;
 array oldring {6} ring0 ring1 ring2 ring3 ring4 ring5;
 array newring {6} cring0 cring1 cring2 cring3 cring4 cring5;
 array oldgrad {6} camgrad rgrad1 rgrad2 rgrad3 rgrad4 rgrad5;
 array newgrad {6} ccagrad crgrad1 crgrad2 crgrad3 crgrad4 crgrad5;
  do i = 1 to 6;
   newring {i} = oldring {i};
   newgrad {i} = oldgrad {i};
  end;
run;

data drgn (drop = i rtie ring0 ring1 ring2 ring3 ring4 ring5
       camgrad rgrad1 rgrad2 rgrad3 rgrad4 rgrad5);
 set include;
 if rtie = 4 ;
 array oldring {6} ring0 ring1 ring2 ring3 ring4 ring5;
 array newring {6} dring0 dring1 dring2 dring3 dring4 dring5;
 array oldgrad {6} camgrad rgrad1 rgrad2 rgrad3 rgrad4 rgrad5;
 array newgrad {6} dcagrad drgrad1 drgrad2 drgrad3 drgrad4 drgrad5;
  do i = 1 to 6;
   newring {i} = oldring {i};
   newgrad {i} = oldgrad {i};
  end;
run;

data ergn (drop = i rtie ring0 ring1 ring2 ring3 ring4 ring5
       camgrad rgrad1 rgrad2 rgrad3 rgrad4 rgrad5);
 set include;
 if rtie = 5 ;
 array oldring {6} ring0 ring1 ring2 ring3 ring4 ring5;
 array newring {6} ering0 ering1 ering2 ering3 ering4 ering5;
```

```
 array oldgrad {6} camgrad rgrad1 rgrad2 rgrad3 rgrad4 rgrad5;
 array newgrad {6} ecagrad ergrad1 ergrad2 ergrad3 ergrad4 ergrad5;
  do i = 1 to 6;
   newring {i} = oldring {i};
   newgrad {i} = oldgrad {i};
  end;
run;

data frgn (drop = i rtie ring0 ring1 ring2 ring3 ring4 ring5
       camgrad rgrad1 rgrad2 rgrad3 rgrad4 rgrad5);
 set include;
 if rtie = 6 ;
 array oldring {6} ring0 ring1 ring2 ring3 ring4 ring5;
 array newring {6} fring0 fring1 fring2 fring3 fring4 fring5;
 array oldgrad {6} camgrad rgrad1 rgrad2 rgrad3 rgrad4 rgrad5;
 array newgrad {6} fcagrad frgrad1 frgrad2 frgrad3 frgrad4 frgrad5;
  do i = 1 to 6;
   newring {i} = oldring {i};
   newgrad {i} = oldgrad {i};
  end;
run;

data grgn (drop = i rtie ring0 ring1 ring2 ring3 ring4 ring5
       camgrad rgrad1 rgrad2 rgrad3 rgrad4 rgrad5);
 set include;
 if rtie = 7 ;
 array oldring {6} ring0 ring1 ring2 ring3 ring4 ring5;
 array newring {6} gring0 gring1 gring2 gring3 gring4 gring5;
 array oldgrad {6} camgrad rgrad1 rgrad2 rgrad3 rgrad4 rgrad5;
 array newgrad {6} gcagrad grgrad1 grgrad2 grgrad3 grgrad4 grgrad5;
  do i = 1 to 6;
   newring {i} = oldring {i};
   newgrad {i} = oldgrad {i};
  end;
run;

data hrgn (drop = i rtie ring0 ring1 ring2 ring3 ring4 ring5
       camgrad rgrad1 rgrad2 rgrad3 rgrad4 rgrad5);
 set include;
 if rtie = 8 ;
 array oldring {6} ring0 ring1 ring2 ring3 ring4 ring5;
 array newring {6} hring0 hring1 hring2 hring3 hring4 hring5;
 array oldgrad {6} camgrad rgrad1 rgrad2 rgrad3 rgrad4 rgrad5;
 array newgrad {6} hcagrad hrgrad1 hrgrad2 hrgrad3 hrgrad4 hrgrad5;
  do i = 1 to 6;
   newring {i} = oldring {i};
   newgrad {i} = oldgrad {i};
  end;
run;

data irgn (drop = i rtie ring0 ring1 ring2 ring3 ring4 ring5
       camgrad rgrad1 rgrad2 rgrad3 rgrad4 rgrad5);
 set include;
 if rtie = 9 ;
 array oldring {6} ring0 ring1 ring2 ring3 ring4 ring5;
 array newring {6} iring0 iring1 iring2 iring3 iring4 iring5;
 array oldgrad {6} camgrad rgrad1 rgrad2 rgrad3 rgrad4 rgrad5;
 array newgrad {6} icagrad irgrad1 irgrad2 irgrad3 irgrad4 irgrad5;
```

```
   do i = 1 to 6;
    newring {i} = oldring {i};
    newgrad {i} = oldgrad {i};
   end;
run;

data jrgn (drop = i rtie ring0 ring1 ring2 ring3 ring4 ring5
        camgrad rgrad1 rgrad2 rgrad3 rgrad4 rgrad5);
 set include;
 if rtie = 10 ;
  array oldring {6} ring0 ring1 ring2 ring3 ring4 ring5;
  array newring {6} jring0 jring1 jring2 jring3 jring4 jring5;
  array oldgrad {6} camgrad rgrad1 rgrad2 rgrad3 rgrad4 rgrad5;
  array newgrad {6} jcagrad jrgrad1 jrgrad2 jrgrad3 jrgrad4 jrgrad5;
   do i = 1 to 6;
    newring {i} = oldring {i};
    newgrad {i} = oldgrad {i};
   end;
run;

data reform1;
 merge argn brgn crgn drgn ergn frgn grgn hrgn irgn jrgn;
 by row col rank;
run;

data svyfile ;
 set input.svyfile1;
run;

proc sort;
 by row col rank;
run;

data output.rowform;
 merge reform1 svyfile;
 by row col rank;
run;

proc print;
run;_
```

A3.B.8. PROGRAM 6B

```
/*****************************************************,
 * TITLE.            rowforb1.sas                     *
 *                                                    *
 * INPUT FILE.       formsam.ssd                      *
 *                   svyfile1.ssd                     *
 *                                                    *
 * OUTPUT FILE.      rowformb.ssd                     *
 *                                                    *
 *****************************************************/;

libname input 'f:\sas\alan\ringtran\working';
libname output 'f:\sas\alan\ringtran\working';
```

```
data include;
 set input.formsam;
run;

data convert (drop = camtp rtp1 rtp2 rtp3 rtp4 rtp5);
 set include;
 if camtp = '+' then tp0 = 1;
 if camtp = '-' then tp0 = 0;
 if rtp1 = '+' then tp1 = 1;
 if rtp1 = '-' then tp1 = 0;
 if rtp2 = '+' then tp2 = 1;
 if rtp2 = '-' then tp2 = 0;
 if rtp3 = '+' then tp3 = 1;
 if rtp3 = '-' then tp3 = 0;
 if rtp4 = '+' then tp4 = 1;
 if rtp4 = '-' then tp4 = 0;
 if rtp5 = '+' then tp5 = 1;
 if rtp5 = '-' then tp5 = 0;
run;

data atur (drop = i rtie ring0 ring1 ring2 ring3 ring4 ring5
        camgrad rgrad1 rgrad2 rgrad3 rgrad4 rgrad5
        tp0 tp1 tp2 tp3 tp4 tp5);
 set convert;
 if rtie = 1 ;
  array oldturn {6} tp0 tp1 tp2 tp3 tp4 tp5;
  array newturn {6} aturn0 aturn1 aturn2 aturn3 aturn4 aturn5;
    do i = 1 to 6;
      newturn {i} = oldturn {i};
    end;
run;

data btur (drop = i rtie ring0 ring1 ring2 ring3 ring4 ring5
        camgrad rgrad1 rgrad2 rgrad3 rgrad4 rgrad5
        tp0 tp1 tp2 tp3 tp4 tp5);
 set convert;
 if rtie = 2 ;
  array oldturn {6} tp0 tp1 tp2 tp3 tp4 tp5;
  array newturn {6} bturn0 bturn1 bturn2 bturn3 bturn4 bturn5;
    do i = 1 to 6;
      newturn {i} = oldturn {i};
    end;
run;

data ctur (drop = i rtie ring0 ring1 ring2 ring3 ring4 ring5
        camgrad rgrad1 rgrad2 rgrad3 rgrad4 rgrad5
        tp0 tp1 tp2 tp3 tp4 tp5);
 set convert;
 if rtie = 3 ;
  array oldturn {6} tp0 tp1 tp2 tp3 tp4 tp5;
  array newturn {6} cturn0 cturn1 cturn2 cturn3 cturn4 cturn5;
    do i = 1 to 6;
      newturn {i} = oldturn {i};
    end;
run;

data dtur (drop = i rtie ring0 ring1 ring2 ring3 ring4 ring5
```

```
        camgrad rgrad1 rgrad2 rgrad3 rgrad4 rgrad5
        tp0 tp1 tp2 tp3 tp4 tp5);
 set convert;
 if rtie = 4 ;
  array oldturn {6} tp0 tp1 tp2 tp3 tp4 tp5;
  array newturn {6} dturn0 dturn1 dturn2 dturn3 dturn4 dturn5;
    do i = 1 to 6;
      newturn {i} = oldturn {i};
    end;
run;

data etur (drop = i rtie ring0 ring1 ring2 ring3 ring4 ring5
        camgrad rgrad1 rgrad2 rgrad3 rgrad4 rgrad5
        tp0 tp1 tp2 tp3 tp4 tp5);
 set convert;
 if rtie = 5 ;
  array oldturn {6} tp0 tp1 tp2 tp3 tp4 tp5;
  array newturn {6} eturn0 eturn1 eturn2 eturn3 eturn4 eturn5;
    do i = 1 to 6;
      newturn {i} = oldturn {i};
    end;
run;

data ftur (drop = i rtie ring0 ring1 ring2 ring3 ring4 ring5
        camgrad rgrad1 rgrad2 rgrad3 rgrad4 rgrad5
        tp0 tp1 tp2 tp3 tp4 tp5);
 set convert;
 if rtie = 6 ;
  array oldturn {6} tp0 tp1 tp2 tp3 tp4 tp5;
  array newturn {6} fturn0 fturn1 fturn2 fturn3 fturn4 fturn5;
    do i = 1 to 6;
      newturn {i} = oldturn {i};
    end;
run;

data gtur (drop = i rtie ring0 ring1 ring2 ring3 ring4 ring5
        camgrad rgrad1 rgrad2 rgrad3 rgrad4 rgrad5
        tp0 tp1 tp2 tp3 tp4 tp5);
 set convert;
 if rtie = 7 ;
  array oldturn {6} tp0 tp1 tp2 tp3 tp4 tp5;
  array newturn {6} gturn0 gturn1 gturn2 gturn3 gturn4 gturn5;
    do i = 1 to 6;
      newturn {i} = oldturn {i};
    end;
run;

data htur (drop = i rtie ring0 ring1 ring2 ring3 ring4 ring5
        camgrad rgrad1 rgrad2 rgrad3 rgrad4 rgrad5
        tp0 tp1 tp2 tp3 tp4 tp5);
 set convert;
 if rtie = 8 ;
  array oldturn {6} tp0 tp1 tp2 tp3 tp4 tp5;
  array newturn {6} hturn0 hturn1 hturn2 hturn3 hturn4 hturn5;
    do i = 1 to 6;
      newturn {i} = oldturn {i};
    end;
run;
```

```
data itur (drop = i rtie ring0 ring1 ring2 ring3 ring4 ring5
        camgrad rgrad1 rgrad2 rgrad3 rgrad4 rgrad5
        tp0 tp1 tp2 tp3 tp4 tp5);
 set convert;
 if rtie = 9 ;
  array oldturn {6} tp0 tp1 tp2 tp3 tp4 tp5;
  array newturn {6} iturn0 iturn1 iturn2 iturn3 iturn4 iturn5;
    do i = 1 to 6;
     newturn {i} = oldturn {i};
    end;
run;

data jtur (drop = i rtie ring0 ring1 ring2 ring3 ring4 ring5
        camgrad rgrad1 rgrad2 rgrad3 rgrad4 rgrad5
        tp0 tp1 tp2 tp3 tp4 tp5);
 set convert;
 if rtie = 10;
  array oldturn {6} tp0 tp1 tp2 tp3 tp4 tp5;
  array newturn {6} jturn0 jturn1 jturn2 jturn3 jturn4 jturn5;
    do i = 1 to 6;
     newturn {i} = oldturn {i};
    end;
run;

data reform1;
 merge atur btur ctur dtur etur ftur gtur htur itur jtur;
 by row col rank;
run;

data svyfile ;
 set input.svyfile1;
run;

proc sort;
 by row col rank;
run;

data output.rowformb;
 merge reform1 svyfile;
 by row col rank;
run;

proc print;

run;
```

A3.B.9. PROGRAM 7

```
*********************************************************.
* TITLE.          samring.sas                            *
*                                                        *
* INPUT FILE.     rowform.ssd                            *
*                 rowformb.ssd                           *
*                 svyfile1.ssd                           *
*                                                        *
* OUTPUT FILE     turns.ssd                              *
*                                                        *
*********************************************************/;

libname input 'f:\sas\alan\ringtran\working';
libname output 'f:\sas\alan\ringtran\working';

data zones;
 set input.rowform;
  if row = 1 then do;
    if number > aring5 then zone = 0;
    if number < aring0 then zone = 0;
    if aring5 >= number > aring4 then zone = 5;
    if aring4 >= number > aring3 then zone = 4;
    if aring3 >= number > aring2 then zone = 3;
    if aring2 >= number > aring1 then zone = 2;
    if aring1 >= number > aring0 then zone = 1;
  end;
  if row = 2 then do;
    if number > bring5 then zone = 0;
    if number < bring0 then zone = 0;
    if bring5 >= number > bring4 then zone = 5;
    if bring4 >= number > bring3 then zone = 4;
    if bring3 >= number > bring2 then zone = 3;
    if bring2 >= number > bring1 then zone = 2;
    if bring1 >= number > bring0 then zone = 1;
  end;
  if row = 3 then do;
    if number > cring5 then zone = 0;
    if number < cring0 then zone = 0;
    if cring5 >= number > cring4 then zone = 5;
    if cring4 >= number > cring3 then zone = 4;
    if cring3 >= number > cring2 then zone = 3;
    if cring2 >= number > cring1 then zone = 2;
    if cring1 >= number > cring0 then zone = 1;
  end;
  if row = 4 then do;
    if number > dring5 then zone = 0;
    if number < dring0 then zone = 0;
    if dring5 >= number > dring4 then zone = 5;
    if dring4 >= number > dring3 then zone = 4;
    if dring3 >= number > dring2 then zone = 3;
    if dring2 >= number > dring1 then zone = 2;
    if dring1 >= number > dring0 then zone = 1;
  end;
  if row = 5 then do;
    if number > ering5 then zone = 0;
    if number < ering0 then zone = 0;
```

```
  if ering5 >= number > ering4 then zone = 5;
  if ering4 >= number > ering3 then zone = 4;
  if ering3 >= number > ering2 then zone = 3;
  if ering2 >= number > ering1 then zone = 2;
  if ering1 >= number > ering0 then zone = 1;
 end;
 if row = 6 then do;
  if number > fring5 then zone = 0;
  if number < fring0 then zone = 0;
  if fring5 >= number > fring4 then zone = 5;
  if fring4 >= number > fring3 then zone = 4;
  if fring3 >= number > fring2 then zone = 3;
  if fring2 >= number > fring1 then zone = 2;
  if fring1 >= number > fring0 then zone = 1;
 end;
 if row = 7 then do;
  if number > gring5 then zone = 0;
  if number < gring0 then zone = 0;
  if gring5 >= number > gring4 then zone = 5;
  if gring4 >= number > gring3 then zone = 4;
  if gring3 >= number > gring2 then zone = 3;
  if gring2 >= number > gring1 then zone = 2;
  if gring1 >= number > gring0 then zone = 1;
 end;
 if row = 8 then do;
  if number > hring5 then zone = 0;
  if number < hring0 then zone = 0;
  if hring5 >= number > hring4 then zone = 5;
  if hring4 >= number > hring3 then zone = 4;
  if hring3 >= number > hring2 then zone = 3;
  if hring2 >= number > hring1 then zone = 2;
  if hring1 >= number > hring0 then zone = 1;
 end;
 if row = 9 then do;
  if number > iring5 then zone = 0;
  if number < iring0 then zone = 0;
  if iring5 >= number > iring4 then zone = 5;
  if iring4 >= number > iring3 then zone = 4;
  if iring3 >= number > iring2 then zone = 3;
  if iring2 >= number > iring1 then zone = 2;
  if iring1 >= number > iring0 then zone = 1;
 end;
 if row = 10 then do;
  if number > jring5 then zone = 0;
  if number < jring0 then zone = 0;
  if jring5 >= number > jring4 then zone = 5;
  if jring4 >= number > jring3 then zone = 4;
  if jring3 >= number > jring2 then zone = 3;
  if jring2 >= number > jring1 then zone = 2;
  if jring1 >= number > jring0 then zone = 1;
 end;
run;

data position (drop = aring0 aring1 aring2 aring3 aring4
          aring5
               bring0 bring1 bring2 bring3 bring4
          bring5
               cring0 cring1 cring2 cring3 cring4
```

```
        cring5
            dring0 dring1 dring2 dring3 dring4
        dring5
            ering0 ering1 ering2 ering3 ering4
        ering5
            fring0 fring1 fring2 fring3 fring4
        fring5
            gring0 gring1 gring2 gring3 gring4
        gring5
            hring0 hring1 hring2 hring3 hring4
        hring5
            iring0 iring1 iring2 iring3 iring4
        iring5
            jring0 jring1 jring2 jring3 jring4
        jring5);
set zones;
array rows {10} row1 row2 row3 row4 row5 row6 row7 row8 row9 row10;
array relpos {10} pos1 pos2 pos3 pos4 pos5 pos6 pos7 pos8 pos9 pos10;
array ring0 {10} aring0 bring0 cring0 dring0 ering0 fring0 gring0 hring0 iring0 jring0;
array ring1 {10} aring1 bring1 cring1 dring1 ering1 fring1 gring1 hring1 iring1 jring1;
array ring2 {10} aring2 bring2 cring2 dring2 ering2 fring2 gring2 hring2 iring2 jring2;
array ring3 {10} aring3 bring3 cring3 dring3 ering3 fring3 gring3 hring3 iring3 jring3;
array ring4 {10} aring4 bring4 cring4 dring4 ering4 fring4 gring4 hring4 iring4 jring4;
array ring5 {10} aring5 bring5 cring5 dring5 ering5 fring5 gring5 hring5 iring5 jring5;
do i = 1 to 10;
 if rows{i}  = 1 then do;
  if zone = 1 then do;
   relpos{i} = round(((number - ring1{i})/(ring0{i} - ring1{i})),0.01);
  end;
  if zone = 2 then do;
   relpos{i} = round(((number - ring2{i})/(ring1{i} - ring2{i})),0.01);
  end;
  if zone = 3 then do;
   relpos{i} = round(((number - ring3{i})/(ring2{i} - ring3{i})),0.01);
  end;
  if zone = 4 then do;
   relpos{i} = round(((number - ring4{i})/(ring3{i} - ring4{i})),0.01);
  end;
  if zone = 5 then do;
   relpos{i} = round(((number - ring5{i})/(ring4{i} - ring5{i})),0.01);
  end;
 end;
end;
run;

data weights;
 set position;
 array relpos {10} pos1 pos2 pos3 pos4 pos5 pos6 pos7 pos8 pos9 pos10;
 array weight {10} wt1 wt2 wt3 wt4 wt5 wt6 wt7 wt8 wt9 wt10;
 do i = 1 to 10;
 if relpos{i} = . then weight{i} = .;
 if 0 <= relpos{i} < 0.25 then weight{i} = 1;
 if 0.25 <= relpos{i} < 0.50 then weight{i} = 0.66;
 if 0.50 <= relpos{i} < 0.75 then weight{i} = 0.34;
 if relpos{i} >= 0.75 then weight{i} = 0;
 end;
run;
```

```
data grades (drop = acagrad argrad1 argrad2 argrad3 argrad4
          argrad5
               bcagrad brgrad1 brgrad2 brgrad3 brgrad4
          brgrad5
               ccagrad crgrad1 crgrad2 crgrad3 crgrad4
          crgrad5
               dcagrad drgrad1 drgrad2 drgrad3 drgrad4
          drgrad5
               ecagrad ergrad1 ergrad2 ergrad3 ergrad4
          ergrad5
               fcagrad frgrad1 frgrad2 frgrad3 frgrad4
          frgrad5
               gcagrad grgrad1 grgrad2 grgrad3 grgrad4
          grgrad5
               hcagrad hrgrad1 hrgrad2 hrgrad3 hrgrad4
          hrgrad5
               icagrad irgrad1 irgrad2 irgrad3 irgrad4
          irgrad5
               jcagrad jrgrad1 jrgrad2 jrgrad3 jrgrad4
          jrgrad5 i );
 set weights;
 array rows {10} row1 row2 row3 row4 row5 row6 row7 row8 row9 row10;
 array rlgrad {10} gra1 gra2 gra3 gra4 gra5 gra6 gra7 gra8 gra9 gra10;
 array weight {10} wt1 wt2 wt3 wt4 wt5 wt6 wt7 wt8 wt9 wt10;
 array grad0 {10} acagrad bcagrad ccagrad dcagrad ecagrad fcagrad gcagrad hcagrad icagrad
jcagrad;
 array grad1 {10} argrad1 brgrad1 crgrad1 drgrad1 ergrad1 frgrad1 grgrad1 hrgrad1 irgrad1
jrgrad1;
 array grad2 {10} argrad2 brgrad2 crgrad2 drgrad2 ergrad2 frgrad2 grgrad2 hrgrad2 irgrad2
jrgrad2;
 array grad3 {10} argrad3 brgrad3 crgrad3 drgrad3 ergrad3 frgrad3 grgrad3 hrgrad3 irgrad3
jrgrad3;
 array grad4 {10} argrad4 brgrad4 crgrad4 drgrad4 ergrad4 frgrad4 grgrad4 hrgrad4 irgrad4
jrgrad4;
 array grad5 {10} argrad5 brgrad5 crgrad5 drgrad5 ergrad5 frgrad5 grgrad5 hrgrad5 irgrad5
jrgrad5;
 do i = 1 to 10;
  if rows{i}  = 1 then do;
   if zone = 1 then do;
    rlgrad{i}=round((((grad1{i}*weight{i})+(grad0{i}*(1-weight{i})))
          /2),0.01);
   end;
  if zone = 2 then do;
    rlgrad{i}=round((((grad2{i}*weight{i})+(grad1{i}*(1-weight{i})))
          /2),0.01);
   end;
   if zone = 3 then do;
    rlgrad{i}=round((((grad3{i}*weight{i})+(grad2{i}*(1-weight{i})))
          /2),0.01);
   end;
   if zone = 4 then do;
    rlgrad{i}=round((((grad4{i}*weight{i})+(grad3{i}*(1-weight{i})))
          /2),0.01);
   end;
   if zone = 5 then do;
    rlgrad{i}=round((((grad5{i}*weight{i})+(grad4{i}*(1-weight{i})))
          /2),0.01);
   end;
```

```
 end;
end;
run;

data addturn;
 merge grades input.rowformb;
 by row col rank;
run;

data output.turns (drop = aturn0 aturn1 aturn2 aturn3 aturn4
                          aturn5
                          bturn0 bturn1 bturn2 bturn3 bturn4 bturn5
                          cturn0 cturn1 cturn2 cturn3 cturn4 cturn5
                          dturn0 dturn1 dturn2 dturn3 dturn4 dturn5
                          eturn0 eturn1 eturn2 eturn3 eturn4 eturn5
                          fturn0 fturn1 fturn2 fturn3 fturn4 fturn5
                          gturn0 gturn1 gturn2 gturn3 gturn4 gturn5
                          hturn0 hturn1 hturn2 hturn3 hturn4 hturn5
                          iturn0 iturn1 iturn2 iturn3 iturn4 iturn5
                          jturn0 jturn1 jturn2 jturn3 jturn4 jturn5
                          row1 row2 row3 row4 row5 row6 row7 row8
                          row9 row10);
 set addturn;
 array rows {10} row1 row2 row3 row4 row5 row6 row7 row8 row9 row10;
 array turns {10} $ tp1 tp2 tp3 tp4 tp5 tp6 tp7 tp8 tp9 tp10;
 array turn0 {10} aturn0 bturn0 cturn0 dturn0 eturn0 fturn0 gturn0 hturn0 iturn0 jturn0;
 array turn1 {10} aturn1 bturn1 cturn1 dturn1 eturn1 fturn1 gturn1 hturn1 iturn1 jturn1;
 array turn2 {10} aturn2 bturn2 cturn2 dturn2 eturn2 fturn2 gturn2 hturn2 iturn2 jturn2;
 array turn3 {10} aturn3 bturn3 cturn3 dturn3 eturn3 fturn3 gturn3 hturn3 iturn3 jturn3;
 array turn4 {10} aturn4 bturn4 cturn4 dturn4 eturn4 fturn4 gturn4 hturn4 iturn4 jturn4;
 array turn5 {10} aturn5 bturn5 cturn5 dturn5 eturn5 fturn5 gturn5 hturn5 iturn5 jturn5;
 do i = 1 to 10;
  if rows{i}  = 1 then do;
   if zone = 1 then do;
    if turn0{i} = . and turn1{i} = . then turns{i} = ' ';
    if turn0{i} = . and turn1{i} = 1 then turns{i} = '+';
    if turn0{i} = . and turn1{i} = 0 then turns{i} = '-';
    if turn0{i} = 1 and turn1{i} = . then turns{i} = '+';
    if turn0{i} = 0 and turn1{i} = . then turns{i} = '-';
    if turn0{i} = 0 and turn1{i} = 0 then turns{i} = '-';
    if turn0{i} = 1 and turn1{i} = 1 then turns{i} = '+';
    if turn0{i} = 1 and turn1{i} = 0 then turns{i} = '*';
    if turn0{i} = 0 and turn1{i} = 1 then turns{i} = '*';
   end;
  if zone = 2 then do;
    if turn1{i} = . and turn2{i} = . then turns{i} = ' ';
    if turn1{i} = . and turn2{i} = 1 then turns{i} = '+';
    if turn1{i} = . and turn2{i} = 0 then turns{i} = '-';
    if turn1{i} = 1 and turn2{i} = . then turns{i} = '+';
    if turn1{i} = 0 and turn2{i} = . then turns{i} = '-';
    if turn1{i} = 0 and turn2{i} = 0 then turns{i} = '-';
    if turn1{i} = 1 and turn2{i} = 1 then turns{i} = '+';
    if turn1{i} = 1 and turn2{i} = 0 then turns{i} = '*';
    if turn1{i} = 0 and turn2{i} = 1 then turns{i} = '*';
   end;
   if zone = 3 then do;
    if turn2{i} = . and turn3{i} = . then turns{i} = ' ';
    if turn2{i} = . and turn3{i} = 1 then turns{i} = '+';
```

```
  if turn2{i} = . and turn3{i} = 0 then turns{i} = '-';
  if turn2{i} = 1 and turn3{i} = . then turns{i} = '+';
  if turn2{i} = 0 and turn3{i} = . then turns{i} = '-';
  if turn2{i} = 0 and turn3{i} = 0 then turns{i} = '-';
  if turn2{i} = 1 and turn3{i} = 1 then turns{i} = '+';
  if turn2{i} = 1 and turn3{i} = 0 then turns{i} = '*';
  if turn2{i} = 0 and turn3{i} = 1 then turns{i} = '*';
 end;
 if zone = 4 then do;
  if turn3{i} = . and turn4{i} = . then turns{i} = ' ';
  if turn3{i} = . and turn4{i} = 1 then turns{i} = '+';
  if turn3{i} = . and turn4{i} = 0 then turns{i} = '-';
  if turn3{i} = 1 and turn4{i} = . then turns{i} = '+';
  if turn3{i} = 0 and turn4{i} = . then turns{i} = '-';
  if turn3{i} = 0 and turn4{i} = 0 then turns{i} = '-';
  if turn3{i} = 1 and turn4{i} = 1 then turns{i} = '+';
  if turn3{i} = 1 and turn4{i} = 0 then turns{i} = '*';
  if turn3{i} = 0 and turn4{i} = 1 then turns{i} = '*';
 end;
 if zone = 5 then do;
  if turn4{i} = . and turn5{i} = . then turns{i} = ' ';
  if turn4{i} = . and turn5{i} = 1 then turns{i} = '+';
  if turn4{i} = . and turn5{i} = 0 then turns{i} = '-';
  if turn4{i} = 1 and turn5{i} = . then turns{i} = '+';
  if turn4{i} = 0 and turn5{i} = . then turns{i} = '-';
  if turn4{i} = 0 and turn5{i} = 0 then turns{i} = '-';
  if turn4{i} = 1 and turn5{i} = 1 then turns{i} = '+';
  if turn4{i} = 1 and turn5{i} = 0 then turns{i} = '*';
  if turn4{i} = 0 and turn5{i} = 1 then turns{i} = '*';
 end;
 end;
end;
run;
```

ACKNOWLEDGEMENTS

I would like to thank my supervisor, Dr. BG Butterfield, and other members of my thesis committee: Dr. BA Fineran; Dr. JM Harris; and Professor WR Philipson, for their guidance and constructive criticism.

I also wish to thank the staff of the Department of Plant and Microbial Sciences, especially: Reijel Gardiner (histology and field work); Graeme Young (computing requirements); and Dougal Holmes (photography).

I would also like to thank fellow students: Dr. James Condon; and Dr. David Burritt, for our many useful discussions.

On a more personal note, I wish to again thank Reijel (and the cats: Boris and Tardis).

REFERENCES

Allan, HH. (1961) Flora of New Zealand. vol. I. Government Printer, Wellington.

Bailey, IW. (1910a) Notes on the wood structure of the Betulaceae and Fagaceae. Forestry Quarterly 8:176-185

Bailey, IW. (1910b) Reversionary characters of traumatic oak woods. Botanical Gazette 50:374-380

Bailey, IW. (1911) The relation of the leaf-trace to the formation of compound rays in the lower dicotyledons. Annals of Botany 25:225-241

Bailey, IW. (1912) The evolutionary history of the foliar ray in the wood of the dicotyledons : and its phylogenetic significance. Annals of Botany 26:647-661

Bailey, IW. (1920) The cambium and its derivative tissues. II. Size variations of cambial initials in gymnosperms and angiosperms. American Journal of Botany 7:355-367

Bailey, IW. (1923) The cambium and its derivative tissues IV. The increase in girth of the cambium. American Journal of Botany 10:499-509

Bailey, IW and Sinnott, EW. (1914) Investigations on the phylogeny of the angiosperms. No.2. Anatomical evidences of the reduction in certain of the amentiferae. Botanical Gazette 58:36-60

Bannan, MW. (1950a) Abnormal xylem rays in *Chamaecyparis*. American Journal of Botany 37:232-237

Bannan, MW. (1950b) The frequency of anticlinal divisions in fusiform cambial cells of *Chamaecyparis*. American Journal of Botany 37:511-519

Bannan, MW. (1951) The reduction of fusiform cambial cells in *Chamaecyparis* and *Thuja*. Canadian Journal of Botany 29:57-67

Bannan, MW. (1957a) Girth increase in white cedar stems of irregular form. Canadian Journal of Botany 35:425-434

Bannan, MW. (1957b) The structure and growth of the cambium. TAPPI 40:220-225

Bannan, MW. (1959) Some factors influencing cell size in conifer cambium. Proceedings.- 9th international Botanical Congress :1704-1709

Bannan, MW. (1965) The rate of elongation of fusiform initials in the cambium of Pinaceae. Canadian Journal of Botany 43:429-435

Bannan, MW and Bayly, LL. (1956) Cell size and survival in conifer cambium. Canadian Journal of Botany 34:769-776

Barghoorn, ES. (1940) The ontogenetic development and phylogenetic specialization of rays in the xylem of dicotyledons. I. The primitive ray structure. American Journal of Botany 27:918-928

Barghoorn, ES. (1941) The ontogenetic development and phylogenetic specialization of rays in the xylem of dicotyledons. II. Modification of the multiseriate and uniseriate rays. American Journal of Botany 28:273-282

Beck, CB; Schmid, R and Rothwell, GW. (1982) Stelar morphology and the primary vascular system of seed plants. The Botanical Review 48:691-815

Bhat, KM. (1980) Pith flecks and ray abnormalities in birch wood. Silva Fennica 14:277-285

Bhat, KM. (1983) A note on aggregate rays of *Betula* species. IAWA Bulletin n.s. 4:183-185

Biro, RL and Jaffe, MJ. (1984) Thigmomorphogenesis - ethylene evolution and its role in the changes observed in mechanically perturbed bean plants. Physiologica Plantarum 62:289-296

Bissing, DR. (1974) Haupt's gelatin adhesive mixed with formalin for affixing paraffin sections to slides. Stain Technology 49:116-117

Bosshard, HH. (1976) Functional tropism. Holztechnologie 17:107-112

Brown, CL and Sax, K. (1962) The influence of pressure on the differentiation of secondary tissues. American Journal of Botany 49:683-691

Carlquist, S. (1982) The use of ethylenediamine in softening hard plant structures for paraffin sectioning. Stain Technology 57:311-317

Carlquist, S. (1988) Comparative wood anatomy: systematic, ecological, and evolutionary aspects of dicotyledon wood. Springer-Verlag, Berlin Heidelberg.

Cronquist, A. (1988) The evolution and classification of flowering plants. 2nd ed. The New York Botanical Garden, Bronx, New York.

Cumbie, BG. (1967) Developmental changes in the vascular cambium in *Leitneria floridana*. American Journal of Botany 54:414-424

D'Agostino, RB and Tietjen, GL. (1973) Approaches to the null distribution of $\sqrt{b1}$. Biometrika 60:169-173

Davies, PJ. (1987) The plant hormones: their nature, occurrence, and functions. In Davies, PJ. Hormones and their role in plant growth and development. Martinus Nijhoff Publishers, Dordrecht

Denne, MP and Whitbread, V. (1978) Variation of fibre length within trees of *Fraxinus excelsior*. Canadian Journal of Forestry Research 8:253-260

Donaldson, LA. (1982) Abnormal rays in the wood of Eucalypts. IAWA Bulletin n.s. 3:214-215

Eames, AJ. (1910) On the origin of the broad ray in *Quercus*. Botanical Gazette 49:161-167

Eames, AJ. (1911) The origin of the herbaceous type in the angiosperms. Annals of Botany 25:215-224

Evert, RF. (1961) Some aspects of cambial development in *Pyrus communis*. American Journal of Botany 48:479-488

Feder, N and O'Brien, TP. (1986) Plant microtechnique: some principles and new methods. American Journal of Botany 55:123-142

Fink, S. (1982) Adventitious root primordia - the cause of abnormally broad xylem rays in hard - and softwoods. IAWA Bulletin n.s. 3:31-38

Flores, EM. (1980) Shoot vascular system and phyllotaxis of *Casuarina* (Casuarinaceae). American Journal of Botany 67:131-140

Groom, P. (1911) The evolution of the annual ring and medullary rays of Quercus. Annals of Botany 25:983-1003

Hejnowicz, Z. (1980) Tensional stress in the cambium and its developmental significance. American Journal of Botany 67:1-5

Hoar, CS. (1916) The anatomy and phylogenetic position of the Betulaceae. American Journal of Botany 3:415-435

Holdheide, W. (1955) Über das abnorme dickenwachstum der hainbuche (*Carpinus betulus* L.) und die rolle der falschen markstrahlen. Botanische Studien 4:132-164

Howard, RA. (1974) The stem-node-leaf continuum of the Dicotyledoneae. Journal of the Arnold Arboretum 55:125-173

IAWA Committee. (1989) IAWA list of microscopic features for hardwood identification. IAWA Bulletin n.s. 10:219-332

IAWA Committee on Nomenclature. (1964) Multilingual glossary of terms used in wood anatomy. Konkordia, Winterthur, Switzerland.

Imamura, Y. (1978) Abnormal ray tissues in excrescence featured wood of sugi (*Cryptomeria japonica* D.Don). Mokuzai Gakkai Shi 24:71-75

Jaffe, MJ. (1973) Thigmomorphogenesis: The response of plant growth and development to mechanical stimulation. Planta 114:143-157

Jeffrey, EC. (1917) The anatomy of woody plants. The University of Chicago Press, Chicago.

Jeffrey, EC and Torrey, RE. (1921a) Physiological and morphological correlations in herbaceous angiosperms. Botanical Gazette 71:1-31

Jeffrey, EC and Torrey, RE. (1921b) Transitional herbaceous dicotyledons. Annals of Botany 35:227-249

Jenkins, R. (1993) The origin of the Fagaceous cupule. Botanical Gazette 59:81-111

Jensen, WA. (1962) Botanical histochemistry: principles and practice. WH Freeman and Company, San Francisco.

Johansen, DA. (1940) Plant microtechnique. McGraw-Hill Book Company Inc., New York.

Jones, JH. (1986) Evolution of the Fagaceae: the implications of foliar features. Annals of the Missouri Botanical Garden 73:228-275

Kribs, DA. (1935) Salient lines of structural specialization in the wood rays of dicotyledons. Botanical Gazette 96:547-557

Kucera, L; Bosshard, HH and Katz, E. (1980) Über den Keilwuchs und den welligen Jahrringverlauf in Buche (*Fagus sylvatica* L.). Holz als Roh- und Werkstoff 38:161-168

Kuroda, K and Shimaji, K. (1985) Wound effects on cytodifferentiation in hardwood xylem. IAWA Bulletin n.s. 6:107-118

Langdon, LM. (1947) The comparative morphology of the Fagaceae. I. The genus *Nothofagus*. Botanical Gazette 108:350-371

Lev-Yadun, S and Aloni, R. (1991a) Natural and experimentally induced dispersion of aggregate rays in shoots of *Quercus ithaburensis* Decne. and *Q. calliprinos* Webb. Annals of Botany 68:85-91

Lev-Yadun, S and Aloni, R. (1991b) An experimental method of inducing 'hazel' wood in *Pinus halepensis* (Pinaceae). IAWA Bulletin n.s. 12:445-451

Lintilhac, PM and Vesecky, TB. (1981) Mechanical stress and cell wall orientation in plants. II. The Application of controlled directional stress to growing plants; with a discussion on the nature of the wound reaction. American Journal of Botany 68:1222-1230

Makino, R; Kuroda, H and Shimaji, K. (1983) Callus formation and effects of applied pressure to the cultured cambial explant of sugi (*Cryptomeria japonica* D.Don). Wood Research 69:1-11

Metcalfe, CR and Chalk, L. (1950) Anatomy of the dicotyledons: leaves, stem and wood in relation to taxonomy. With notes on economic uses. vol. I. Claredon Press, Oxford.

Metcalfe, CR and Chalk, L. (1983) Anatomy of dicotyledons. 2nd ed. vol. II. Clarendon Press, Oxford.

Métraux, J-P. (1987) Gibberellins and plant cell elongation. In Davies, PJ. Hormones and their role in plant growth and development. Martinus Nijhoff Publishers, Dordrecht

Middleton, TM. (1987) Aggregate rays in New Zealand Nothofagus Blume (Fagaceae) stem wood and their influence on vessel distribution. IAWA Bulletin n.s. 8:53-57

Morgan, DC and Smith, H. (1978) The relationship between phytochrome photoequilibrium and development in light grown *Chenopodium album* L. Planta 142:187-193

Moseley, MF. (1948) Comparative anatomy and phylogeny of the Casuarinaceae. Botanical Gazette 110:231-280

Newman, IV. (1956) On fluting of the trunk in young trees of *Pinus taeda* L. (loblolly pine). Australian Journal of Botany 4:1-12

Newton, M; El Hassen, BA and Zavitkovski, J. (1968) Role of red alder in Western Oregon forest succession. In Trappe, JM; Franklin, JF; Tarrant, RF and Hansen, GM. Biology of Alder. Pacific Northwest and Range Experimental Station, Forest Service, US Department of Agriculture, Portland, Oregon

Nixon, KC. (1982) Support of recognition of the family Nothofagaceae Kuprianova. Publications - Botanical Society of America. Incorporated miscellaneous series. 162:102

Noskowiak, AF. (1978) Distribution of aggregate rays in red alder. Wood and Fiber 10:58-68

Ohtani, J; Fukuzawa, K and Fukumorita, T. (1987) SEM observations of indented rings. IAWA Bulletin n.s. 8:113-124

Parham, BE. (1930) An introductory study of the genus "*Nothofagus*" Blume: the secondary xylem, with special reference to the New Zealand species. MA (Honours) in Botany. Thesis. University of New Zealand

Parham, BE. (1933a) New Zealand beech timbers: their structure and identification. The New Zealand Journal of Science and Technology 14:233-240

Parham, BE. (1933b) New Zealand beech timbers: their structure and identification. The New Zealand Journal of Science and Technology 14:372-382

Patel, RN. (1965) A comparison of the anatomy of secondary xylem in roots and stems. Holzforschung 19:72-79

Patel, RN. (1986) Wood anatomy of the dicotyledons indigenous to New Zealand. 15. Fagaceae. New Zealand Journal of Botany 24:189-202

Patel, RN and Shand, JE. (1985) Bark anatomy of *Nothofagus* species indigenous to New Zealand. New Zealand Journal of Botany 23:511-532

Philipson, WR; Ward, JM and Butterfield, BG. (1971) The vascular cambium: Its development and activity. Chapman and Hall Ltd., London.

Roberts, LW; Gahan, PB and Aloni, R. (1988) Vascular differentiation and plant growth regulators. Springer-Verlag, Berlin, Heidelberg.

Ruth, RH. (1968) First season growth of red alder seedlings under gradients in solar radiation. In Trappe, JM; Franklin, JF; Tarrant, RF and Hansen, GM. Biology of Alder. Pacific Northwest and Range Experimental Station, Forest Service, US Department of Agriculture, Portland, Oregon

Schultze-Dewitz, G and Gotze, H. (1986) Abnorme holzstrukturen. Teil 1. Haselwuchs and wimmerwuchs. Drevársky Výskum 111:1-10

Shimaji, K. (1954a) Anatomical studies on the wood of Japanese *Quercus*. 1. On subgenus Lepidobalanus (Nara group). Bulletin of the Tokyo University Forests 46:193-210

Shimaji, K. (1954b) Anatomical studies on the wood of Japanese *Quercus*. 2. On subgenus Cyclobalanopsis (Kashi group). Bulletin of the Tokyo University Forests 47:125-143

Sinnott, EW and Bailey, IW. (1914) Investigations on the phylogeny of the angiosperms: No.4. The origin and dispersal of herbaceous angiosperms. Annals of Botany 28:547-600

Sinnott, EW and Bailey, IW. (1922) The significance of the 'foliar ray' in the evolution of herbaceous angiosperms. Annals of Botany 36:523-533

Sugawa, T and Fujii, T. (1993) Aggregate rays of *Thujopsis dolabrata* var. *hondai* (Cupressaceae). IAWA Journal 14:315-323

Thompson, WP. (1911) On the origin of the multiseriate ray of the dicotyledons. Annals of Botany 25:1005-1014

Wardle, JA. (1984) The New Zealand beeches. Ecology, utilisation and management.. N.Z. Forest Service, .

Wardrop, AB. (1948) The influence of pressure on the cell wall organisation of conifer tracheids. Leeds Philosophical and Literary Society Proceedings. Scientific Section 5:128-135

Waring, PF and Phillips, IDJ. (1981) Growth and differentiation in plants. 3rd edn. Pergamon Press, Oxford.

Wenham, MW and Cusick, F. (1975) The growth of secondary wood fibres. New Phytologist 74:247-261

Ziegler, H and Merz, W. (1961) 'Hazel' Growth. On the relationship between irregular secondary thickening and the distribution of rays. Holz als Roh- und Werkstoff 19:1-8